Multi-temporal shoreline dynamics of the repeatedly nourished coast of Egmond-Bergen quantified from satellite imagery

MSc Thesis Earth Surface and Water

Coastal dynamics and Fluvial systems

J. S. Löhr

6803288

1st supervisor: Prof Dr. Gerben Ruessink

2nd supervisor: Dr. Timothy Price

Utrecht University
Faculty of Geosciences
Department of Physical Geography

Utrecht, 2 February 2024

Acknowledgements

This thesis would not have been possible without the help and guidance I received from several people. First of all, I would like to express my sincere gratitude to my supervisors, Gerben Ruessink and Timothy Price, who motivated and inspired me with their invaluable knowledge and experience. Thank you for the weekly meetings, guidance and valuable feedback. I would also like to thank my friends and family, especially my parents, for their unconditional support during the making of this thesis.

Abstract

Climate change is expected to worsen coastal erosion in the future related to sea level rise, changes in wave climate and an increase in storm activity. Consequently, it is becoming more and more relevant to understand and quantify the present-day dynamics of the shoreline and its underlying drivers of change. In line with the dynamic coastline preservation policy adopted in the Netherlands since 1990, many sand nourishments have been carried out over the past 30 years to protect the Dutch coastline against erosion. These sand nourishments mainly comprised of beach and shoreface nourishments. However, knowledge is still limited on the effects of beach and shoreface nourishments on the dynamics of the shoreline and its (long-term) temporal trends, especially in the case of repeated sand nourishments. The latter being important given that nourishment efforts are likely to increase in the future due to rising sea levels. This study focused on a stretch of the Holland coast along Castricum, Egmond and Bergen, where in the northern part at Egmond and Bergen 23 beach nourishments and 10 shoreface nourishments have been performed. In the south near Castricum, on the other hand, beaches remained unnourished. The Python toolkit CoastSat was used to obtain time-series of cross-shore shoreline positions along the entire study area over a time period of 1985 – 2023. In this toolkit satellite images from Landsat 5-9 and Sentinel-2 are utilised to extract the instantaneous position of the shoreline. By analysing the temporal and spatial variability of the shoreline, this study shows that the repeated nourishments had a large influence on the long-term interannual trend of the coastline leading to considerable shoreline advance and an increasing trend of 2.00 m/year for the nourished coast at Egmond and Bergen, while the unnourished coast remained more or less stable. Shoreface nourishments, especially in combination with a beach nourishment, attributed most to the expansion of the shoreline (~50 m). Although no considerable shoreline sedimentation was observed at the scale of only one shoreface nourishment, over time the repeated shoreface nourishments led to a large cumulative effect with shoreline expansion becoming more pronounced over time. Beach nourishments only resulted in relatively minor sustainable shoreline advance (< 10 m) and were often completely eroded within 1 or 2 years. For individual beach nourishments typically between 10 and 40 m of shoreline progradation occurred after construction. It was found that the effect of the sand nourishments was very localised to the initial extent of the nourishments and did not exhibit large alongshore migration to the adjacent, unnourished coast. Only after 2016, sand also slightly started to spread to the adjacent coastlines, related to the cumulative effect of the shoreface nourishments. Furthermore, in terms of temporal variability, it was found that seasonality in shoreline position along the entire study area was very limited, the amplitude of the seasonality typically was less than 10 m. A distinct response of the shoreline to storm events was also limited. Future studies will have to tell if the shoreline progradation trend at Egmond and Bergen will continue under the current nourishment strategy or if, due to climate change, nourishment efforts will have to increase.

Keywords: *Coastal morphodynamics; beach nourishments; shoreface nourishments; shoreline evolution; Holland coast*

Contents

List of Figures

List of Tables

1. Introduction

With more than 9 million people in the Netherlands living below sea level and with the majority of economic activities also situated in the lower-lying regions, protection of the hinterland against flooding has always been of utmost importance in Dutch coastal management (Mulder et al., 2011). Especially after the disastrous impact of the storm surge of 1953 in the southwestern part of the Netherlands, large-scale reinforcement of the flood protection structures (e.g. dikes, dunes) was initiated across the entire country. Higher fluvial and coastal flood protection standards were established and also laid down in legislation, and multiple dams and storm surge barriers (Delta works) were built to reduce the length of the coastline (Pilarczyk, 2007; Van Alphen, 2016). Without flood protection structures large parts of the Netherlands would flood during storm conditions due to the accompanying high water levels (e.g. nowadays approximately two-thirds of the country) (Pilarczyk, 2007).

Dutch coastal policy

Before 1990 coastal protection was mainly focused on defensive measures, that is, measures were only implemented when urgent erosion problems came to pass threatening the safety of the land and requiring immediate solving (De Ruig & Hillen, 1997). An important shift took place in 1990, from the defensive coastal policy a more offensive coastal policy was adopted. In earlier years, in particular starting from the 1980s, already the general idea came into existence that the coastal policy of the time would not be sustainable in the future. The ongoing coastal retreat would not only jeopardise the safety function of the coastal area (e.g. dunes) but also its other functional uses (e.g. economical, recreational) (De Ruig & Hillen, 1997; Lodder & Slinger, 2022). Therefore, a new coastal policy called 'Dynamic Preservation' was developed and from 1990 and onwards the Dutch government decided to pro-actively preserve the coastline thereby counteracting all structural erosion of the coastline. This new approach also incorporated other aspects that were concerned with the ecological values of the dunes and beaches, allowing for the presence of more natural dynamics. This way, the natural character and dynamics of the Dutch coastal zone could be sustained besides the primary function of the policy for safety against flooding. To be able to dynamically maintain the coastline, the position of the 1990-coastline was chosen as a fixed reference point which is not to be exceeded in landward direction. The term 'Basiskustlijn' (BKL) or Basal Coastline was adopted to refer to this reference coastline (De Ruig & Hillen, 1997; Hillen & Roelse, 1995). But given that the approach of the basal coastline did not consider the longer-term influence of sea level rise or loss of sand at greater water depths, in 1995 an even larger scale management approach came into practice as well. This made sure that the active sand volume contained between the -20 m depth contour and the dune foot is maintained, the so-called Coastal Foundation (Mulder et al., 2007). A third and smallest scale was also developed during that time and included the preservation of the dune strength and the protection against flooding they provide. Since then, every 5 years the residual dune strength has been evaluated with a dune erosion model to test the dunes under design storm conditions to ensure that the local safety standard is still met (Mulder & Tonnon, 2011). On the whole, the Dutch coastal policy thus uses three different indicators for safety, translating into three different scale levels of coastal management (Figure 1.1). The overarching concept behind this is that the larger scale defines the boundary conditions for the smaller scale. For instance, maintaining the residual dune strength establishes boundary conditions for the momentaneous safety against flooding. Moreover, conservation of the basal coastline sets boundary conditions for sustaining the residual dune strength considering longshore distances of kilometres and a time period of years. Lastly, keeping the sediment budget in the Coastal Foundation at the right level establishes the boundary conditions for preserving the basal coastline over time periods ranging from decades to centuries and longshore distances of tens to hundreds of kilometres (Mulder et al., 2007; Mulder & Tonnon, 2011).

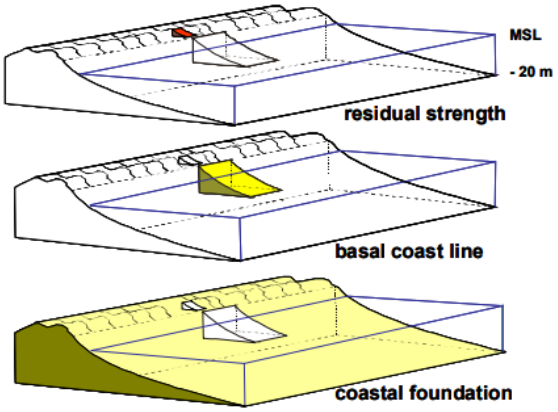

Figure 1.1: The three different scales incorporated in the Dutch coastal erosion management. Retrieved from: Mulder & Tonnon (2011).

Sand nourishments

With an eye on the preservation of the natural value of the beach and dune area, soft measures instead of hard measures (e.g. groynes, breakwaters) became the preferred strategy to sustain the coastline after 1990. Hence, sand nourishments were selected as the main method to compensate for the sand loss within the Coastal Foundation and (structural) erosion of the coastline (Lodder & Slinger, 2022). The positive effects of the added sediment supply also worked through to the smallest level, the dunes (Mulder & Tonnon, 2011). The sand nourishments proved to be an effective measure and for many beaches along the Dutch coastline erosional trends were brought to a halt, while at the same time nourishments also fulfilled other purposes regarding recreation and nature conservation (De Ruig & Hillen, 1997). However, it is important to note that the implementation of nourishments did not eliminate the underlying causes of erosion of the coastline. Over time, the nourished sand also eroded and nourishments had to be repeated to be able to maintain the basal coastline. Nourishments efforts not only increased over time, but also the initial, frequently-used beach nourishments got more and more replaced by cheaper and equally effective shoreface nourishments (Brand et al., 2022).

Several studies have reported on the implementation of beach and shoreface nourishments along the Dutch coastline (e.g. Cohen & Brière, 2007; de Sonneville & Van der Spek, 2012; Huisman et al., 2019; Ojeda et al., 2008; Quartel & Grasmeijer, 2007; Roelse, 1996; Van Duin et al., 2004; Vermaas et al., 2013). Nourished locations include for example Terschelling, Ameland, Noordwijk aan Zee, Egmond aan Zee, and Zandvoort. Many of these studies investigated the behaviour and effects of individual nourishments but only on a typical timescale of years. Often the collected data comprised of annual bathymetric measurements (Jarkus data) (e.g. de Sonneville & Van der Spek, 2012), sometimes supplemented with additional bathymetric surveys or other measurements (e.g. Grunnet & Ruessink, 2005; Huisman et al., 2019; Vermaas et al., 2013). In Van Duin et al. (2004) available bathymetric data was for the most part collected two times per year. Van Duin et al. (2004) evaluated the morphological response of the subtidal bars and the effects on the shoreline after a shoreface nourishment performed in front of Egmond on a temporal scale of years. They found that the shoreface nourishment barely influenced the shoreline and volume of the beach with very little redistribution of the nourished sand in the first two years. Similar studies but then for beach nourishments are very sparse in the Netherlands. Most importantly, most of the studies limited their research to the effects of individual nourishments on the shoreline and nearshore zone, while almost none of them examined the effects of repeated beach and shoreface nourishments on the temporal trends and dynamics of the shoreline. As sand nourishments often have to be repeated in certain locations that experience rapid erosion of the coastline, it is crucial to increase the understanding on the influence of repeated nourishments.

Therefore, this thesis aims to unravel the spatiotemporal shoreline evolution for high-energy and low-sloping beaches that are repeatedly nourished. The research will be carried out at Bergen and Egmond along the Dutch Holland coast, where since 1990 a large number of beach and shoreface nourishments

have been performed. With CoastSat, a freely-accessible toolkit to derive shorelines from 30+ years of satellite imagery (Vos et al., 2019b), time-series of shoreline positions at the Egmond-Bergen coast will be studied from 1985-2023. The position of the shoreline will be used to analyse the temporal variability in the shoreline but also to examine the spatial effects of the repeated sand nourishments on the coast. Experts in the field of coasts often view the position of the shoreline as a fundamental factor in gaining insight into the evolution of a coastline. Thereby measurements and observations of the variability in the shoreline are widely used to determine potential accreting or erosional trends, also with regard to coastal monitoring and safety (Vos et al., 2019a). Additionally, the rich source of satellite imagery has shown a gradual increase in satellite revisit period over the years due to technical advancements and the addition of Landsat 5-9 and Sentinel-2 missions (Vos et al., 2019a). Consequently, this allows for investigation of shoreline dynamics on shorter timescales, that is, from seasonal to multi-decadal timescales including changes on the event-scale (e.g. storms, nourishments). This is in contrast to earlier studies which were often based on one or two surveys per year.

The outline of this thesis is as follows: First a comprehensive literature review is provided discussing natural shoreline behaviour and nourishments in Chapter 2. This is followed by the objective and research questions in Chapter 3. In Chapter 4 a description of the Holland Coast and the Egmond-Bergen coast is given, whereafter in Chapter 5 the use of CoastSat and the methods to answer the research questions will be explained. The results are presented in Chapter 6 and they are discussed in the Chapter 7 with the use of relevant literature. In the final chapter the conclusions are drawn.

2. Literature review

In this chapter an extensive overview will be given about sand nourishments, including the different types of nourishments, their design and behaviour, and their effect on the coastline. In order to provide a complete picture, first, a short review is provided about autonomous coastal behaviour as this may interact with nourishments. Then the historical context of coastal erosion and the nourishment strategy of the Netherlands is described, after which information and knowledge on nourishments is given. In this literature review, there will be a focus on the Netherlands and Egmond-Bergen as this is most relevant for this thesis and because the Netherlands is recognised as having one of the most extensive nourishment records in the world.

2.1 Autonomous coastal behaviour

This section aims to provide insight into the natural dynamics of the coastline and the dynamics of the subtidal bar system. Changes in morphology that result from feedbacks between the morphology and the hydrodynamics will be explained.

2.1.1 Natural dynamics of the coastline

Autonomous shoreline behaviour encompasses the natural behaviour of the coast without the presence of human interventions. Natural shoreline variability occurs at different timescales. The shortest timescale that is considered within the field of coastal management includes the seasonal and interseasonal timescale. Hereby, variations are examined on the timescale of storms (single events) to seasons (Stive et al., 2002). Classically, a beach often shows clear fluctuations throughout the seasons if there is a clear distinction present between seasons. During winter it is common that a storm profile develops, which is characterised by a relatively low slope and a narrow beach. This is the result of the higher energetic wave conditions that prevail during winter. The beach is eroded during storms by the high and long waves, depositing the sediment in the surf zone. For this reason, sometimes a storm profile is also called a winter profile (Figure 2.1) (Bosboom & Stive, 2022; Stive et al., 2002). During summer, wave conditions are much more calm and accretion of the beach typically occurs by onshore movement of sandbars. The sediment is returned to the beach by the lower and smaller waves. Subsequently, a relatively steep 'swell' profile develops with a berm (Figure 2.1) (Bosboom & Stive, 2022; Stive et al., 2002). On the event time scale, large storms can cause substantial erosion of the coastline, while in between almost uninterrupted sedimentation of the beach takes place (Stive et al., 2002). Note that the mean position of the coastline is not changed by these periodic fluctuations in the coastline (Bosboom & Stive, 2022).

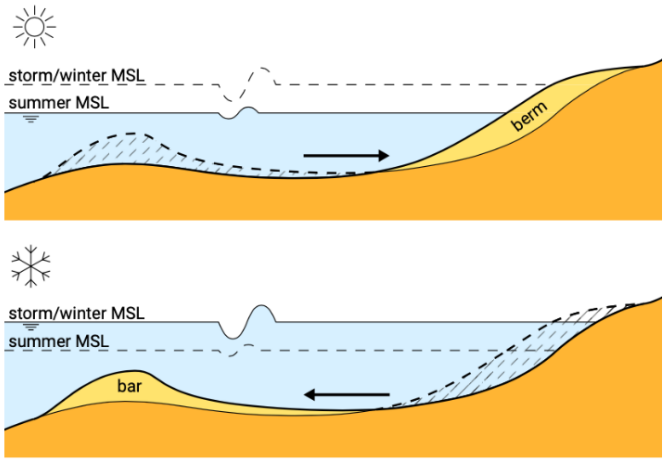

Figure 2.1: (a) Beach profile during summer; (b) beach profile during the storm season/winter. Retrieved from: Bosboom & Stive (2022).

The above described was mostly focused on swell-dominated beaches, for storm-dominated beaches the situation is slightly different. The characteristics of a storm-dominated beach are often described by a 'storm-post storm' model (Quartel et al., 2008). According to this model, considerable short-term erosion is predicted during a storm event by the generation of a surge and offshore currents (e.g. undertow), while after a storm slow and gradual accretion takes place. Typically, an intertidal bar-trough morphology with intertidal rip channels is present, whereby the beach flattens and the intertidal bar disappears during a storm. Without necessarily a volume change of the beach, a flattened beach would also suggest a wider beach. Post-storm conditions include propagating bores and swash, responsible for onshore sediment transport, leading to the formation or growth of new intertidal bars which may eventually weld to the beach (Quartel et al., 2008; Quartel & Grasmeijer, 2007). Generally, this model is deemed to be applicable to a range of storm-dominated coasts. Furthermore, the 'storm- post storm' model also has a seasonal aspect because seasonality in the frequency and intensity of storms also occurs, often with more and higher-energy storms during winter than during summer (Quartel et al., 2008).

On longer timescales, such as (inter-) annual timescales and inter-(decadal) timescales, changes in the mean position of the coastline do happen. Structural loss or gain of sediment leads to erosional or accretional trends. Guillén et al. (1999) studied the decadal variability of the shoreline for the Holland coast. They propose that the behaviour of the subtidal bars is an important factor controlling the decadal shoreline evolution. Bars could act as a wave filter, thereby influencing the actual wave energy that is transferred to the shoreline. Guillén et al. (1999) suggest that this process of wave-dampening is an important factor in the occurrence of the longshore rhythmic features that occur along the Holland coast (e.g. sand waves).

2.1.2 Natural dynamics of subtidal bars

At the Dutch coastline, typically one to three subtidal bars (max. 5) are present in the cross-shore profile, which has been described by numerous authors (e.g. Grunnet & Ruessink, 2005; Ojeda et al., 2008; Radermacher et al., 2018; Ruessink & Kroon, 1994; Shand et al., 1999). These bars show a pattern in their behaviour. During more energetic or storm conditions, bars experience relatively large offshore migration and during less energetic conditions, nonlinear waves lead to a slight onshore transport of the bars (Figure 2.2). This results in net offshore movement of the subtidal bars. Subtidal bars have a multi-annual lifetime and often they are characterised by cyclic behaviour (Bosboom & Stive, 2022; Walstra et al., 2012). Generally, three stages are recognised in the offshore bar cycle (Ojeda et al., 2008; Ruessink & Kroon, 1994):

1. Bar generation in the intertidal zone near the beach
2. Net seaward migration
3. Degeneration at the zone of decay and disappearance from the active profile

During their offshore migration, an increase in bar height and bar width occurs until they start their degeneration in the outer surf zone (Ruessink et al., 2003; Walstra et al., 2012). After a bar has disappeared, the formation of a new bar and the offshore migration of the remaining inner bars are stimulated, whereafter the cycle repeats itself (Ojeda et al., 2008; Ruessink & Kroon, 1994). The duration of the offshore bar cycle varies along the Dutch coast. For instance, the cycle is about 4 to 5 years long in the southern part of the Holland coast and about 15 years in the northern part of the Holland coast (Bosboom & Stive, 2022). This difference seems to be related to the size of the bars and the slope of the shoreface: in North Holland the bars are of larger scale and the shoreface has a steeper slope. Therefore, in order to facilitate an adequate level of sediment transport, an increased amount of energy is required (Bosboom & Stive, 2022). Near the Egmond-Bergen coast the bar cycle is about 15 years (Spanhoff et al., 2004). Guillén et al. (1999) observed a similar periodicity of 10-15 years

in the occurrence of so-called sand waves (i.e. rhythmic features) in the shoreline along the Holland coast, thereby suggesting that bar behaviour and the evolution of these rhythmic patterns in the shoreline are strongly related. They further found that the length of crescentic shapes in the bars also coincided with the wavelength of these sand waves (2-3 km). Though, the processes responsible for this potential relation between the development of subtidal bars and shoreline evolution are largely unknown.

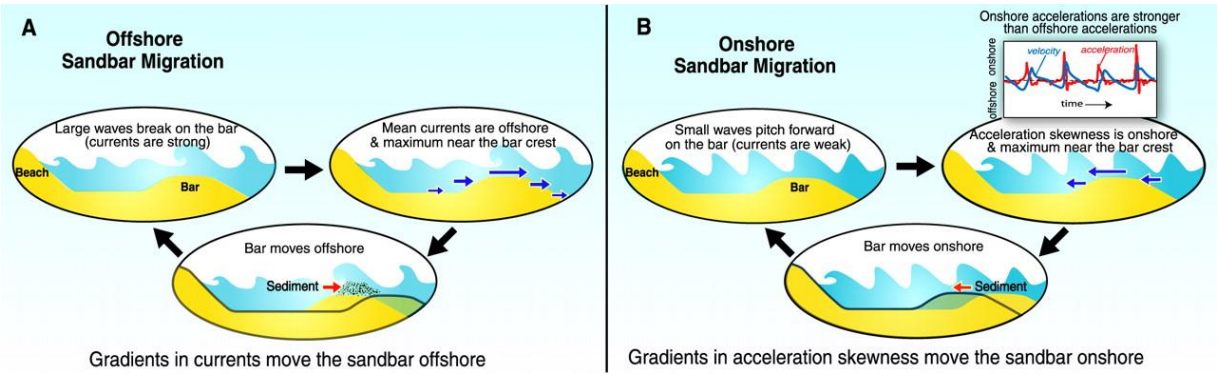

Figure 2.2: Processes responsible for the migration of sandbars: (a) Energetic conditions drive offshore bar migration, whereby an undertow is generated; (b) Calmer wave conditions induce onshore migration. Retrieved from: Hoefel & Elgar (2003).

Wright & Short (1984) described the morphology of different beach states, which also included the behaviour of one subtidal bar at a certain beach state. They distinguished six individual beach states for single-bar systems, which range from 'dissipative' (most upstate) to 'reflective' (most downstate). In between these two states, four 'intermediate' beach states are recognised, these include from highest to lowest state: the Longshore Bar Trough (LBT), Rhythmic Bar and Beach (RBB), Transverse Bar and Rip (TBR), and Low-Tide Terrace (LTT) (Stive et al., 2002; Wright & Short, 1984). The dissipative beach is sometimes also seen as the 'winter' profile (storm-dominated) and the reflective is seen as the 'summer' profile (Bosboom & Stive, 2022). The parameter in the format of $\Omega = H_b/(w_s \cdot T)$ is used to distinguish the beach states as it is based on both wave (T = wave period, H_b = breaking wave height) and sediment (w_s = fall velocity) characteristics. When the parameter Ω is smaller than 1, this indicates the reflective state, and when Ω is larger than 6 this indicates the dissipative state (Stive et al., 2002; Wright & Short, 1984). However, these beach states were based on single-bar beaches, while multiple longshore bars can also be present at the shore. In the case of two or three subtidal bars, the same beach states can be used but often the outer and inner bars behave differently from each other. Often the shallower inner subtidal bars are more mobile than the outer bar, with the outer bar only being active during large storm events. Consequently, in most cases the inner bars are more downstate or leaning towards the intermediate-reflective states than the outer bars (Short & Aagaard, 1993).

2.2 Nourishment motivation and history

In this section a short description will be given about former coastal retreat in the Netherlands, after which the nourishment history and motivation to nourish in the Netherlands is discussed.

2.2.1 History coastal erosion

The Dutch coast can be divided into three regions: the Wadden coast north of Den Helder, the Holland coast, and the Delta coast south of Hoek van Holland (Van Rijn, 1995). In this chapter, the focus will be on the Holland coast and Egmond since this is most relevant for this study.

For centuries, the Dutch Holland coast has been experiencing coastal erosion, especially in the north and south of the Holland coast while the central part remained more or less stable (Stolk, 1989). Van Rijn (1995) gives an outline of the coastal retreat that occurred along the Dutch coastline over roughly 400 years based on old manuscripts and charts. The results for the Holland coast are presented in Table 2.1. Especially between 1600-1700 substantial retreat of the coastline was documented. Near Huisduinen, which is located near Den Helder in the north, erosion of approximately 5 to 7 m/year could be observed (Van Rijn, 1995). Stolk (1989) describes that between 1600 and 1750 a retreat of approximately 1500 m occurred at Den Helder. However, after the construction of the Helderse Zeewering in 1774, coastal erosion largely ceased at Den Helder. At the Hondsbossche zeewering about 700 m was lost in the same time period, whereafter another 375 m was lost after 1750. Coastal retreat at Callantsoog (beneath Den Helder) amounted to 3 to 4 m/year between 1600-1700. In the south of the Holland coast, similar erosion rates were documented at Terheide, where erosion of 3 to 5 m/year took place. Near Egmond a coastal retreat of approximately 100 m was determined between 1665 and 1717. Between 1717 and 1864 even more land disappeared in sea; an additional retreat occurred of about 120 m (Van Rijn, 1995). Stolk (1989) reports similar erosion rates for Egmond: a retreat of 160 m between 1600 and 1750, and 130 m erosion after 1750. The coastal retreat had large consequences for the local population, whereby parts of the village were even lost to the sea (Figure 2.3). Between 1850 and 1950 coastal erosion still amounted to 0.5 to 1 m/year north of Egmond (Van Rijn, 1995). However, since 1990, structural erosion of the coastline does no longer occur as a result of the dynamic preservation policy in the Netherlands (Ministerie van Verkeer en Waterstaat, 2000).

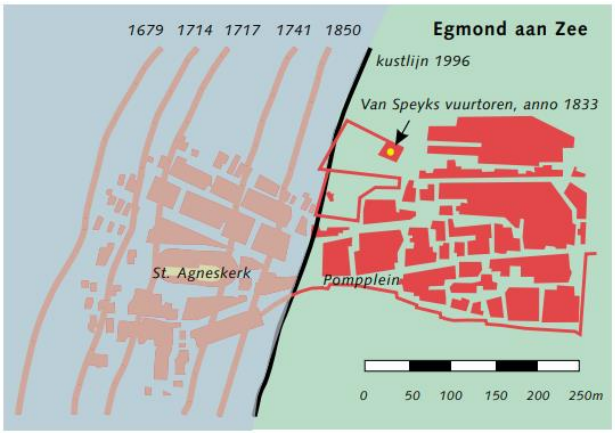

Figure 2.3: Historical coastal retreat at Egmond aan Zee, the lines represent the position of the coastline. This includes the position at 1679, 1714, 1717, 1741, 1850, and 1996. Retrieved from: Ministerie van Verkeer en Waterstaat (2000).

At IJmuiden local sedimentation of the coastline takes place due to the construction of two harbour jetties in ca. 1870. These obstruct the longshore transport along the coast, thereby resulting in very localised coastal advance (Boers, 1999; Stolk, 1989).

Table 2.1: Coastal retreat (rough estimates) for the Dutch Holland coast from 1600 to 1990. Adjusted from: Rijn (1995).

Location	Coastline retreat (in m)				Total
	1600-1700	1700-1800	1800-1900	1900-1990	
Huisduinen (0 km)	450	300	150	100	1000
Callantsoog (13 km)	250	150	80	70	550
Seawall Petten (23 km)	400	300	100	100	900
Egmond (38 km)	150	100	30	0	280
Scheveningen (100 km)	100	80	40	30	250
Terheide (110 km)	500	300	100	50	950
Terheide (115 km)	700	400	100	- 50*	1050

* Effect of harbour dam near Hoek van Holland.

2.2.2 Nourishment motivation

A beach nourishment can be applied to a stretch of coast for multiple reasons. According to Verhagen (1992), the three main reasons to nourish can be described as:

1. Counteracting coastal erosion (structural erosion)
2. Protecting the hinterland against flooding (safety)
3. Preservation of a wide beach for recreation

With the dynamic coastline preservation policy adopted in the Netherlands, aiming to maintain the coastline position of 1990, the main purpose of implementing sand nourishments is to prevent (chronic) coastal retreat. Since the middle of the 19th century annual measurements have been taken of the position of the dune-foot and the high- and low-water lines along the Dutch coast. The long-term monitoring allows for the documentation of the changes in coastal zone morphology while at the same time it guarantees the safety of the inhabited hinterland. The measurements are taken along transects oriented perpendicular to the coastline. Beach posts placed on the beach along the entire Dutch coast at intervals of 250 m mark the positions of these transects. Since 1963 it was decided by Rijkswaterstaat, which is the executive agency of the Ministry of Infrastructure and Water Management in the Netherlands, that along every transect the whole coastal profile should be determined for each year. To accomplish this, remote sensing (onland) and sounding techniques (nearshore) were applied to measure the coastal profile from approximately 800 m seaward from the beach posts up to a distance of 200 m inland from the posts (Heuvel et al., 1996; Hillen & Roelse, 1995). The annual coastal profiles are stored in a database called JARKUS, which is an abbreviation for 'JAaRlijkse KUStmetingen' (Dutch for 'annual coastal measurements'). An important purpose of the JARKUS transects is the annual determination of the MKL-position (Momentary coastline or Momentane KustLijn), which is a proxy for the present coastline position.

Following the dynamic coastline preservation approach, sand nourishments are implemented when the MKL-position is shifted landward of the BKL-position (Basal Coastline or BasisKustLijn), to pro-actively prevent coastal erosion and to maintain the coastline (Brand et al., 2022). The assessment of the MKL in relation to the BKL occurs every year and is executed in a specific manner. To evaluate the position of the coastline for a particular year, the annual MKL-measurements from the preceding 10 years are taken to determine a trendline through the points, and then by extrapolation, the position of the 'to be assessed coastline' (TKL position) can be found. The BKL-position has been calculated similarly, whereby a trendline is determined based on the period between 1980 and 1989 (Figure 2.5). Subsequently, the position of the basal coastline can be inferred from the trendline position on

January 1, 1990 (Boers, 1999; Heuvel et al., 1996). The computation of the MKL requires knowledge of the position of the dune foot and the mean low water line, which can be derived from the JARKUS transects. The MKL-position, which is with respect to a chosen reference line, is determined by taking the weighted average of the volume of sand contained in the yellow zone shown in Figure 2.4. The vertical boundary of this zone is established by twice the height between the dune foot and the lower water line, naturally creating a triangle shape. The calculation of the MKL is as follows:

$$MKL = \frac{A}{2h} \pm x_{RSP}$$

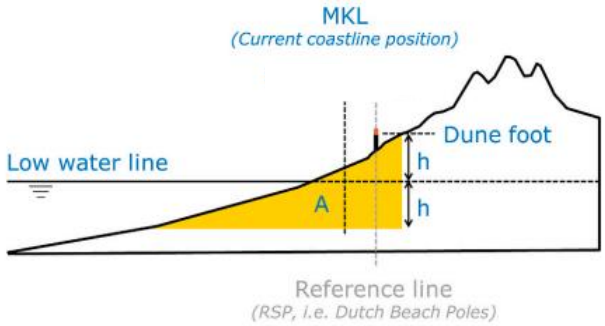

A = area for calculation [m^2]

h = difference between dune foot and low water line [m]

$\mathbf{x_{RSP}}$ = reference line

Figure 2.4: The method for computation of the MKL. The area contained in the yellow zone (A) is divided by twice the difference between the dune foot and lower water line (h), whereafter it is expressed towards a reference line. Retrieved from: Brand et al. (2022).

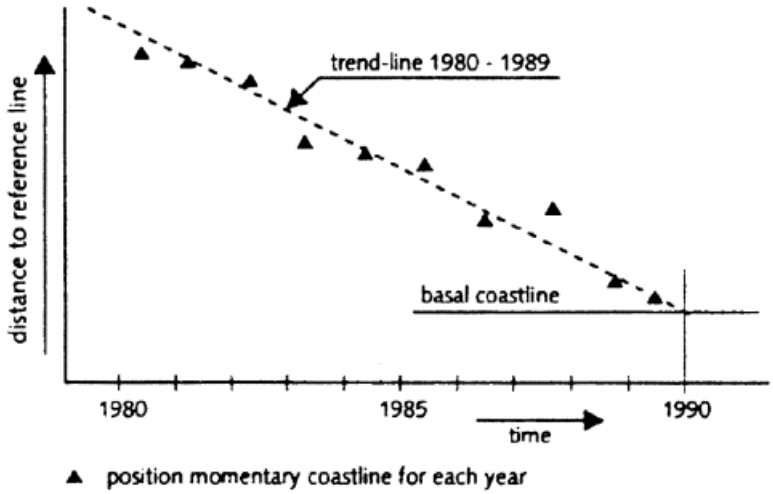

Figure 2.5: Trendline position drawn for the period of 1980-1989 in order to determine the position of the basal coastline in 1990. Retrieved from: De Ruig & Hillen (1997).

2.2.3 History nourishments

The Netherlands can be seen as one of the first countries to implement a beach nourishment as a compensation for coastal erosion; the first nourishments were carried out in the 1950s. Globally the first nourishments were carried out since the 1990s. Initially, the Dutch nourishment approach was characterised by reactive management, whereby nourishments were solely implemented as a reaction to a storm event. The volume of these nourishments was relatively small, that is, less than 0.5 mln. m^3 per year (Brand et al., 2022). Between the 1970s and the 1990s, new technical development led to an increase in the volume and frequency of beach nourishments, increasing the nourished volume to roughly 3.5 mln. m^3 per year along the Dutch coastline. With the dynamic preservation policy adopted since 1990, the nourished volume increased further and annually a volume of 6.4 mln. m^3 had to be nourished to maintain the coastline (Brand et al., 2022). When sea level rise became more and more prominent, it also became a necessity to account for coastal retreat caused by sea level rise. Accordingly, to keep the active sand volume in equilibrium with sea level rise, the nourished volume almost doubled since 2000 and now amounts to 12 mln. m^3 (Brand et al., 2022; Ministerie van Verkeer en Waterstaat, 2000). The sediment budget to sustain is defined as the Coastal Foundation, which, as aforementioned, is the region contained within the -20 m depth contour and the dune foot at +3 m NAP (Lodder & Slinger, 2022). The decision of 12 mln. m^3 is grounded on the sand budget computations by Mulder (2000) and without additional sea level rise, this was estimated for the years 2000 - 2040. However, new estimations of the Dutch sediment budget and its deficit performed by De Ronde (2008) already indicate that the 12 mln. m^3 is no longer enough to maintain the coastal foundation and needs to be upscaled to 20 mln. m^3 per year, considering a relative sea level rise of 2 mm/year. Sea level rise is also likely to increase and with scenarios of relative sea level rise of 6-12 mm/year (65 - 130 cm in 2100) nourishment efforts would have to increase by 40-85 mln. m^3 annually (Deltacommissie, 2008).

This increase in nourishment volume to 12 mln. m^3 was mainly translated into larger-sized nourishments but did not necessarily lead to an increase in the frequency of nourishment practices. Nowadays, about 10 sand nourishments are carried out every year. In Figure 2.6, the timeline of nourishing can be seen from 1950 to 2020, whereby the nourishment volume over time is shown as well as the number of nourishment projects per year. Apart from the aforementioned sand nourishments which are purely applied to sustain the Dutch coastline, several nourishments have also been performed to serve other purposes (Figure 2.6). This includes land reclamation and flood defence, and to improve nourishment techniques and to increase the understanding on this subject. Over the last 70 years, this has been a total volume of 623 mln. m^3. Two examples of projects clearly identifiable in Figure 2.6 are the construction of the Sand Engine in 2011, and the Hondsbossche Dunes in 2014 (Brand et al., 2022). Especially the Maasvlakte 2 project demanded a large volume of sand, namely 170 mln. m^3. However, in this literature review, only the 'regular' nourishments are considered. Sand required for the nourishments is generally extracted offshore in the North Sea, below the -20 m NAP contour, outside of the zone defined by the Coastal Foundation. Although shipping distances are shorter when sand is extracted within this zone of 20 km, this could result in coastal erosion and is thus avoided (Brand et al., 2022).

These nourishment efforts make that the Netherlands is recognised as one of the world's most extensively nourished coasts (Brand et al., 2022; Hanson et al., 2002). Since the 1990s, more than 300 nourishments have been carried out along the Dutch coast (Brand et al., 2022). Nourishments are usually executed on a fairly large scale because Dutch coastal maintenance is laid down in legislation, which is not the case in many other countries (Hanson et al., 2002). In other countries, nourishments are often much smaller in size and are mainly applied to benefit the recreational function of the beach (De Schipper et al., 2020). Although, it is important to note that aside from the safety function of

nourishments in the Netherlands, often values and functions on the short-term are also taken into account. For instance, beach nourishments can also serve societal functions, by enhancing the local economy (e.g. recreation), by considering ecology and by increasing scientific knowledge (Brand et al., 2022). In practice this means that the State first consults Provinces, Water Boards and municipalities and stakeholder organisations before coastline management in the form of nourishments is carried out (Mulder et al., 2011).

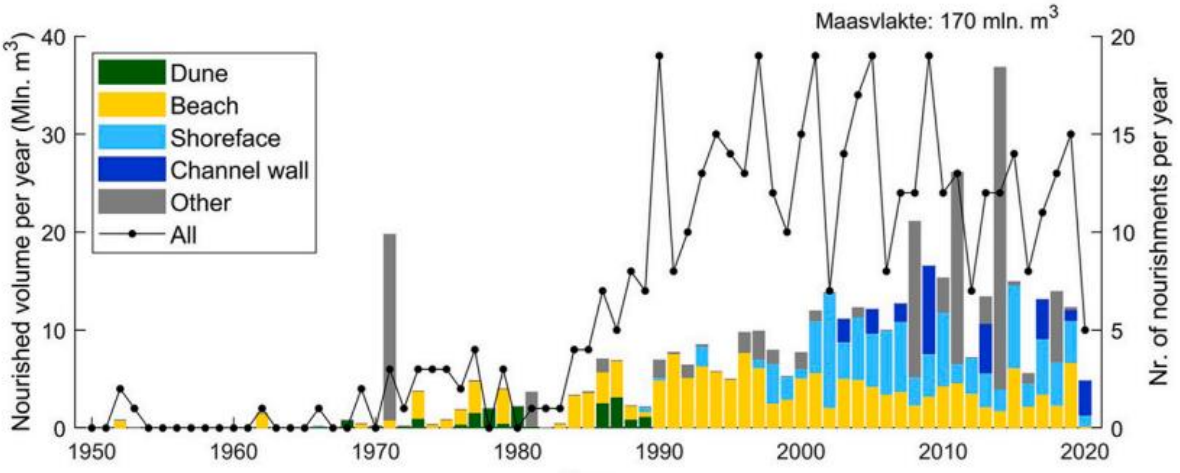

Figure 2.6: The annually nourished volume for the period of 1950-2020 for each type of nourishment, represented by the bars. The number of nourishments is also given for each year and is represented by the black line. Retrieved from: Brand et al. (2022).

2.3 Types of nourishments

In this section the different types of nourishments will be discussed. Subsequently, the two most common nourishment types implemented in the Netherlands will be further elaborated on in terms of their design and behaviour. Some examples of their implementation will also be given, with a focus on the Netherlands and in particular the Egmond-Bergen coast.

Over the years, the evolution of nourishments in terms of size and volume is not the only aspect that changed; there have also been continuous developments in nourishment techniques. Brand et al. (2022) distinguishes four types of 'traditional' nourishments, depending on the location of the sand positioning within the coastal profile:

1. Dune nourishments – sand is placed above the dune foot
2. Beach nourishments – sand is placed on the beach in the MKL-zone
3. Shoreface nourishments – sand is placed a bit seaward from the MKL-zone or just within
4. Channel wall nourishments – sand is placed against the landward side of a channel wall

In Figure 2.7 the three most common types of nourishments (2, 3, 4) are illustrated. Some papers also include mega nourishments in their classification (e.g. Stive et al., 2013), an example of a mega nourishment is the Sand Engine in the Netherlands.

Until the early 1990s, only beach and dune nourishments were carried out. Later on, also shoreface nourishments were invented and these had the advantage that they were less costly and decreased the disturbance on the beach. Channel wall nourishments were the last to be implemented, the first to be performed was in 2003 (Brand et al., 2022). Channel wall nourishments are only executed in the tidal inlets between the barrier islands (Wadden Islands) in the north and in the southwestern part of the Netherlands. These are thus not relevant to this study, and the same applies to dune nourishments. Therefore, in this literature review only beach and shoreface nourishments will be considered.

Beach and shoreface nourishments are both very common along the Holland coast. Beach nourishments are used more often than shoreface nourishments, about 70% of the time it is decided to implement a beach nourishment. However, in general beach nourishments are smaller than shoreface nourishments (Table 2.2), therefore, with regard to volume, beach nourishments only encompass 40% of the total nourished volume. In terms of costs, beach nourishments are involved with less costs than shoreface nourishments (Table 2.2) (Brand et al., 2022).

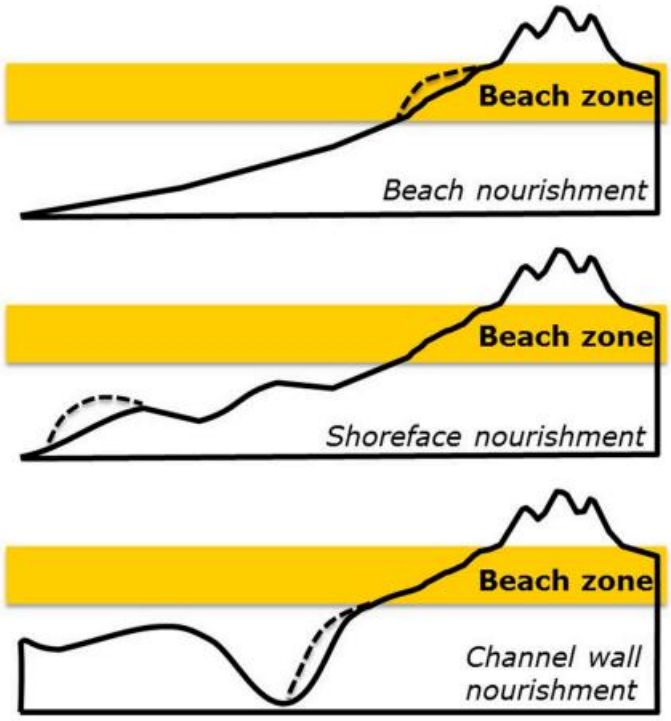

Figure 2.7: The three most regularly applied types of nourishments in the Netherlands. Retrieved from: Brand et al. (2022).

Table 2.2: Comparison between a beach and a shoreface nourishment. Based on: Brand et al. (2022).

	Type of nourishment	
	Beach	**Shoreface**
Average length	2.3 km	4 km
Average volume	200 m^3/m	450 m^3 /m
Initial decrease in volume	Fast	Gradual
Lifetime	1-5 years	4-10 years
Average cost	5.5 €/m^3	3.5 €/m^3
Visibility	High	Low

2.3.1 Beach nourishments

Design and behaviour

Beach nourishments are mainly positioned on the above-water beach but the sand can also (partially) extend to the part of the beach that is underwater. Often the landward limit of a beach nourishment is defined as the dune foot (NAP +3 m) (Brand et al., 2022; De Schipper et al., 2020). To deviate as little as possible from the natural planform of the beach and to avoid possible scarping of a nourishment, the slope and thickness of a beach nourishment are site-specific and adapted to the beach. Beach nourishments with a limited thickness help impede the possible formation of a scarp. The slope of a

beach nourishment should be comparable to the natural slope of the beach, inferring that the maximum slope of a nourishment is about 1:20 in the Netherlands, as naturally, the beach would want to return to its initial equilibrium profile (Brand et al., 2022). Another side effect that could emerge from a beach nourishment includes the generation of spits in the longshore-direction (Figure 2.8a) (Elko & Wang, 2007). In many cases, tapered ends on both sides (in longshore direction) of the nourishment with a gradual decrease in volume are applied. This helps minimising large alongshore gradients in sediment transport that otherwise would emerge from the large angles of the nourishment with the coast (Brand et al., 2022; De Schipper et al., 2020). On average, beach nourishments have a volume of 200 m^3/m and are 2.3 km long in longshore direction, taking into account the accommodation capacity of most Dutch beaches (Table 2.2).

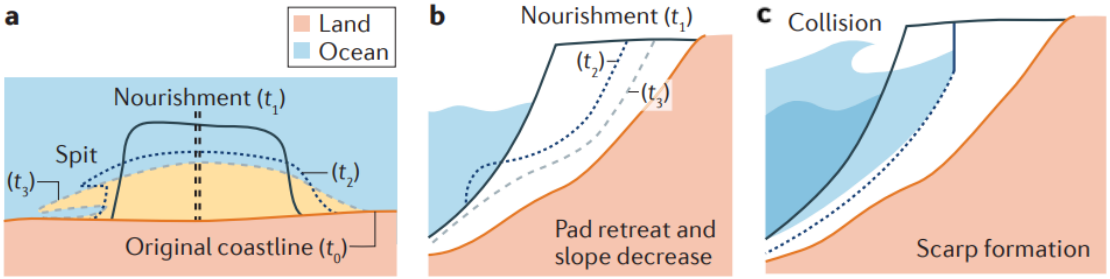

Figure 2.8: (a) Erosion of the beach nourishment, with possible spit formation; (b) Decrease of the slope of a nourishment after its construction; (c) The formation of a scarp. Retrieved from: De Schipper et al. (2020).

As beach nourishments are constructed within the MKL-zone, their effect is instantly felt in the coastal zone. After implementation, the nourishment volume decreases relatively fast through rapid erosion of the sand (Figure 2.8) (Brand et al., 2022). The erosion follows from the widening and steepening of the beach. The added sand locally enlarges the volume of the sediment body at a specific stretch of the coast, which acts as a large nearshore perturbation in the system. As a consequence, forcing conditions including waves, currents, wind are changed, thereby altering the sediment transport at the nourished site (Dean, 2002). Through both cross-shore and alongshore transport the disturbed beach will then readjust itself to restore its initial situation, so-called profile equilibration (Dean, 2002; Elko et al., 2005). Together with the hydrodynamic climate, the perturbation's 'amplitude and wavelength' in relation to natural scales determines the degree to which transport of the nourished sand occurs. In broad terms, greater sand transport takes place when the amplitude is larger, the wavelength is shorter, and when the hydrodynamic climate is more energetic (Hamm et al., 2002). The redistribution of a beach nourishment is thus strongly related to location and for instance, the strength of cross-shore and longshore currents. The grain size of the nourished sand also plays a role in the redistribution of a nourishment, it appears that finer sand is more easily picked up by the waves, implying that beach nourishments consisting of finer sand disappear quicker (De Schipper et al., 2020; Hamm et al., 2002). In contrast, nourishments with coarser sand lead to wider and steeper beaches that may persist longer (De Schipper et al., 2020; Dean, 2002). Often the development of a beach nourishment follows the so-called saw-tooth concept which describes gradual erosion until a threshold is reached (e.g. BKL-position), whereafter a peak in sedimentation occurs due to a nourishment with again gradual erosion after the beach nourishment. This is a common concept used to determine the lifetime of beach nourishments (Van Koningsveld & Lescinski, 2006).

A part of the sand is transported by the wind in landward direction to the dunes but mostly the sand disappears in seaward direction, whereby the sand usually first ends up in the lower MKL-zone but eventually erodes completely from this zone (Brand et al., 2022; De Schipper et al., 2020). The sand that is transported in longshore direction due to wave-driven currents can lead to accretion of adjacent beaches (Dean & Campbell, 2016). In the first months after the placement of a beach nourishment the

erosion rate is greatest and after one year up to 40-50% of the nourishment volume can disappear from the MKL-zone (Figure 2.9) (Brand et al., 2022). Storms are likely to exacerbate this process (De Schipper et al., 2020). Important to note is that the erosion rate does not remain constant, over time the erosion rate reduces and the process becomes more gradual, as shown in Figure 2.9. Brand et al. (2022) found that after about 2.9 years a beach nourishment along the Dutch coast is completely redistributed and the coastline is back to its original position before nourishing. In contrast, Van der Spek et al. (2007) reports a lifespan for beach nourishments of approximately 5 years. Thus, this suggests that there are large differences in lifespan across individual beach nourishments along the Dutch coastline, which is probably related to local conditions and the configuration of a particular nourishment.

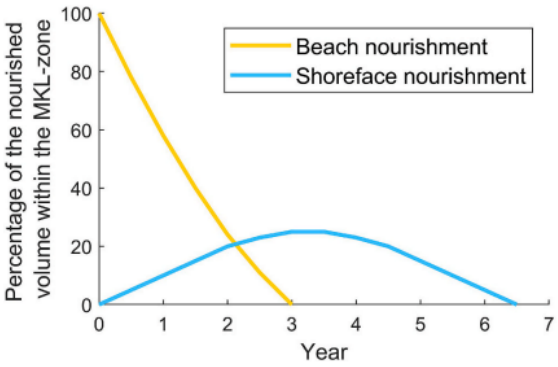

Figure 2.9: Evolution over time of the nourished sand volume within the MKL-zone (in %), for a beach nourishment and a shoreface nourishment. Retrieved from: Brand et al. (2022).

Previous experience with beach nourishments

There have been only a few studies on beach nourishments in the Netherlands, some examples will be discussed below.

Roelse (1996) evaluated five sections along the Dutch coast where between 1975 and 1994 several beach nourishments were performed. The locations included Ameland, Texel, North-Holland, Schouwen and Walcheren. At every location 3 to 6 nourishments were carried out during this period. Predominantly beach nourishments were constructed, sometimes in combination with a dune nourishment and in very few cases in combination with a shoreface nourishment. For every section he studied the development of the coastline and the volume changes in the MKL-zone over time. In addition, the effects of nourishments with regard to recreation, natural values and flood protection were examined. He found that overall beach nourishments proved to be an effective method to maintain the coastline at nearly all sites. At four of the five sites the sediment budget changed from negative to positive after nourishing. The only exception was Texel, where erosion was of such large proportions that it turned out to be cheaper to also make use of hard measures to counteract the erosion of the coastline. Roelse (1996) confirms that in the first years post-nourishing, rapid erosion of the nourished sand occurred. For instance, the volume of a beach nourishment carried out in Ameland in 1992 had been reduced by half after one year. Computations regarding the effectiveness of 10 beach nourishments showed that on average a nourishment appears to be effective for 80%. However, this can strongly vary per location, which is, among other things, mainly related to the accommodation space of the beach and the natural dynamics present at each location (Roelse, 1996).

Van der Wal (2004) studied the effect of a nourishment on beach-dune interactions along the Dutch coast. Over a 15-year period, the annual volume changes of the beach and the foredune were analysed for several locations along the coast. An important finding was that the beach nourishments in this study considerably contributed to sand deposition in the dunes. After the first year post-nourishing, a significant increase in sand transport to the foredunes could be observed, signified by the increased

deposition at the dune toe and in the foredunes. During this period, also more erosion of the beach occurred between +1 and +3 m NAP. During the second and third year, erosion of the nourishment in this area decreased, which coincides with the aforementioned fact that in the first year after a nourishment is carried out, most erosion takes place. Transport to the foredunes also decreased in the second and third year but still, until the fourth year the foredunes barely experienced erosion caused by storm surges. This shows that through beach nourishments the foredunes can be temporarily protected against the attack of waves. In the fourth year, the barrier that the nourishment provided was weakened and erosion of the foredune returned to its initial rate. A study by Van der Meulen et al. (2014) also looked at beach-dune interactions and they examined the creation of a new dune area through the construction of a beach nourishment along the Delfland coast as part of the so-called Delfland 'weak link' project. Similar results were found, whereby a significant amount of sand was transported into the dunes by aeolian processes after 4 years, making the area very dynamic.

Other research on the Delfland coast was carried out by Radermacher et al. (2018). They analysed 13 beach nourishments and found that the construction of a beach nourishment encouraged the development of sandbars. They attributed this phenomenon to the cross-shore sediment transport that occurs directly after a nourishment is placed in an attempt to restore the original beach profile.

Egmond-Bergen

The Egmond-Bergen coast is one the most heavily nourished coasts in the Netherlands and several studies have looked at the dynamics of nourishments in the proximity of Egmond-Bergen. At certain locations along the North Sea coast the lifespan of sand nourishments is very low, being so-called erosion hotspots, and these locations need to be nourished very regularly. Egmond aan Zee is considered to be such a location with rapid erosion of the coastline (Briere et al., 2008; Van Duin et al., 2004). From several studies it appears that the lifespan of nourishments near Egmond is very short, beach nourishments usually only persist for 1 or 2 years (Boers, 1999).

At the Egmond and the Bergen sites, the urban area behind the dunes is situated relatively close to the beach. In order to guarantee the safety of the hinterland, the BKL-position at Egmond-Bergen has been established further seaward than its original position (i.e. 1990 position). This takes into account that storm conditions with a probability of 1 per 500 years do not pose risks to the urban areas. However, to sustain the coastline at this seaward position, more frequent nourishing is required (Boers, 1999; Cohen & Brière, 2007).

Boers (1999) analysed beach nourishments at the location of Egmond-Bergen and tried to find an explanation for their limited lifetime. The study shows that wave-driven longshore currents at the Egmond-Bergen coast could play an important role in the redistribution of the nourished sand; transporting the sand to adjacent beaches. The further a nourishment protrudes in seaward direction, the larger the alongshore transport gradients can become. It was found that sand is also transported by cross-shore processes, partly through the presence of rip currents and horizontal circulation patterns which lead to a large mobility of the sand on the beach and foreshore (Boers, 1999; Van Duin et al., 2004). Van Duin et al. (2004) explain the presence of rip currents by bathymetric longshore irregularities in the coastline of Egmond-Bergen. Thus, previous studies report that both cross-shore and longshore processes seem to be involved in the short lifespan of beach nourishments at Egmond.

Wijnberg et al. (2007) made an effort to examine the response of a sand wave to the construction of a beach nourishment in the trough of a sand wave. As briefly mentioned in Section 2.1, sand waves can be seen as longshore migrating features along a coast, giving the coastline a wave-like appearance. They exist along the entire Dutch coastline. Based on Ruessink & Jeuken (2002) and Verhagen (1989) sand waves along the Holland coast typically have an alongshore wavelength in the order of 1 km, an

amplitude between 40-60 m, a period between 75-100 yr, and a celerity with which they migrate of 0-200 m/yr. Note that this periodicity is largely in contrast to the periodicity of 10-15 yr reported by Guillén et al. (1999). After the beach nourishment was placed, the sand wave near Egmond showed an increase in its amplitude after about half a year but also decreased again in the years after (Wijnberg et al., 2007). However, there have been ample studies on the interactions between sand waves and beach nourishments in the Netherlands, therefore, this still requires more research.

In an attempt to increase the lifespan of beach nourishments near Egmond, it was tried several times to combine a beach nourishment with a shoreface nourishment. Spanhoff et al. (2004) studied two combinations of a beach and shoreface nourishment, one took place in 1999 near Egmond and the second one in 2000 near Bergen. Their findings indicate that it seems that the underwater nourishments extended the life of the beach nourishments. Cohen & Briere (2007) came to a similar conclusion for a combined beach-shoreface nourishment in 2004/2005 but they do state that for a shoreface nourishment to have a stabilising effect on a beach nourishment, the shoreface nourishment is required to have a certain geometry and minimum volume, on which they could not draw conclusions yet. Boers (1996) attributes the stabilising effect of a shoreface nourishment to its wave-damping function. This could also lead to a change in the patterns of rip currents at the site, however, this remains to be largely unknown. There are still many uncertainties about this combined type of nourishing (Boers, 1999; Van der Spek et al., 2007). Too little time has passed to be able to draw clear conclusions about the effectiveness of these projects.

2.3.2 Shoreface nourishments

Design and behaviour

Besides beach nourishments, shoreface nourishments are also regularly applied at the Dutch coast. Shoreface nourishments are a relatively novel type of nourishing, they only emerged in the early nineties. Therefore, knowledge on their typical morphodynamic behaviour is still uncertain.

Similarly to beach nourishments, shoreface nourishments aim to increase the sand volume in the MKL-zone to protect the coastline against erosion. Though, shoreface nourishments are performed in a different way than beach nourishments. Shoreface nourishments are constructed below the MKL-zone, generally their crest is at -5 m NAP, where they are considered to be most efficient and result in the quickest readjustment of the coastal profile (Brand et al., 2022; Van der Spek et al., 2007). Shoreface nourishments do not have a direct effect on the beach and MKL-zone after their placement, it generally takes one year to see a 10% increase in the volume of the MKL-zone and it takes a few more years to see the maximum increase of approximately 20-30% (Figure 2.9) (Pwa & Nieboer, 2006). The lifespan of shoreface nourishments differs from beach nourishments, shoreface nourishments can persist for 4-10 years so their influence on the coast is present over a longer period of time (Brand et al., 2022; Pwa & Nieboer, 2006; Vermaas et al., 2021). In research of Huisman et al. (2019) larger shoreface nourishments still contained 40-80% of their initial volume after three years. Van Duin et al. (2004) found similar results, where the studied shoreface nourishment was still intact for 45% after three years had passed. As shoreface nourishments are also less costly than beach nourishments (Table 2.2) and have similar contributions as beach nourishments to coastal maintenance and to the goal of nourishing 12 mln.m^3 sand per year, they can be considered to be more cost-effective than beach nourishments. Because of this, shoreface nourishments are nowadays preferred over beach nourishments. They also lead to less disturbance of the beach in contrast to beach nourishments (Brand et al., 2022; Pwa & Nieboer, 2006). Typically, shoreface nourishments are 4 km in length and on average their volume amounts to 450 m^3/m. When their volume is larger, shoreface nourishments tend to persist longer (Vermaas et al., 2013). Similar to beach nourishments, the design of shoreface nourishments is adapted to their natural surroundings to prevent side effects. This means that shoreface nourishments also contain tapered edges in longshore direction, whereby the volume at both edges gradually diminishes (Brand et al., 2022).

Positive effects of a shoreface nourishment can extend up to 2 km in longshore direction from each side of the shoreface nourishment (considering a 3 km long nourishment) (Van der Spek et al., 2007). Sand is transported by both cross-shore and alongshore processes from a nourished shoreface, however, because shoreface nourishments are placed underwater and a bit seaward from the coast, additional processes come into play that further complicate their behaviour. Cohen & Briere (2007) and Van Duin et al. (2004) both hypothesise two processes responsible for the accretion of a beach after a shoreface nourishment. First of all, the shoreface nourishment is expected to act as a sort of submerged berm or wave filter for incoming waves. This is called the 'lee-effect' (Figure 2.10a). Large waves are supposed to break at the nourishment, by which a milder wave climate is created shoreward of the nourishment. As a consequence of the remaining smaller waves, the longshore current diminishes in strength in the lee of the nourishment. This leads to a decrease in sand transport directly behind the nourishment, causing an updrift accretion of sand. However, a side effect encompasses downdrift erosion of the coast because downstream of the nourishment the longshore current increases in strength again. Secondly, a cross-shore effect can be present that has the potential to generate onshore transport. While large waves already break at the seaward side of the nourishment, other smaller waves are shoaling across the nourishment and lead to onshore transport due to wave non-linearity. Moreover, the less energetic waves also create less stirring of the sand in the lee of the nourishment and they reduce the return currents that occur on the sides of the nourishment, diminishing the

offshore transport of sand. This is called the 'feeder effect' (Figure 2.10b) (Van Duin et al., 2004). In their conclusions, Van Duin et al. (2004) confirm that both the lee and the feeder effect seemed to have played a role in the redistribution of sand after analysing a shoreface nourishment near Egmond with two process-based models in combination with bathymetric data between May 1999 to April 2002.

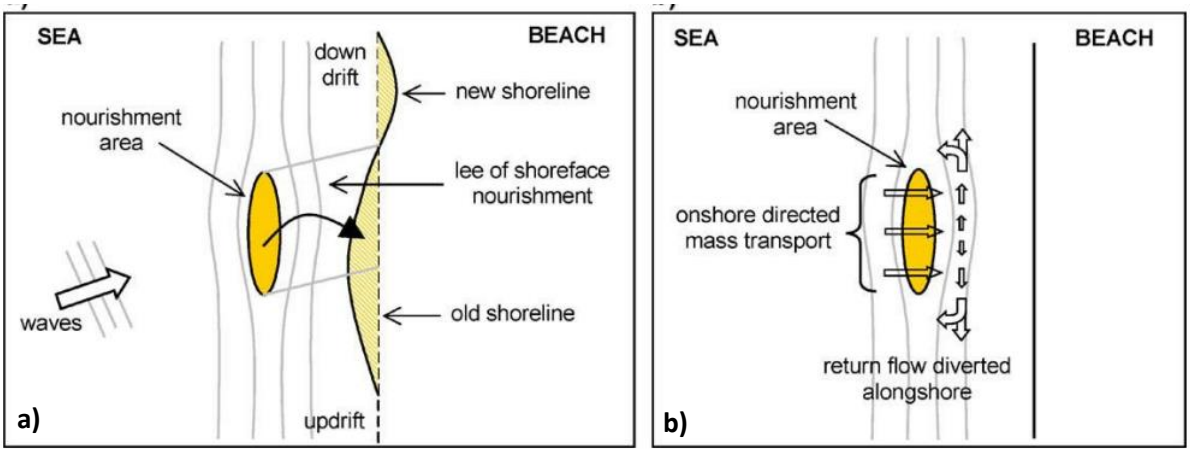

Figure 2.10: Possible alongshore (left) and cross-shore (right) effects of a shoreface nourishment. Retrieved from: Cohen & Brière (2007).

Huisman et al. (2019) further elaborate on the behaviour of shoreface nourishments after studying 19 individual shoreface nourishments carried out along the Dutch coast, based on bathymetric data and numerical model simulation. One of their main findings includes the fact that significant cross-shore profile change was observed in response to a shoreface nourishment, while any longshore changes were less pronounced. The hydrodynamic processes and inferred erosion rates influencing the shoreface nourishments were evaluated with a numerical model. In their modelling results, 60 to 85% of the erosion from the shoreface nourishments was the result of onshore transport. Especially in the middle part of a nourishment the model showed that onshore mass transport was produced by currents driven by water-level setup (e.g. rip currents) and by enhanced velocity asymmetry of the waves across the nourishment (Figure 2.11), as Van Duin et al. (2004) also stated. Huisman et al. (2019) also add that erosion of the nourishment mainly occurred when the waves were more energetic and breaking ($H_{m0} \geq 3$ m). The dominance of the cross-shore transport was expressed by a change in the shape of the shoreface nourishments. After one year, shoreface nourishments often possessed a 'triangular' landward protruding shape, as the result of onshore sand transport to the 'nourishment crest'. Usually after two to four years, the sediment is depleted from the seaward side of the shoreface nourishment, whereafter the onshore transport becomes less strong (Huisman et al., 2019).

Alongshore transport contributed much less to the erosion of the considered shoreface nourishments, only 15 to 40% of sand was lost by alongshore transport. Alongshore transport took place at the seaward side of the shoreface nourishment when storm conditions were present ($H_{m0} \geq 3$ m), as waves were required to be breaking and obliquely incident at the nourishment for a current to develop. Important to note is that the geometry of a shoreface nourishment influences the erosion rate. Shorter nourishments experienced relatively more erosion and more impact of longshore currents than longer ones (Huisman et al., 2019).

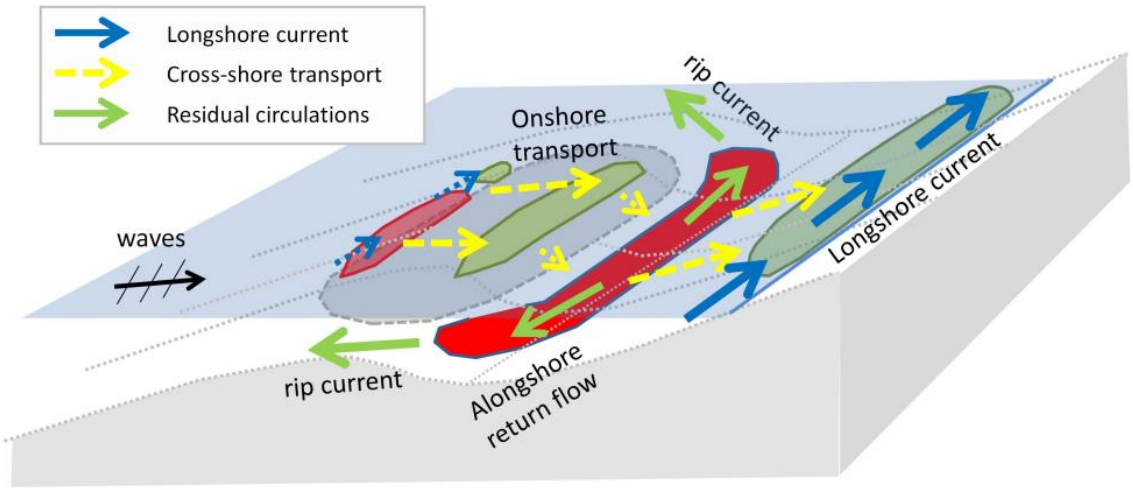

Figure 2.11: Processes responsible for the redistribution of sand in a shoreface nourishment. Green = sedimentation, Red = erosion. Retrieved from: Huisman et al. (2019).

Furthermore, landward of most shoreface nourishments a trough developed. A portion of the sand eroded from this trough was transported onshore and deposited in the shallower nearshore region. According to the model, the rest of the eroded sediment was brought offshore by rip currents on the lateral sides of the nourishments when incoming waves were shore-normal to mildly oblique (Figure 2.11). The offshore directed rip currents on the lateral sides of the shoreface nourishments also explain why next to the nourishments almost no sedimentation occurred. After approximately three years, when onshore transport diminished, the trough was filled up again and sedimentation of the nearshore decreased. Wave shielding or filtering, also described by Van Duin et al. (2004), also seems to have contributed to the accretion in the nearshore zone through a local decrease in the alongshore transport. However, Huisman et al. (2019) state that this latter effect could only have been present during energetic wave conditions. Overall, shoreface nourishments seem to affect the coast the most during storm conditions, during which they protect the coast from storm erosion by acting as a sub-tidal buffer volume (Huisman et al., 2019). Quartel & Grasmeijer (2007) roughly come to a similar conclusion, whereby they state that shoreface nourishments primarily have a protective function to the beach and to a lesser extent a feeding effect.

Previous experience and sandbar response to shoreface nourishments

Although this study does not focus on bar behaviour in response to a shoreface nourishment, still this section gives a short review of subtidal sandbar response to shoreface nourishments because they can have important interactions with each other, also relevant for the evolution of a shoreface nourishment and the accretion of the shoreline. In addition, in this section relevant case studies on the effects of individual shoreface nourishments on the shoreline are given, including Egmond-Bergen.

Ideal locations for the placement of shoreface nourishments include stretches of the coast where subtidal sandbars are present, such as near Egmond-Bergen. The placement of a shoreface nourishment can disturb the natural net offshore directed cycle of bar growth and decay, as shown by several studies (e.g. Grinten & Ruessink, 2012; Grunnet & Ruessink, 2005; Ojeda et al., 2008; Van Duin et al., 2004). Important to note is that for a shoreface nourishment to affect bar migration, it must be of the same order of magnitude as the subtidal bars (Van der Spek et al., 2007). Grunnet & Ruessink (2005) studied bar behaviour at the Dutch barrier island of Terschelling after a shoreface nourishment was carried out in the trough between the middle and outer bar in 1993 (Figure 2.12). They found that initially, the bar system adapted relatively fast to the nourishment by forming a new trough and

integrating the nourished sand, that is, in about half a year. Though, after this first period, adjustments occurred in a more gradual manner and only after 6 to 7 years the full bar-trough morphology was completely restored. In these 6 to 7 years a significant impact on the autonomous bar behaviour could be seen. Cross-shore bar development, including their migration, ceased for multiple years whereby the bars did no longer change in height, width, depth and volume, except for natural fluctuations. Moreover, the shoreface nourishment positively affected the shoreline position near Terschelling, as the shoreline retreat was temporarily reverted to shoreline advance for about 6-7 years. However, during the implementation of the nourishment also sand waves appeared in the study area perturbing the nearshore zone. These sand waves resulted in a similar expansion of the shoreline as was observed in the nourished area, consequently, it is still debated if the reported shoreline advance in the nourished area could be attributed to the actual shoreface nourishment or that the appearance of sand waves also played a large role (Grunnet & Ruessink, 2005).

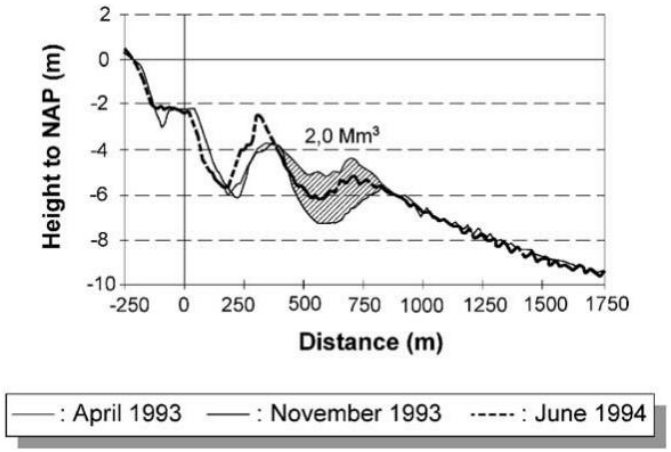

Figure 2.12: The placement of the shoreface nourishment at Terschelling between the middle and outer bar in 1993. A total volume of 2 Mm3 of sand was used to construct the shoreface nourishment. Retrieved from: Hamm et al. (2002).

At Noordwijk, a shoreface nourishment was placed at the seaward side of the outer bar in 1998. After construction, the nourishment started migrating towards the coast and approached the outer bar. During the entire period, it moved approximately 300 m onshore. Although the shoreface nourishment moved shoreward, the portion of the subtidal bars that were affected by the nourishment did not and came to a halt in their migration. The latter also led to bar switching events, as described in Ojeda et al. (2008). In contrast to Grunnet & Ruessink (2005), the shoreface nourishment at Noordwijk aan Zee in 1998 did not result in shoreline advance, neither did it alter the trend in shoreline position (Ojeda et al., 2008).

Besides the complete stop in bar migration that may take place after a shoreface nourishment, the cross-shore bar cycle can even be reversed from seaward migration to landward migration (e.g. Van Duin et al. 2004), in particular, if the outer bar is still present and the shoreface nourishment is positioned against it (Van der Spek et al., 2007). This sometimes leads to sediment accretion in the shallow nearshore zone, on the beach and in the dunes (Van der Spek et al., 2007).

At the Delfland coast different subtidal bar behaviour was documented by Radermacher et al. (2018) than was found in other coastal sections, which were for example studied by Grunnet & Ruessink (2005), Grinten & Ruessink (2012), and Ojeda et al. (2008). After their placement, shoreface nourishments at the Delfland coast started migrating with 20 to 60 m/year to the shore, compelling existing sandbars to also shift towards the shore at a fast pace. Because of their onshore migration, this

even resulted in bar attachment to the beach for most shoreface nourishments. This is in contrast to the other coastal sections (e.g. Terschelling, Noordwijk, Egmond) where either an arrest in bar development was detected, or at most, only some slight onshore bar migration. Most of the shoreface nourishments themselves also stayed put in their initial location, whereas at Delfland these experienced rapid onshore migration (Radermacher et al., 2018).

Egmond-Bergen

Van Duin et al. (2004) studied a large shoreface nourishment (combined with a beach nourishment) implemented at Egmond in 1999 at the seaward side of the outer bar (Figure 2.13). Based on bathymetric data, they found that in the first two years the nourishment stayed roughly the same size, with very little redistribution of the sand. This was presumably related to the large scale of the nourishment, leading to little or no interaction with the morphodynamic system. The sand nourishment also remained at the same location during the entire nourishment period. At the same time, the bars did show change as a response to the nourishment, substantial onshore migration could be seen whereby a trough developed between the nourishment and the outer bar. The onshore migrating bars also increased in height. The nourishment itself remained at its initial cross-shore position and presumably started acting as the new outer bar. The shoreface nourishment did have a positive effect on the sediment budget in the surf zone, however, it had barely any effect on the beach width at Egmond. Van Duin et al. (2004) attribute this phenomenon to the disappearance of the nourished sand before it could end up at the beach.

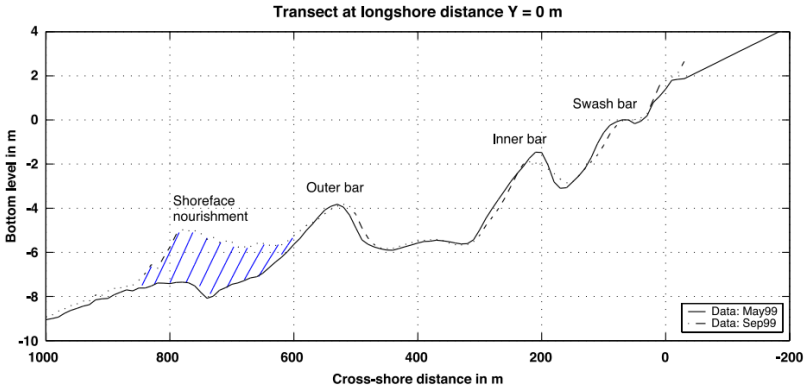

Figure 2.13: Cross-shore location of the shoreface nourishment at Egmond constructed in 1999. Retrieved from: Duin et al. (2004).

Another shoreface nourishment was implemented at Egmond in 2004, which was studied by Cohen & Brière (2007). This shoreface nourishment had a length of 4 km and was almost twice as long as the shoreface nourishment in 1999. This shoreface nourishment was combined with a beach nourishment, which was carried out in 2005. They observed that the shoreface nourishment of 2004 positively influenced the sediment budget in the MKL-zone during a longer time period than the nourishment in 1999. The authors suggested that this was related to the larger volume and length and the calmer wave climate present during the second shoreface nourishment. In terms of bar behaviour: the outer bar showed a temporal arrest in its migration, while the middle bar started migrating in onshore direction. Moreover, the effect of the shoreface nourishment on the bars was not limited to the nourished area but also extended at least 2 km south from the shoreface nourishment (Cohen & Brière, 2007).

Comparison of shoreface nourishments

Effect on shoreline position

Most shoreface nourishments are thus implemented either at the seaward face of the outer bar or seaward of the zone of decay (Brand et al., 2022; Radermacher et al., 2018; Van der Spek et al., 2007).

Both the shoreface nourishments at Noordwijk and Egmond were placed against the seaward part of the outer sandbar and barely resulted in sedimentation of the beach. However, at Terschelling considerable shoreline advance took place after a beach nourishment was placed between the middle and outer bar, though, there are still some doubts if the shoreline advance was the result of the nourishment itself or from the appearance of a sand wave. The difference in effect on the beach may thus be associated with the cross-shore position of the shoreface nourishment, but this is not entirely certain. Van Duin et al. (2004) proposed that the lack of beach accretion might be related to the diffusion of the nourished sand before it could even reach the beach. Ojeda et al. (2008) further add that the increase in height of the middle bar at Terschelling could have enhanced the lee effect, whereas at Egmond and Noordwijk this was not the case.

Nourishment migration

Furthermore, differences in the migration of the nourishment itself were also apparent. At Egmond the nourishment stayed in its initial cross-shore position, while at Delfland and Noordwijk the shoreface nourishments showed onshore migration. Bruins (2016) investigated this behaviour and came to a possible conclusion that shoreface nourishments, similar to subtidal bars, migrate to the zone of decay. Consequently, if a shoreface nourishment is placed seaward of the zone of decay, it will start migrating onshore until it reaches this zone (e.g. Noordwijk). And if the nourishment is placed landward of the zone of decay, the opposite occurs and the nourishment will migrate offshore. A shoreface nourishment implemented at the zone of decay will remain at this location without migrating, such as at Egmond. It further appears that the total volume, length and volume per metre (m^3/m) of a shoreface nourishment exert no influence on this behaviour. Important to note is that a larger volume per metre did result in enhanced accretion of the MKL-zone.

Lifespan

After a few years the bars returned to their natural behaviour at all coastal stretches but at some locations the shoreface nourishments persisted longer than at other locations. For example, at Noordwijk the effects of a shoreface nourishment were visible for the longest time period. After 6 years, the bar system still did not show any signs of returning to its autonomous behaviour (Ojeda et al., 2008). At Terschelling the shoreface nourishment remained in place for approximately 6-7 years (Grunnet & Ruessink, 2005), whereas at Egmond the nourishment only influenced the bars for 2-3 years (Van Duin et al., 2004). Ojeda et al. (2008) give three plausible reasons for the longer lifespan of the Noordwijk nourishment: 1) the more seaward position of the nourishment, whereas at Egmond and Terschelling the nourishments were located more onshore; 2) the larger grain size of the nourished sand, presumably causing smaller onshore transport rates; 3) the larger size of the nourishment in respect to the sandbars (Table 2.3). The latter is relevant because sandbars are typically of a smaller scale at the Noordwijk site compared to the other two sites, while the relative volume in m^3/m was greatest at Noordwijk (Ojeda et al., 2008).

Table 2.3: Length, total volume, relative volume and grain size for the aforementioned shoreface nourishments implemented at Terschelling, Noordwijk and Egmond. Adjusted from: Ojeda et al. (2008).

Location	Year	Length (km)	Total Volume Mm^3	Volume (m^3/m)	D50 (µm)
Terschelling	1993	4.6	2.0	435	194-207
Noordwijk	1998	3.0	1.7	570	±400
Egmond	1999	2.2	0.9	400	±228

3. Objective and research questions

3.1 Problem description

Most of the aforementioned studies only looked at the short-term effects of one or two nourishments per location at the time in their research on relatively small spatial scales (e.g. Huisman et al., 2019; Ojeda et al., 2008; Van Duin et al., 2004; Wijnberg et al., 2007). These studies did gain a decent insight into the temporary effects of individual beach and shoreface nourishments on, for example, the development of the beach, dunes and behaviour of subtidal sandbars. However, none of them investigated the longer-term influence of repeated sand nourishments on the shoreline. Therefore, the effects of repeated sand nourishments on the dynamics and long-term temporal trends of the shoreline are still largely unknown. As sand nourishments often have to be repeated in locations that are subject to structural erosion of the coastline, this poses a clear need to increase the understanding on the effects of repeated sand nourishments on the spatiotemporal evolution of the shoreline. This is further stressed by the expectation of nourishment efforts to considerably increase in the future considering global climate change and the accompanying sea level rise (Deltacommissie, 2008). Furthermore, multiple studies investigated the behaviour and effects of individual nourishments but only on a typical timescale of years, with the obtained data mainly comprising of annual bathymetric measurements (e.g. de Sonneville & Van der Spek, 2012; Grunnet & Ruessink, 2005; Van Duin et al., 2004). Therefore, knowledge is still limited on which timescales nourishments change and disappear (storms, seasons, years). This also includes whether the nourished sand of (repeated) beach and shoreface nourishments diffuses alongshore to adjacent, non-nourished beaches or that it rather stays put in its initial location.

For the Netherlands, over 30 years of regular satellite data is now available to the public. Nowadays, with the gradual increase in the satellite revisit period (every 16 or 5 days in the last years), it is possible to investigate the dynamics of the shoreline and the effects of repeated beach and shoreface nourishments on timescales ranging from seasonal to years to even several decades, but also on the single event timescale (Vos et al., 2019a). Additionally, the global coverage of satellite imagery allows for the analysis of shoreline dynamics on much larger spatial scales compared to previous studies, making it possible to address the abovementioned knowledge gaps (Vos et al., 2019a).

3.2 Objective and research questions

The objective of this thesis is to quantify and obtain a better understanding of shoreline dynamics and the underlying drivers of change, specifically for high-energy, storm-dominated coasts that are repeatedly nourished. The knowledge acquired from this research can aid in the development of future coastal policy and help validate and improve the current shoreline evolution models, especially in view of global climate change (Brand et al., 2022). Moreover, the results of this study can contribute to the design and implementation of future nourishment projects. The main goal of this thesis is described by:

“To increase the understanding of shoreline dynamics for high energetic, low-sloping, repeatedly nourished beaches.”

To address the main objective, this research will focus on the coast of Egmond-Bergen in the Netherlands over a time span of 1985 - present. The Egmond-Bergen coast is chosen for this research as it is one of the most heavily nourished stretches of the Holland coast. While usually, beach nourishments have a lifespan of about 5 years along the Dutch coast, near Egmond-Bergen nourishments only last for 1 or 2 years (Boers, 1999; Brand et al., 2022). This can be attributed to the rapid erosion of the coastline near Egmond, and therefore, several authors have identified Egmond as a significant ‘hotspot’ for erosion. To the south of Egmond, near Castricum, beaches remained unnourished.

Two research questions have been defined to study the Egmond-Bergen coast, which are described below.

Question 1: What is the temporal variability in shoreline position that can be observed along Egmond-Bergen?

- What are temporal trends (storms, seasons, long-term trends) in shoreline position along Egmond-Bergen?
- What is the relative importance of these time scales of change (storms, seasons, long-term trends) for shoreline dynamics along Egmond-Bergen?

Question 2: How do beach and shoreface nourishments affect shoreline dynamics along the coast of Egmond-Bergen on a spatial scale and what are the typical dynamics of a beach nourishment?

- What are the spatial changes in shoreline position and dynamics along the coast of Egmond-Bergen as a response to the implementation of repeated nourishments and how does a beach nourishment compare to a shoreface nourishment in that matter?
- What is the impact of repeated beach and shoreface nourishments near Egmond-Bergen on nearby non-nourished beaches?
- In what manner and on which timescales are beach nourishments completely redistributed at the coast of Egmond-Bergen?

The first research question aims to unravel the temporal variability in shoreline position along Egmond-Bergen to first create a more general overview of shoreline dynamics for the site for the nourished and unnourished beaches. Then, with the second research question, the effect of beach and shoreface nourishments on the shoreline is assessed on a spatial scale, whereby also the effects on a nearby natural non-nourished beach are investigated. Lastly, with the second question also the typical behaviour of beach nourishments along the coast of Egmond-Bergen is analysed.

4. Study site

In this chapter a description of the Holland coast will be given and light will be shed on the setting of the Holland coast, the hydrodynamics and its characteristics, whereafter the Egmond-Bergen coast will be introduced within the setting of the Holland coast. Lastly, the nourishment practices at Egmond-Bergen will be described.

4.1 Holland coast

4.1.1 Setting

The Holland coast is situated along the central part of the Dutch coast and is about 120 km long. In total the Dutch coast has a length of 432 km (Stolk, 1989). Its primary defence against coastal flooding comprises of sand dunes, protecting about 75% of the coastline, but hard structures are also used (15%), and about 10% of the coastline consists of tidal flats (Brand et al., 2022; Ministerie van Verkeer en Waterstaat, 2000). The closed central or Holland coast has an almost uninterrupted strip of dunes (Brand et al., 2022; Guillén et al., 1999; Van Rijn, 1995). The Holland coast is the region defined between the Marsdiep, a tidal inlet in the north, and the harbour jetties of Rotterdam in the south, where the Rhine flows into the North Sea. The Holland coastline has a slightly curved shape and has an orientation of NNE-SSW (Wijnberg, 2002). At several locations man-made structures are present, including sluices and harbour jetties, which interrupt the coastline at IJmuiden, Scheveningen and Hoek van Holland (Brand et al., 2022). Furthermore, the Hondsbossche and Pettemer seawall a bit south of Den Helder (between 20-26 km) acts as a barrier to counteract the effects of wave attack in this coastal stretch (Van Rijn, 1995). In 2014-2015 this seawall was reinforced with 35 million m^3 of sand placed on the seaward side of the dike and it was renamed to the 'Hondsbossche dunes' (Wittebrood et al., 2018).

In Figure 4.1 a part of the Holland coast is shown with the location of the Hondsbossche and Pettemer seawall/dunes and the harbour of IJmuiden.

4.1.2 Hydrodynamics

The Holland coast can be considered as a wave-dominated coast with a micro-tidal regime. The tide is semi-diurnal with a mean tidal range of 1.6 m (Van Rijn, 1995), during neap tide the tidal range amounts to approximately 1.4 m while during spring tide the tidal range amounts to 1.8 m (Ojeda et al., 2008). From the south near Hoek van Holland to the north near Den Helder a small increase in tidal range can be witnessed from 1.4 m to 1.7 m (Van Rijn, 1995). The tide is asymmetric, whereby the rise of the tide occurs faster than the falling of the tide (Wijnberg, 2002). During flood a northward-directed current is generated along the shore with a maximum velocity of about 0.8 m/s (during spring tide), while during ebb a southward-directed current is generated with lower current velocities that are at maximum 0.7 m/s. This discrepancy in maximum velocities induces a northward-directed residual current along the Dutch coast (Van Rijn, 1995). The typically moderate waves approaching the Holland coast are characterised by a mean wave height of 1.1 m. Van Rijn (1995) reports that waves that entered the breaker zone typically have a height of 1 to 1.5 m with a period of about 5 s. Offshore waves with a larger height than 2 m are detected approximately 10% of the time. Only 2% of the time, waves exceeding a height of 3 m appear in the offshore zone. Waves primarily come from the southwest and the northwest. Both wind-sea and swell waves arrive at the Holland coast, however, the geometry of the North Sea basin only allows swell waves to enter the North Sea from the northwest. The highest waves also tend to come from the northern directions as this part of the North Sea basin provides a longer wind-fetch (Van Rijn, 1995; Wijnberg, 2002). During storms from the northwest, wave heights can become as large as 5 m with periods between 5 to 8 s. In these cases, it is common for storm surges to attain values as high as 1 m (Ojeda et al., 2008). Generally, during summer lower wave heights occur, while generally during winter waves are larger (Van Rijn, 1995).

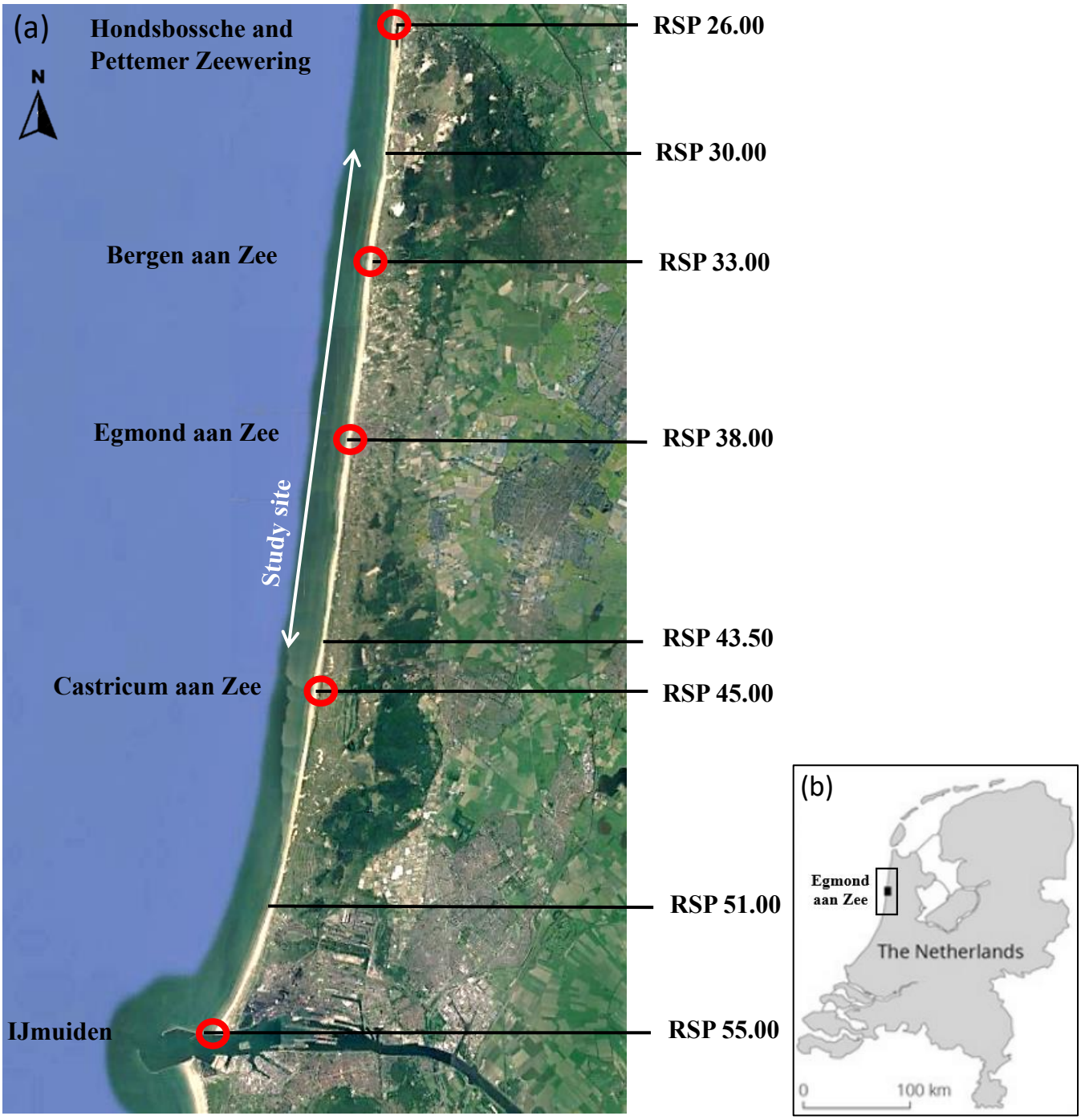

Figure 4.1: (a) Northern part of the Holland coast and the location of the study site. The red RSP points represent important points on the RSP reference line; (b) Overview map of the Netherlands with the extend of the study area indicated in the box.

4.1.3 Characteristics

Along the Holland coast a sequence of multiple alongshore bars is often present on the shoreface. The number of subtidal bars can vary but typically two to three subtidal bars exist (Brand et al., 2022). The subtidal bars along the Holland coast are dynamic and show cyclic behaviour, whereby the bars migrate net offshore until eventually the outer bar decays, triggering the formation of a new bar on the landward side of the breaker zone (Quartel & Grasmeijer, 2007; Spanhoff et al., 2004) (see Chapter 2.1.2). The duration of this cyclicity varies between 4 to 15 years along the entire Dutch coastline. The intertidal zone is also characterised by bars, which are considered to be more dynamic than subtidal

bars since these are strongly influenced by storm events (Quartel & Grasmeijer, 2007). The beaches along the Holland coast are usually around 300 m in width, having a slope of around 1:50 (Brand et al., 2022; Stolk, 1989). Furthermore, shoreface slopes are approximately 1:400 in the northern and southern parts of the Holland coast. In the central part of the coast steeper shoreface slopes are found, such as a shoreface slope of 1:260 near IJmuiden and a slope of 1:136 near Egmond (Stolk, 1989). The sediment contained within the shoreface typically has a grain size of 125-250 µm. However, in the coastal stretch north of IJmuiden also slightly larger grain sizes ranging between 250-500 µm occur. On the beaches of the Holland coast, grain sizes are mostly between 250-300 µm. The grain size thus slightly increases in the landward direction, which was also reported by Stolk (1989). He states that especially at IJmuiden this seaward fining trend is clearly observable. It is important to note that in coastal stretches where sand nourishments are carried out, the local variation in grain size can be relatively large (Stolk, 1989).
Furthermore, along the entire length of the Holland coast a natural dune area is present, except for the artificially placed Hondsbossche dunes, that protects the hinterland from flooding (Brand et al., 2022). As mentioned, a system of beach poles spaced 250 metres apart are permanently positioned on the beach along the whole length of the Dutch coastline (so-called Rijksstrandpaallijn or RSP), to serve as a reference line for the monitoring of coastal change (Wijnberg, 2002).

4.2 Egmond-Bergen coast

4.2.1 Setting

As mentioned, this study will focus on a stretch of the Dutch Holland coast located in front of Egmond and Bergen aan zee, both being small villages in the province of Noord-Holland. The study area comprises of approximately 13.5 km of coastline between RSP 30.00 and 43.50 (Figures 4.1 and 4.2). A little further to the north of this study area the Hondsbossche and Pettemer seawall is present. In the south, the study area is bounded by the town of Castricum aan Zee (Figure 4.1). The coastal stretch near Egmond and Bergen is, on a larger scale, characterised by a relatively alongshore-uniform coastline. However, when looking at a smaller longshore scale, there are also some longshore irregularities to be observed. In the order of km, the coastline shows a rhythmic alternation of 'accreting' and 'erosional' features, giving the coastline a wave-like appearance. This may be referred to as a shoreline sand wave (Guillén et al., 1999; Van Duin et al., 2004; Wijnberg et al., 2007) (see Chapter 2.3.1). Typically, three sandbars exist in the coastal profile of Egmond and Bergen, with two breaker or subtidal bars existing in the surf zone and one swash bar in the intertidal zone (Van Duin et al., 2004). The bar cycle of bar decay and bar formation is about 15 years for Egmond (Spanhoff et al., 2004). The alongshore sandbars in the system are sometimes interrupted by rip channels (Cohen & Brière, 2007). The Egmond-Bergen coast is generally characterised by the Longshore Bar Trough (LBT) beach state with the inner bar being more downstate than the outer subtidal bar (Short & Aagaard,

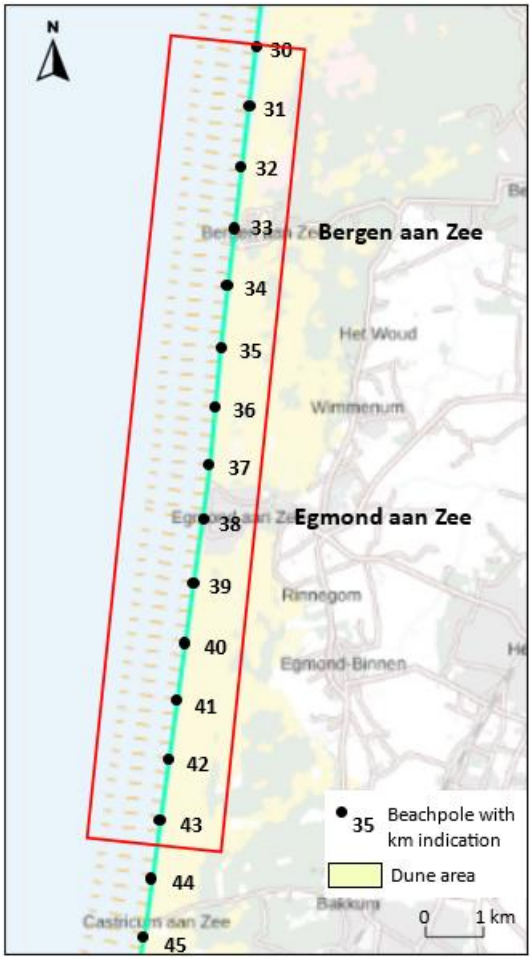

Figure 4.2: More detailed map of the study site. The red box represents the extend of the study area. Beach poles are also depicted, forming an alongshore reference line with km indication in respect to the most northern point of the Holland coast.

1993). The beach within the study area is on average 100 to 125 m in width and the intertidal beach slope varies between 1:30 and 1:50 m. In the immediate surroundings of Egmond no human-made constructions are present (e.g. sluices, jetties) (Cohen & Brière, 2007; Stolk, 1989). As mentioned above, the shoreface in front of Egmond has an average slope of 1:136, which is the steepest shoreface slope for the Holland coast. However, in the rest of the study area, north and south of Egmond, shoreface slopes are less steep and amount to approximately 1:237 and 1:219 for Bergen and Castricum respectively. The average grain size of the beach in the study area is 295 µm. The grain size becomes smaller in seaward direction: approximately 400-500 m offshore of the waterline grain sizes still range between 200 and 300 µm, while further offshore (e.g. 1 km offshore) grain sizes of only 100-200 µm are present.

In Figure 4.3, measurements of significant wave height and wave direction between 2015 and 2022 are shown through a wave rose. Measurements of the wave conditions during this period were carried out every 10 minutes at the measurement location IJmuiden Munitiestortplaats, which is located to the south of the study area, approximately 25 km offshore of IJmuiden. Mean significant wave height during this period was 1.17 m and the mean significant wave period amounted to 5.46 s. As can be clearly seen, the Holland coast is characterised by a wave climate where the majority of waves are coming from the northwest and southwest directions.

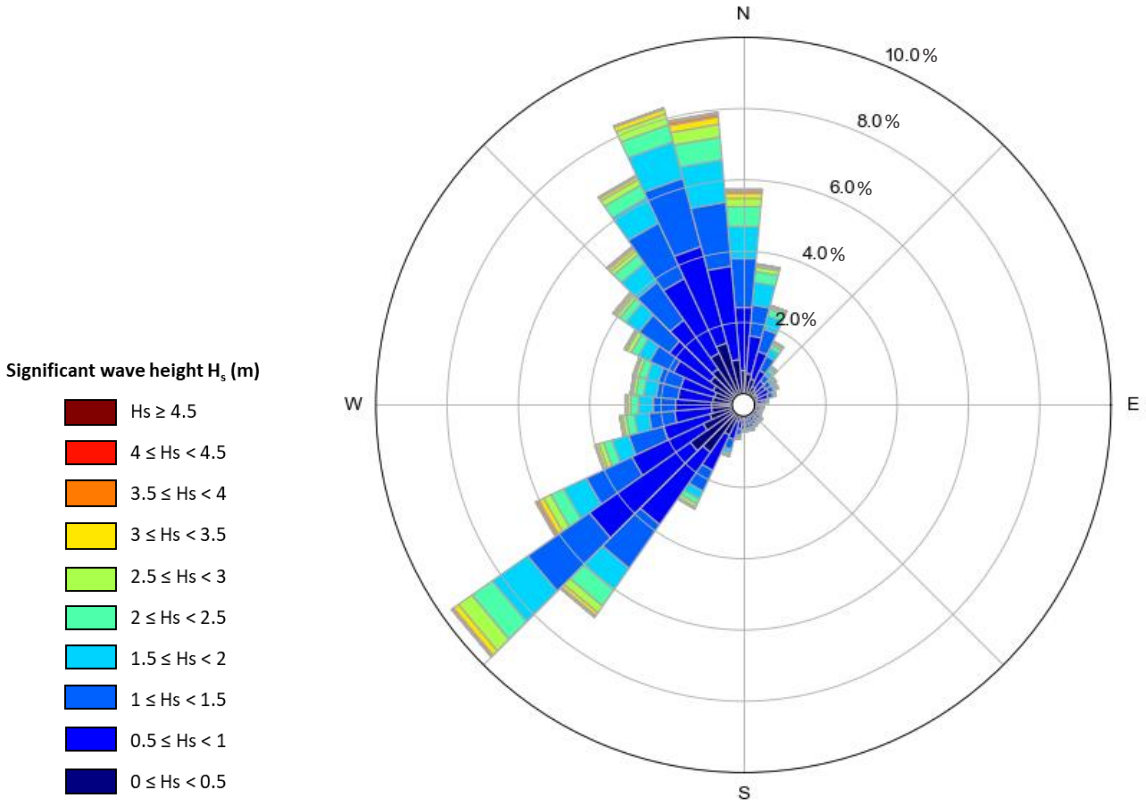

Figure 4.3: Wave rose from wave measurements at IJmuiden Munitiestortplaats for the period of 2015-2022. The measurement station IJmuiden Munitiestortplaats is located approximately 25 km offshore from IJmuiden.

4.2.2 Nourishment practices

Egmond aan zee is considered to be one of the most heavily nourished parts of the Holland coast. Different authors refer to the stretch of coast in front of Egmond as a significant 'hotspot' for erosion, including Van Duin et al. (2004) and De Sonneville and van der Spek (2012). Because the BKL-position of the coastline near Egmond and Bergen is located more in seaward direction than was originally

calculated for the 1990 position, more frequent nourishing is necessary to sustain the coastline (Boers, 1999). Nourishments implemented near Egmond and Bergen only have a lifespan of 1 or 2 years most of the time, in contrast to the rest of the Dutch coast where beach nourishments can last for 5 years (Boers, 1999; Brand et al., 2022; Van der Spek et al., 2007). Within the study area, the area that is heavily nourished comprises of the coastline roughly between RSP 30.00 and 40.00. The other half of the study area between RSP 40.00 and 43.50, south of Egmond, is much more stable and does not experience coastal erosion. Therefore, this stretch of coast has barely received any nourishments and can be seen as a 'natural' unnourished coast. The study area can thus be separated into two distinct parts of coastline: the northern heavily nourished coast and the southern unnourished coastline, which is located near the town of Castricum.

In Table 4.1 an overview is given of all beach and shoreface nourishments carried out in the study area between 1985-2023. On average, beach nourishments in this location were carried out every 1 to 2 years between 1990 and 2000 to maintain the coastline after the Dutch dynamic coastline preservation policy came into practice. After the year 2000 the frequency of beach nourishing decreased to about every 4-5 years, which coincides with the development of the larger shoreface nourishments (Brand et al., 2022; Quartel & Grasmeijer, 2007). In recent years (since 1999), shoreface nourishments have been applied at the site Egmond-Bergen with a frequency of roughly every 4 to 5 years (Brand et al., 2022). In Figure 4.4 the nourishments and their alongshore extent are visualised over time. Clearly observable is the separation between the nourished coast in front of the towns of Egmond and Bergen and the unnourished coast near Castricum. In front of Egmond and Bergen a total maximum amount of 4328 m^3/m of sand was nourished (excluding the last unfinished nourishment) and of this amount 2218 m^3/m was nourished on the beach (Figure 4.5).

Table 4.1: Complete overview of all nourishments that have been carried out in the study area (RSP 30.00-43.50) between 1985 and 2023. (Data: Rijkswaterstaat).

#	Location	Type	Start of construction	End of construction	Begin transect	End transect	Length (m)	Total Volume (m3)	Volume m3/m
1	Bergen	beach	5-1990	6-1990	3225	3375	1500	60,000	40
2	Egmond	beach	5-1990	5-1990	3700	3850	1500	323,318	216
3	Bergen	beach	5-1990	6-1990	3225	3375	1500	385,774	257
4	Egmond-Camperduin	beach*	5-1992	11-1992	2620	3850	12300	1,472,640	120
5	Egmond	beach	9-1992	11-1992	3765	3860	950	69,225	73
6	Bergen	beach	6-1994	6-1994	3290	3350	600	100,683	168
7	Emond	beach	6-1994	6-1994	3785	3820	350	106,343	304
8	Bergen	beach	5-1995	5-1995	3263	3363	1000	306,000	306
9	Egmond	beach	5-1995	5-1995	3725	3875	1500	306,000	204
10	Bergen-Egmond	beach	5-1997	5-1997	3450	3575	1250	158,000	126
11	Egmond	beach	5-1997	5-1997	3625	3880	2550	314,000	123
12	Bergen	other***	6-1997	6-1997	3005	3105	1000	132,690	133
13	Bergen	beach	6-1997	6-1997	3105	3350	2450	352,000	144
14	Schoorl	beach*	6-1997	7-1997	2600	3005	4050	547,000	135
15	Egmond	beach	6-1998	7-1998	3750	3875	1250	244,442	196
16	Bergen	beach	4-1999	5-1999	3250	3375	1250	205,793	165
17	Egmond	beach	4-1999	4-1999	3725	3875	1500	214,515	143
18	Egmond	shoreface	6-1999	9-1999	3690	3910	2200	880,100	400
19	Bergen	shoreface	4-2000	8-2000	3225	3425	2000	994,000	497
20	Egmond	beach	6-2000	7-2000	3800	3900	1000	207,445	207
21	Bergen	beach	6-2000	6-2000	3275	3325	500	225,000	450
22	Egmond	shoreface	6-2004	11-2004	3620	4020	4000	1,800,699	450
23	Bergen	beach	4-2005	4-2005	3225	3375	1500	300,436	200
24	Egmond	beach	4-2005	5-2005	3700	3925	2250	486,023	216
25	Bergen	shoreface	8-2005	9-2005	3150	3620	4700	1,306,114	278
26	Bergen-Egmond	shoreface	8-2010	8-2011	3400	3900	5000	1,713,913	343
27	Bergen	beach	11-2010	8-2011	3150	3400	2500	500,000	200
28	Bergen	shoreface	11-2010	2-2011	3100	3400	3000	1,124,348	375
29	Egmond	beach	3-2011	4-2011	3700	3900	2000	400,000	200
30	Egmond	shoreface	8-2011	9-2011	3900	4000	1000	360,870	361
31	Egmond	beach	4-2015	4-2015	3700	3900	2000	432,500	216
32	Bergen	beach	4-2015	4-2015	3125	3400	2750	605,000	220
33	Bergen-Egmond	shoreface	7-2015	9-2016	3100	4000	9000	2,500,000	278
34	Bergen-Egmond	shoreface	7-2019	9-2019	3100	4000	9000	2,500,000	278
35	Bergen-Egmond	shoreface	3-2023	12-2024**	3250	3900	6500	1,400,000	215

*Nourishment extend exceeds the range of the study area. ** Nourishment construction works are not yet finished during this study. ***Rijkswaterstaat did not provide additional information on the specific type of this nourishment.

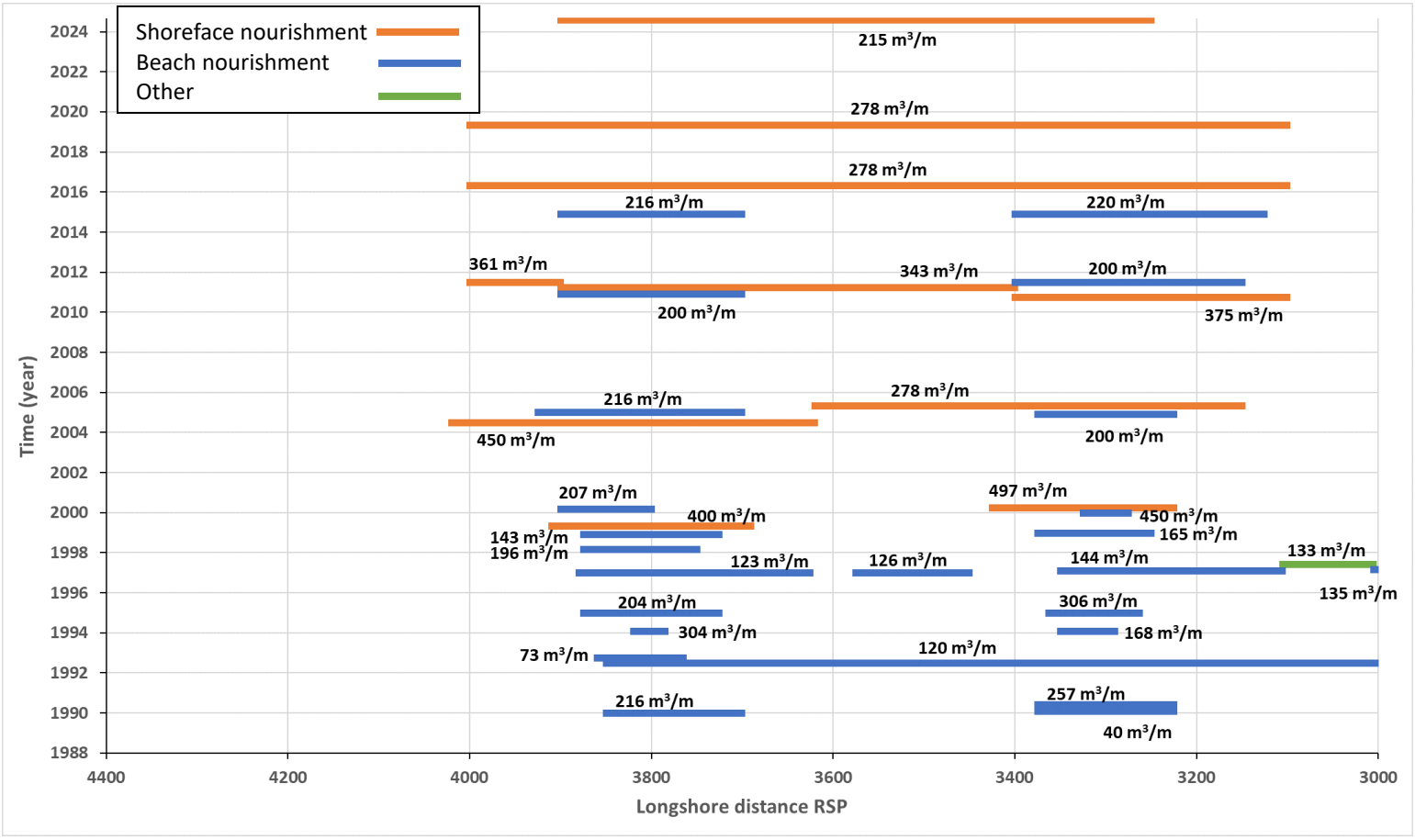

Figure 4.4: Overview of all nourishments constructed in the study area, the date corresponding to the end of the construction in Table 4.1 is plotted against the alongshore distance (RSP line). In a few cases the end of construction date was slightly shifted for clear visualisation of all individual nourishments without overlap obscuring the boundaries of the nourishments. In this figure the last unfinished shoreface nourishment is also shown, though, this nourishment is further not included in the analyses of this study. A distinction is made between beach nourishments, shoreface nourishments and other type of nourishments.

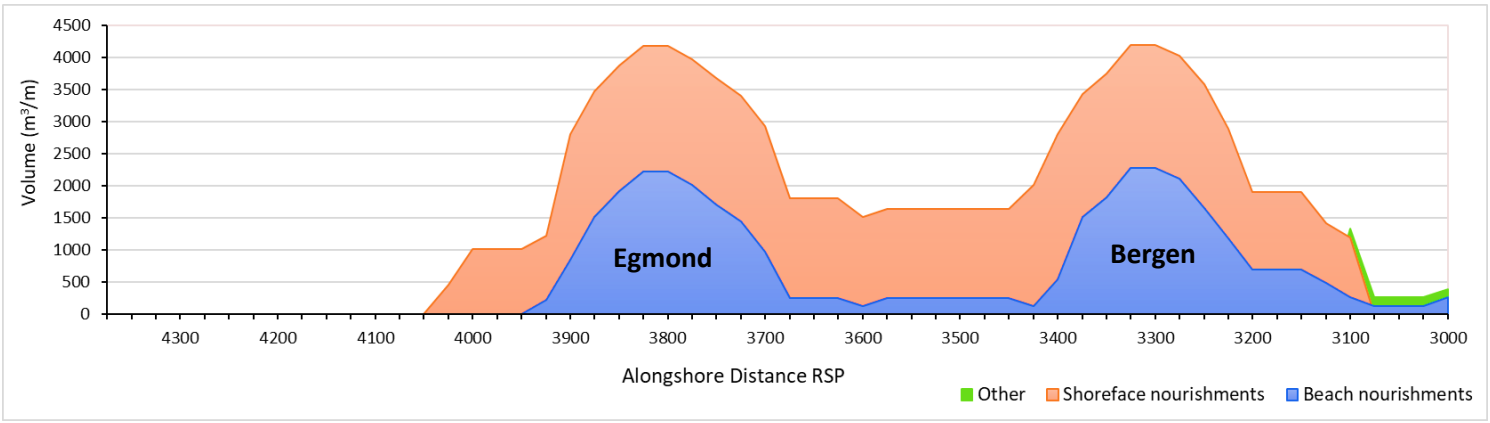

Figure 4.5: Cumulative volume of nourished sand near Egmond and Bergen plotted against the alongshore distance expressed with the RSP beach pole line. The last unfinished shoreface nourishment in 2023/2024 is already included in this figure.

5. Methodology

This section provides insight into the methods that were utilised to unravel the multi-temporal shoreline dynamics at the coast of Egmond-Bergen. First, the workflow of CoastSat will be delineated as well as its limitations. Thereafter, a description of the analyses regarding research question 1 and 2 will be given.

5.1 Data collection

5.1.1 Shoreline extraction with CoastSat

To be able to study shoreline dynamics as a response to nourishing, the Python toolkit CoastSat (Vos et al., 2019b) was used to extract instantaneous shorelines along the northern part of the Dutch Holland coast over a time period of 1985 – present. This toolkit is designed to acquire time-series of cross-shore shoreline position along shore-normal transects at any sandy coastline over the world. Publicly available satellite imagery over more than 30 years is used to extract the positions of the shorelines.

Collection of satellite imagery

With the Google Earth Engine (GEE) Python API package the available satellite images can be retrieved for a user-defined region of interest. Both Landsat and Sentinel-2 images can be accessed from the publicly available satellite imagery. Landsat images can be divided into two categories: Tier 1 and Tier 2 collections. In this study only Landsat Tier 1 scenes were selected to use for shoreline extraction as these are the only products applicable for time-series analysis (Vos et al., 2019a). The reason being that Tier 1 images have reliable geometric accuracy (RMSE < 12m) and a well-characterised radiometry. Every image contained in Tier 1 is stored as three different products and out of these three products, only the TOA (Top-of-Atmosphere) reflectance image is utilised in CoastSat (Vos et al., 2019a). The advantage of TOA reflectance images for time-series analysis is that they allow for a standardised comparison between images captured with various sensors or on different dates (Chander et al., 2009). Sentinel-2 also contains the same TOA reflectance images, but here Tier 1 images are called Level-1C products (Vos et al., 2019a; Vos et al., 2019b). Satellite images from Landsat 5-9 (1984-present) and Sentinel-2 (2015-present) missions were available for the stretch of coast near Egmond-Bergen, with a spatial resolution of the multispectral bands of 10 m for Sentinel-2 and 30 m for Landsat 5-9 (Vos et al., 2019b). Landsat 5-9 and Sentinel-2 satellites respectively have revisit periods of 16 days and 5 days, making it possible to study shoreline variability on different timescales. In Table 5.1 an overview is given of the different satellite imagery that can be used with CoastSat.

Table 5.1: The different collections of satellite imagery that were accessible with CoastSat and which were used in this study. After: Vos et al. (2019b).

Satellite mission	GEE collection	Time coverage	Revisit period	Pixel size
Landsat 5 (TM)	LANDSAT/LT05/ C02/T1_TOA	1984-2013	16 days	30m R, G, B, NIR, SWIR1 band
Landsat 7 (ETM+)	LANDSAT/LE07/ C02/T1_RT_TOA	1999-present	16 days	30 m R, G, B, NIR, SWIR1 bands + 15m panchromatic band
Landsat 8 (OLI)	LANDSAT/LC08/ C02/T1_RT_TOA	2013-present	16 days	30 m R, G, B, NIR, SWIR1 bands + 15m panchromatic band
Landsat 9 (OLI-2)	LANDSAT/LC09/ C02/T1_RT_TOA	2021-present	16 days	30 m R, G, B, NIR, SWIR1 bands + 15m panchromatic band
Sentinel-2 (MSI)	COPERNICUS/S2	2015-present	5 days	10m R, G, B, NIR + 20 m SWIR1

To specifically study the coastal stretch in front of Egmond and Bergen (RSP 30.00-43.50) a region of interest (ROI) was specified by defining a polygon of the study area (15.5 km^2) in Google Earth Pro and importing this polygon as a KML file within CoastSat. As a result, only the cropped images defined by the ROI are downloaded and stored. Furthermore, the CoastSat toolkit only allows the relevant spectral bands necessary for shoreline detection to be downloaded in the cropped images. This includes the three bands in the visible spectrum (Red, Green, Blue), along with the near infrared band (NIR) and the short-wave infrared band (SWIR1). Panchromatic bands available for Landsat 7-9 are also downloaded because they allow for increasing the spatial resolution of the bands. Lastly, because the quality assessment (QA) band holds a cloud mask, this band is also selected for download for each image (Vos et al., 2019a; Vos et al. 2019b). With the download of the images, relevant metadata is stored for each image which consists of the date, the filename, georeferencing accuracy and the coordinate reference system of the image.

Pre-processing

Before the shoreline positions can be extracted from the satellite imagery, first the downloaded images needed to be pre-processed. This includes the application of cloud masking, whereby images with too much cloud cover are excluded from the shoreline detection (Vos et al. 2019b). The number of cloudy pixels is determined from the QA band. For the Egmond-Bergen site, a threshold of 0.4 was defined to exclude all images with a cloud cover of more than 40% as this made it not possible to extract valid shoreline positions. In CoastSat this process is accompanied by panchromatic image sharpening and down-sampling to improve shoreline detection. This has the purpose to increase the spatial resolution of the Landsat images from 30 m to 15 m and to increase the resolution of the SWIR1 band of Sentinel-2 from 20 m to 10 m to have similar resolution across all Sentinel-2 bands. Landsat 7, 8, 9 all contain a higher resolution panchromatic band (Table 5.1), which is utilised to enhance the resolution of the multispectral bands. This executed by the application of a data fusion technique which is grounded on principal component analysis as described in Tu et al. (2001). For Landsat 5 a panchromatic band does not exist. However, it was still established that down-sampling from 30 to 15 m by bilinear interpolation led to a better accuracy in shoreline detection. The SWIR1 band of Sentinel-2 also uses the same method of bilinear interpolation to improve the resolution of this band to 10 m (Vos et al., 2019b).

Shoreline detection

To automatically obtain the position of the shoreline from the satellite images, the machine learning Python package scikit-learn (see Pedregosa et al., 2011) and an image processing package scikit-image (see Van der Walt et al., 2014) are implemented. Shoreline detection is carried out with a robust sub-pixel resolution shoreline detection algorithm. Hereby, the shoreline is expressed as the instantaneous sand/water interface at the time of image retrieval. Each pixel of an image is classified according to four classes: ‘sand’, ‘water’, ‘white-water’, ‘other land features’ with a Neural Network classifier (‘Multilayer Perceptron’ in scikit-learn) (Figure 5.1b) (Vos et al., (2019b). CoastSat allows the user to specify the sand colour in the region of interest, this includes ‘default’, ‘dark’ or ‘bright’ sand. The beach sand at Egmond and Bergen was quite bright in regards to its colour, therefore, using a classifier trained on brighter sand beaches and thus setting the sand colour accordingly provided more accurate classifications. After pixel classification, the boundary between sand and water is determined using the Modified Normalized Difference Water Index (MNDWI). The MNDWI value is computed with the following equation:

$$MNDWI = \frac{SWIR1 - G}{SWIR1 + G} \tag{1}$$

where SWIR1 represents the pixel intensity in the short-wave infrared band and G represents the pixel intensity in the green band. The MNDWI can only have values between -1 and 1. The probability density

function of MNDWI values is presented in a histogram (Figures 5.1c & d), from which can be derived that the sand class clusters itself around positive MNDWI values, whilst the water class represents the negative MNDWI values. The 'white water' and 'other land features' classes do not cluster around specific MNDWI values but rather attain a wider range of MNDWI values. Hence, to calculate a reliable and more refined boundary between sand and water, these two classes are excluded and only the sand and water classes are used. This is in contrast to other studies (e.g. Liu et al., 2017), where they applied a broader 'land-water' thresholding algorithm. However, this does not account for pixels belonging to vegetation, buildings or roads for example, resulting in a less stable and robust shoreline boundary (Vos et al., 2019a). With the histogram, Otsu's thresholding algorithm then computes the 'sand' / 'water' threshold (dotted line in Figure 5.1d) (see Otsu, 1979). This threshold corresponds to the MNDWI value that separates the two sand and water classes with maximum inter-class variance. Lastly, the sub-pixel resolution Marching Squares algorithm (see Cipolletti et al., 2012) leads to the iso-valued contour, which corresponds to the priorly-calculated threshold between sand and water. This iso-valued contour thus portrays the instantaneous shoreline for an image (Vos et al., 2019a; Vos et al., 2019b).

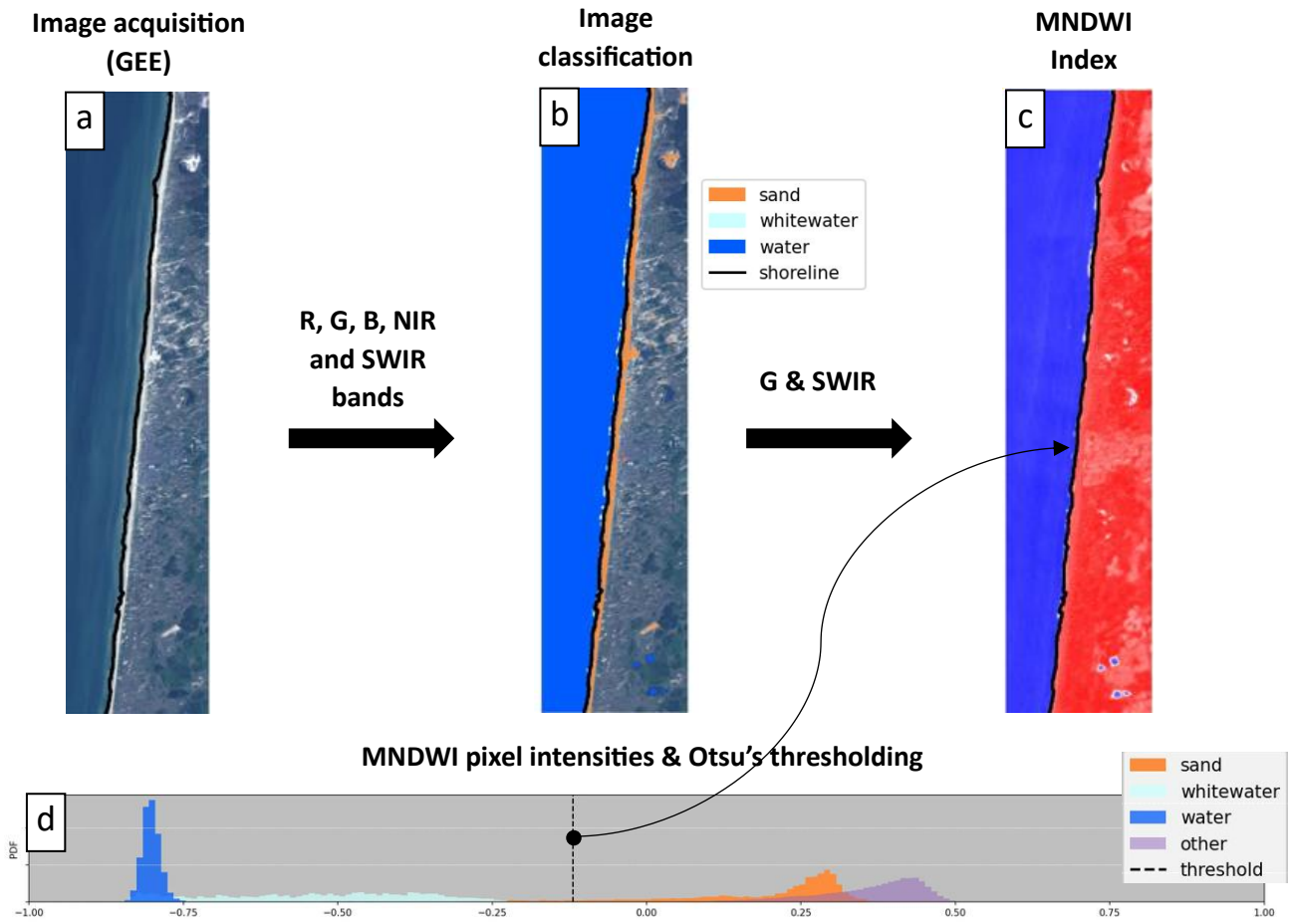

Figure 5.1: Workflow of shoreline detection in CoastSat: (a) Images downloaded from GEE; (b) Classification of the pixels into four classes; (c) The MNDWI value is calculated for each pixel on the image; (d) Otsu's threshold is calculated based on the sand and water classes. This specific case is based on a Landsat 8 (L8) image acquired for the study area on 02-05-2022. (After: Konstantinou et al., 2023).

Vos et al. (2019b) recommend the user to draw a 'reference' shoreline on a cloudless image prior to the detection of all shorelines as this aids in avoiding outliers and incorrect detections. Only points that fall between a specified distance from the reference shoreline are then included in the shoreline mapping. For the Egmond-Bergen study site, a reference shoreline for each year between 1985-2023 was digitised. For some years, 1985 and 1986 no reference shoreline could be digitised as there were no cloudless images available. For these two years a reference shoreline digitised on a S2-image from 2019-02-15 was used. This date was chosen because the last nourishment carried out in the study area before this date was in the beginning of 2015, so that the reference shoreline would not be too much influenced by the effects of nourishing.

For the study area shorelines were detected for each year separately for the period 1985 to 09-2023 (until September 2023 because at that time the images were retrieved). A total number of 2408 satellite images could be downloaded for Bergen-Egmond between 1985 and September 2023. However, many of these images could not be used for the analysis because their cloud cover exceeded the defined threshold of 40%. Approximately half of the images were removed, whereafter 1212 images remained available for shoreline detection. Within these initial 1212 images, also some duplicate Landsat images existed because in the range of the study area two Landsat tiles were present. One tile covered the entire study area, while the second tile only covered the southern part of the study area. The CoastSat toolkit did not provide a tool to select only one Landsat tile, therefore, most duplicate images were visually removed during the shoreline detection keeping only the images from the Landsat tile entirely covering the study area. Any remaining duplicate images were removed later on. For Sentinel-2 also two tiles (partly) covered the study area, but in this case CoastSat did have a workflow to select only one tile. Therefore, in these 1212 images no duplicate Sentinel-2 images were present related to this problem. During the actual detection of the shorelines at Egmond-Bergen, each shoreline was validated and accepted or declined based on the visual quality of the detection. Shorelines were discarded for varying reasons, duplicates were removed and often there were still too many clouds covering the beach area or there were shadows of clouds present affecting the position of the shoreline (Figure 5.2b). Important here is that not all shorelines that were not continuous along the entire study area were declined. If enough parts of the shoreline were considered to be present, despite of clouds or other problems (described below) the shoreline was still accepted to be included in the final dataset. Another problem affecting the satellite images was an issue with the cloud mask algorithm that is applied to the Landsat images by USGS, called CFMASK. In the documentation of CoastSat it is described that this algorithm sometimes also identifies very bright features as clouds. This also includes brighter-sand beaches, such as the beach near Egmond-Bergen, and white-water in the ocean. As a result, multiple images for Egmond-Bergen were affected by this issue, whereby the pixels corresponding to the beach were wrongly estimated as cloudy pixels. These pixels showed up as masked pixels on the images and made many satellite images not useful anymore (Figure 5.2c). An additional check to ensure accurate shoreline detection was provided by CoastSat by allowing the user to modify the shoreline position. With an interactive graphical tool built into the programme, the detected shorelines for Egmond were validated and if it was necessary, the shoreline position was manually modified by adjusting the MNDWI threshold to the right position (Castelle et al., 2021). Manual adjustment was for example required when the beach was partly saturated and the algorithm placed the shoreline at the wet sand/dry sand boundary instead of the water/sand boundary. During lower stages of the tide, intertidal features such as shoals, bars and troughs showed up at the coastline (Figure 5.2d). By manual adjustment of the MNDWI threshold the effect of these features on the shoreline position was decreased as much as possible, however, completely avoiding the presence of these features in the mapped shoreline was not always possible.

It has to be noted that satellite images acquired with Landsat 7 from 2003 and onwards were affected by a permanent failure in the Landsat 7 scan line corrector (SLC) (El Fellah et al., 2017). This causes white parallel lines to occur on the satellite images at places where pixels are missing (Figure 5.2a). As a result, shorelines mapped on Landsat 7 images since 2003 were not complete and showed multiple gaps, still, it was decided to use these images to increase the data density. Almost all years containing Landsat 7 images were also accompanied by other satellite missions (e.g. L5, L8), the only exception was 2012, exclusively having Landsat 7.

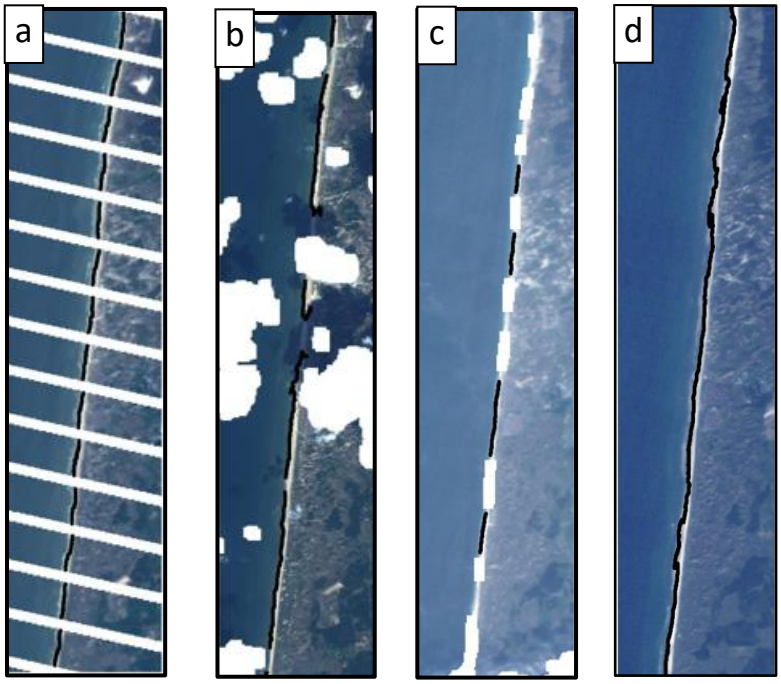

Figure 5.2: Common problems affecting the satellite images and shoreline detection: (a) White lines occur on the images because of the failure in the Landsat 7 scan line corrector; (b) Clouds and shadows of clouds affecting the shoreline detection; (c) Masked pixels occur on the image due to an issue with the cloud mask algorithm; (d) Intertidal features emerging during low water influence the position of the shoreline.

Because the shorelines were mapped for each year separately, afterwards all individual output files with the shorelines were merged into one large output file with corresponding metadata, containing the shorelines, dates, cloud cover, geoaccuracy, and the MNDWI-thresholds. After detection of all shorelines between 1985-2023, a total number of 583 shorelines, each at a different timestep, was the result. These shorelines were not all continuous along the whole study area. After removing duplicates, that is, images within 5 minutes of each other taken by the same satellite, and after removing images with inaccurate georeferencing (with a threshold at 12 m), 572 shorelines remained. The median of the MNDWI threshold of these 572 shorelines was approximately -0.16. Generally, the threshold for inaccurate georeferencing is set to 10 m in CoastSat. Here, a relatively high value of 12 m was chosen because between 1991 and 1997 almost all images were characterised by a geoaccuracy around 10 or 11 m. These were important years containing a significant number of nourishments, so it was decided to set the threshold for removal to 12 m. Thus, it is important to keep in mind that these years may contain measurements that are less accurate in their horizontal accuracy. Although the threshold was set to 12 m, most images had better georeferencing. Of all Landsat images the median geoaccuracy was equivalent to 5.3 m and approximately 74% of Landsat images were attained with a geoaccuracy of 7 m or less. Sentinel-2 images did not provide a geoaccuracy, but worked with a pass or fail system, with 1.0 equivalent to pass and -1.0 to discard the image. All Sentinel-2 images in the final dataset had a value of 1.0.

Over the years the density of the data increased, since Landsat 8 and Sentinel-2 became available a large increase in density of mapped shorelines occurred. For instance, in 1985 only 5 shorelines were detected, while in 2016 this had already increased to 29 shorelines, further increasing to 68 in 2022 when all satellite missions were available. Generally, most shorelines were captured in the spring-summer months (e.g. April, June, July) characterised by less clouds and calmer weather.

To obtain cross-shore time-series of the mapped 2D shorelines, shore-normal transects were drawn along the coast of Egmond-Bergen. Initially, the coordinates of the RSP-points (Rijksstrandpalen, Rijkswaterstaat) served as the locations of the shore-normal transects. The coordinates of every RSP point were used to compute two new points perpendicular to the coast, thereby forming a transect with its origin on the landward side. It was chosen to extend the transect 300 m landward and 400 m seaward of the RSP point. This resulted in 55 transects at an interval of approximately 250 m along the coast. Subsequently, the density of the transects was increased to 271 transects at an interval of 50 m to enhance the resolution of the data. Defining transects at intervals smaller than 50 m was not possible since CoastSat applies a function that uses an alongshore distance of 25 m to calculate the intersections. After computing the intersections, for every transect a cross-shore time-series was available from 1985-2023. In Figure 5.3 all extracted shorelines are depicted and the density and locations of the transects are shown for one particular part of the study area. The shorelines depicted in Figure 5.3 were all acquired at different water levels (e.g. due to tides) and were not post-processed yet, which will be described below.

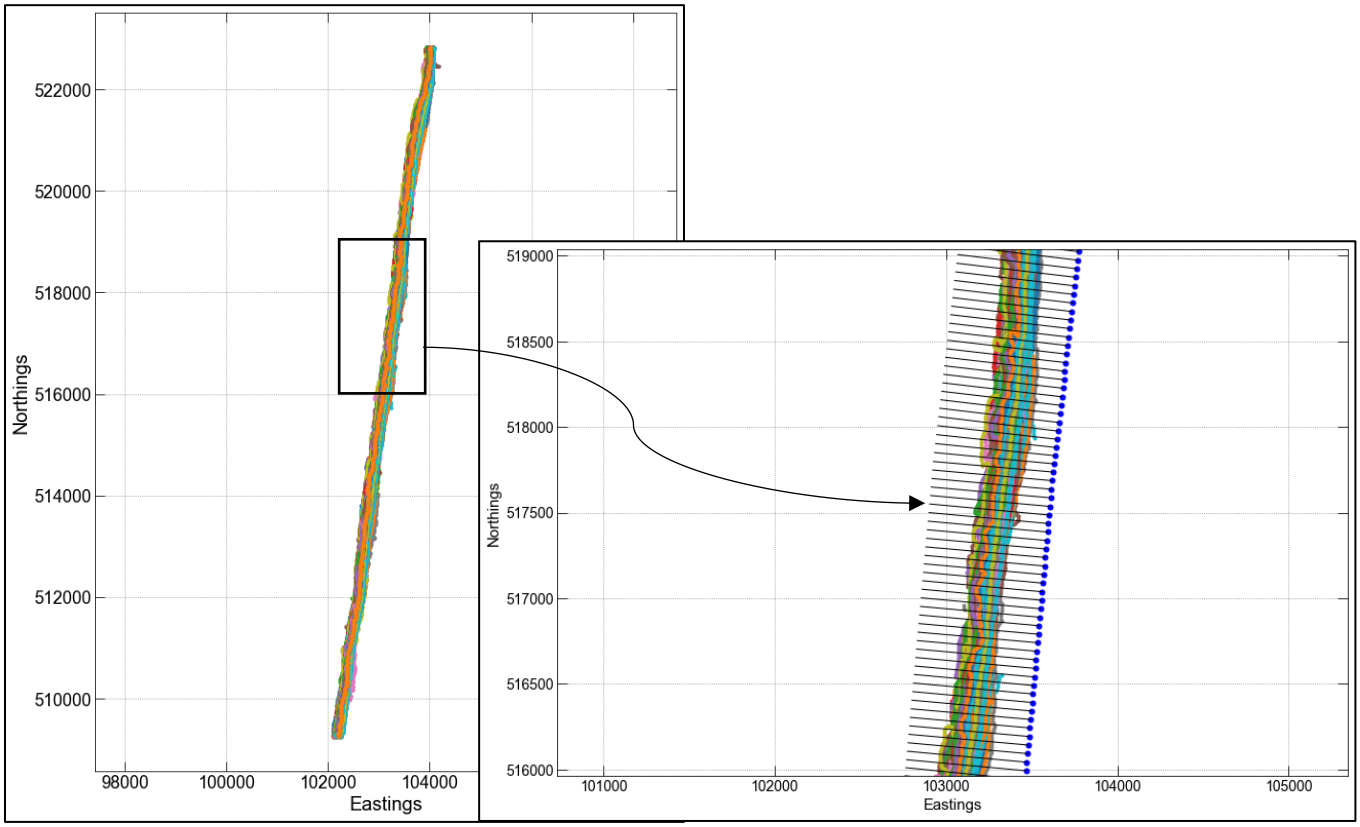

Figure 5.3: Left: the detected 2D shorelines with CoastSat between RSP 30.00 and 43.50 before post-processing the data. Right: A more detailed map of one part of the study area, here also the locations of the transects are shown with their origin (blue dots) on the landward side.

To account for the fact that all satellite images were obtained at different conditions and water levels, a linear water level correction was used which ensured that all instantaneous shoreline positions were projected to a standard reference elevation. The linear water level correction was as follows:

$$\Delta x = \frac{z_{wl} - z_{ref}}{m} \tag{2}$$

where Δx is the cross-shore horizontal displacement, z_{wl} is the measured water level corresponding to the times of image acquisition, z_{ref} is the standard reference elevation (e.g. mean sea level), and *m* is the beach slope in the study area. It was recommended to at least apply a linear tidal correction to the obtained shoreline positions, especially for coastal sites with low-sloping beach profiles and/or a large tidal range (Vos et al., 2019b). However, a study by Castelle et al. (2021) has shown that for coastlines characterised by high-energy incident waves and/or large tidal ranges and low-sloping beaches a tidal correction alone is not enough to improve satellite-derived shoreline positions. For these coastlines, the presence of breaking waves has a considerable influence on the total water level. The coast along Egmond-Bergen is such a case whereby the coastline is characterised by high-energy, low-sloping beaches. Moderate to high-energy breaking waves on a low-sloping beach can lead to significant horizontal translations of the shoreline through wave runup. Wave runup occurs at a beach as the result of two processes: total swash excursion and time-averaged wave setup. To account for these effects at the coast of Egmond-Bergen, not only tides were included in the linear water level correction (Eq. 2) but also wave runup by using the parametrisation of Stockdon et al. (2006). This empirical model is reported to perform well in a variety of different settings and wave conditions and is widely used (Konstantinou et al., 2023). The general runup parametrisation defined by Stockdon et al. (2006) is as follows:

$$R_2 = 1.1\left(0.35\beta_f(H_0L_0)^{\frac{1}{2}} + \frac{[H_0L_0(0.563\beta_f^2 + 0.004)]^{1/2}}{2}\right) \tag{3}$$

where R_2 is the elevation of extreme (2%) runup, β_f is the beach slope, H_0 is the deep-water significant wave height, and L_0 is the deep-water wavelength which can be computed with the linear dispersion relationship:

$$L_0 = \frac{gT^2}{2\pi} \tag{4}$$

where L_0 is the deep-water wavelength, g is the gravitational acceleration (9.81 m/s^2), and T is the wave period. In Equation 3, the first term represents the setup while the second term represents the swash excursion. However, Stockdon et al. (2006) also present a dissipative-specific runup parametrisation in the case of dissipative beaches. If the Iribarren number (Eq. 5) is below 0.3 a beach is considered to be dissipative. Calculating the Iribarren number for the study site gave a value of approximately 0.0047, implying that the dissipative-specific runup parametrisation could be used for Egmond-Bergen. The expression for the latter is given in Equation 6.

$$\xi = \frac{\beta}{(\frac{H}{L_0})^{1/2}} \tag{5}$$

$$R_2 = 0.043(H_0L_0)^{\frac{1}{2}} \qquad for \qquad \xi_0 < 0.3 \tag{6}$$

The total water level is then the sum of the measured tidal water levels and the runup elevations. The measured tidal water levels also include non-tidal water level residuals, consequently, the final correction also accounted for the effects of storm surges on the water level. With the total water level

the final correction could be applied by making use of Equation 2, thereby improving the horizontal accuracy of the cross-shore shoreline positions. On average, the shoreline positions were translated approximately 16.5 m either in landward or seaward direction. In most of these abovementioned equations the beach slope is considered. The beach slope was empirically determined by observing when the corrected cross-shore shoreline positions showed the least dependence on the total water level, indicating a successful water level correction. Consequently, for each transect a linear regression was executed through the data points and the resulting coefficient of determination (R-squared) was determined. This was done for different values of the beach slope, whereby for each value of the beach slope the R-squared was averaged over all transects to represent all transects. The beach slope was then defined as the value that resulted in an R-squared closest to zero (no dependence on water level). This resulted in an average beach slope for the study site of 1:36 m ($\beta \approx 0.0277$). This did correspond to descriptions in other studies, for instance, Ruessink et al. (2019) reported an intertidal beach slope of ≈1:40. Stolk (1989) described a beach slope between 1:35 and 1:60 for the Holland coast with gentler sloping beaches in the northern part, where Egmond and Bergen are situated.

Coastsat also provides the option to post-process the results of the shoreline detection. A despiking algorithm is used to detect and remove outliers. This algorithm removes outliers based on the maximum cross-shore change between two successive data points. The user can define how much cross-shore change is allowed between the two data points. A spike is removed if the shoreline shows a large amount of accretion of erosion (to be defined by the user) but thereafter immediately returns to its previous state. It is expected that after a significant erosion or accretion of the shoreline it takes some time for the shoreline to recover, thus, if the shoreline immediately returns to its previous date the data point is deemed an outlier. For the study site a relatively high maximum value of 70 m cross-shore change (default=40 m) was chosen to account for nourishments which can cause sudden changes in beach width. A value of 70 m was found not to affect the results of the nourishments. The algorithm also ensured that Otsu thresholds that did not fall between a range of -0.5 to 0 were removed. Typically around 6 to 7 data points were dismissed from each transect. The end result comprised of 271 post-processed transects with cross-shore time series over a period of 1985-2023, which were also corrected for tides, storm surge and wave runup. With CoastSat 572 shorelines were detected, but after the removal of outliers, most of the cross-shore time-series contained in each transect were based on roughly 460 data points. Of course, this is also due to the fact that not all detected shorelines were complete, lowering the availability of data points. The cross-shore shoreline change along each transect could be visualised by subtracting the mean cross-shore position for each transect. In such a manner, more landward locations of the beach are shown by values below zero while more seaward locations are shown by values greater than zero. In Figure 5.4 one of the 271 transects is shown as an example, the cross-shore change is presented with respect to the mean shoreline position of that transect, as explained above.

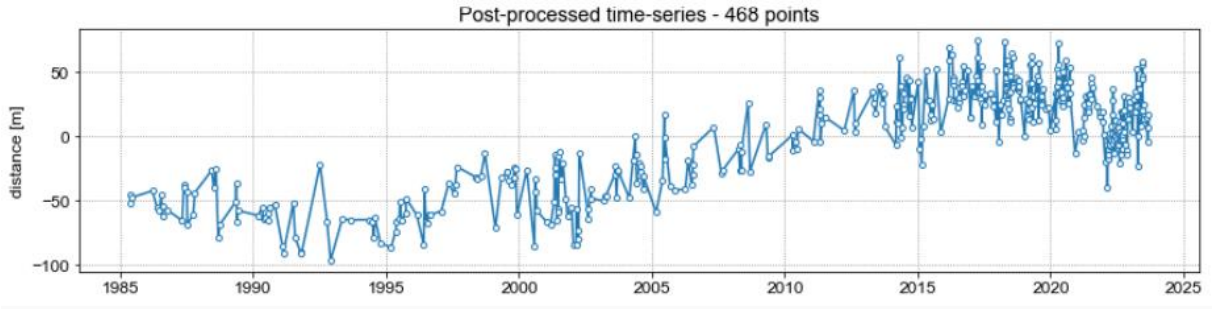

Figure 5.4: Example of a post-processed time-series of cross-shore shoreline positions. The number of data points in this time-series was 468 points.

Overall, this method of detecting shorelines with a sub-pixel resolution results in time-series of cross-shore shoreline positions with a horizontal accuracy of approximately 10 m for different coastal settings (Vos et al., 2019a). Vos et al. (2019a) investigated time-series of shoreline change at five different study sites and compared the results to in-situ measurements of shoreline change. They found that for a microtidal steep beach environment (Tairua, New Zealand) the horizontal accuracy relative to the in-situ surveys (RMSE) amounted to 7.3 m, while for a mesotidal low-sloping beach (Truc Vert, France) the horizontal accuracy was less and amounted to 12.7 m. However, in these cases only a linear tidal correction was applied. Castelle et al. (2021) also studied Truc Vert but did account for wave setup and wave runup and showed that the RMSE was much reduced. This highlights the need for using an appropriate water level parametrisation at low-sloping beaches with a large tidal range or highly energetic waves. Generally, the main sources of error in the instantaneous shoreline position are related to the pixel resolution of the satellite images, the horizontal inaccuracy in the georeferencing of the images, and the fact that the extracted shorelines have to be adjusted to a standard reference elevation using an average beach slope instead of a space and time-varying beach slope. Considering the horizontal accuracy of ~10 m, typically, the satellite imagery is able to capture shoreline variability trends and patterns at timescales of 6 months and longer (Vos et al., 2019a). Seasonal and interannual behaviour can both be inferred from the resulting time-series (Vos et al., 2019b). Rapid shoreline changes as a result of large storms and the construction of sand nourishments are also shown to be well documented by the shoreline detection tool, as described in Vos et al. (2019a).

5.1.2 Water (tide) level and wave data

Time-series of (offshore) water levels and waves were obtained from Rijkswaterstaat from 1985 to September 2023, corresponding to the time of satellite image acquisition. Measured water levels with respect to NAP (Normaal Amsterdams Peil) and calculated (astronomic) water levels with respect to NAP were obtained from measuring buoys located offshore from IJmuiden. Rijkswaterstaat did not provide a complete record of 30+ years of data at one measuring station, therefore, four different measuring stations had to be used to acquire a complete record for 1985-2023. Water levels were provided with an interval of 10 minutes at all stations. In Figure 5.5 the different stations used are shown for the measured water levels and in Table 5.2 the offshore distance and water depth are provided for all buoys. Until March 1987, measured water levels were obtained from the station Zuidelijk Havenhoofd (ZDHV), whereafter the station IJmuiden Buitenhaven (IJMBUI) was used for measurements until October 2002. IJmuiden Stroommeetpaal (IJMSMPL) covered the remaining part of the measurements, except the last 3 months of data which had to be acquired from IJgeul Stroommeetpaal (IJGSMPL). Astronomic water levels are not shown in Figure 5.5, but these were for a large part obtained from IJmuiden Buitenhaven until the end of 2011. From 2012 and onwards measurements were acquired from IJmuiden Stroommeetpaal. In comparison to astronomic water levels, measured water levels also include non-tidal residuals, therefore the measured water levels were preferred as they also account for atmospheric surge. However, when the measured water levels were incomplete, missing data was replaced by the corresponding atmospheric water level. Except for missing data, the measured water level data also contained duplicate data, some obvious outliers, and sometimes (e.g. part of 1987) the data was not measured at a regular interval of 10 minutes but rather at a random interval. Therefore, first the duplicates and the outliers were removed and the data was resampled to 10 minute-interval, whereafter all missing values were replaced by atmospheric water level data. To account for the fact that water levels were taken from measuring stations near IJmuiden instead of in the vicinity of Egmond and Bergen, a travel time of 20 minutes for the tide was added to the original time of the measurement as the tidal wave propagates northward along the Dutch coast.

Deep-water significant wave height ($H_{1/3}$ or H_s) and the corresponding wave period to $H_{1/3}$ were for the most part obtained from one offshore wave buoy, namely, IJmuiden Munitiestortplaats (IJMMNTSPS).

Only between July 2023 and September 2023 measurements were not available at this location and had to be acquired from IJgeul Munitiestort1 (IJGMUN1) (Figure 5.5) (Table 5.2). In these last months also another parameter for the wave period had to be used. Instead of the wave period corresponding to $H_{1/3}$, the wave period was used which belonged to the longest one-third of waves. This may have led to potential bias in the data for these last months. In general, the wave data was also measured on a 10-minute basis, however, until the end of 1989 wave data was only measured every three hours and until approximately the end of 2006 the data consisted of hourly measurements. The collected wave data contained many duplicates and some outliers which had to be removed. After removing these values, the average significant wave height amounted to approximately 1.18 m and the average wave period amounted to 5.46 s. Subsequently, both the wave height and period were resampled to 10-minute data and linearly interpolated to fill missing values. Not all missing values were filled with the technique of interpolation because sometimes gaps longer than a few days in the data existed. For these larger data gaps linear interpolation was deemed to be inaccurate and therefore the missing values still remaining after interpolation were filled with the average of the wave height and period (1.18 m and 5.46 s). To process the water level and wave data with the Coastsat toolkit the date and time of the time-series were required to be in the UTC timezone. To convert the acquired data from the MET/CET timezone to UTC, one hour was subtracted from the time of each data point.

With the wave period, the deep-water wavelength could be calculated following the linear dispersion relationship (Eq. 4). The deep-water wavelength is shown in Figure 5.5. Finally, with the offshore wave height and wavelength, the runup elevation at the coast could be computed with the Stockdon parametrisation for dissipative conditions (Eq. 6) (Figure 5.5).

Table 5.2: Additional information about the different measuring stations used to collect the water level and wave data. The distance offshore and the water depth are both approximations. The first two measuring stations were not located offshore but near the harbour of IJmuiden.

Measuring buoy	**Distance offshore from IJmuiden (km)**	**Water depth (m)**
Zuidelijk Havenhoofd (ZDHV),	- situated near outer end southern harbour jetty IJmuiden	16
IJmuiden Buitenhaven (IJMBUI)	- situated near southern harbour jetty IJmuiden	2
IJmuiden Stroommeetpaal (IJMSMPL)	3	17
IJgeul Stroommeetpaal (IJGSMPL)	3	17
IJmuiden Munitiestortplaats (IJMMNTSPS)	25	20
IJgeul Munitiestort1 (IJGMUN1)	25	21

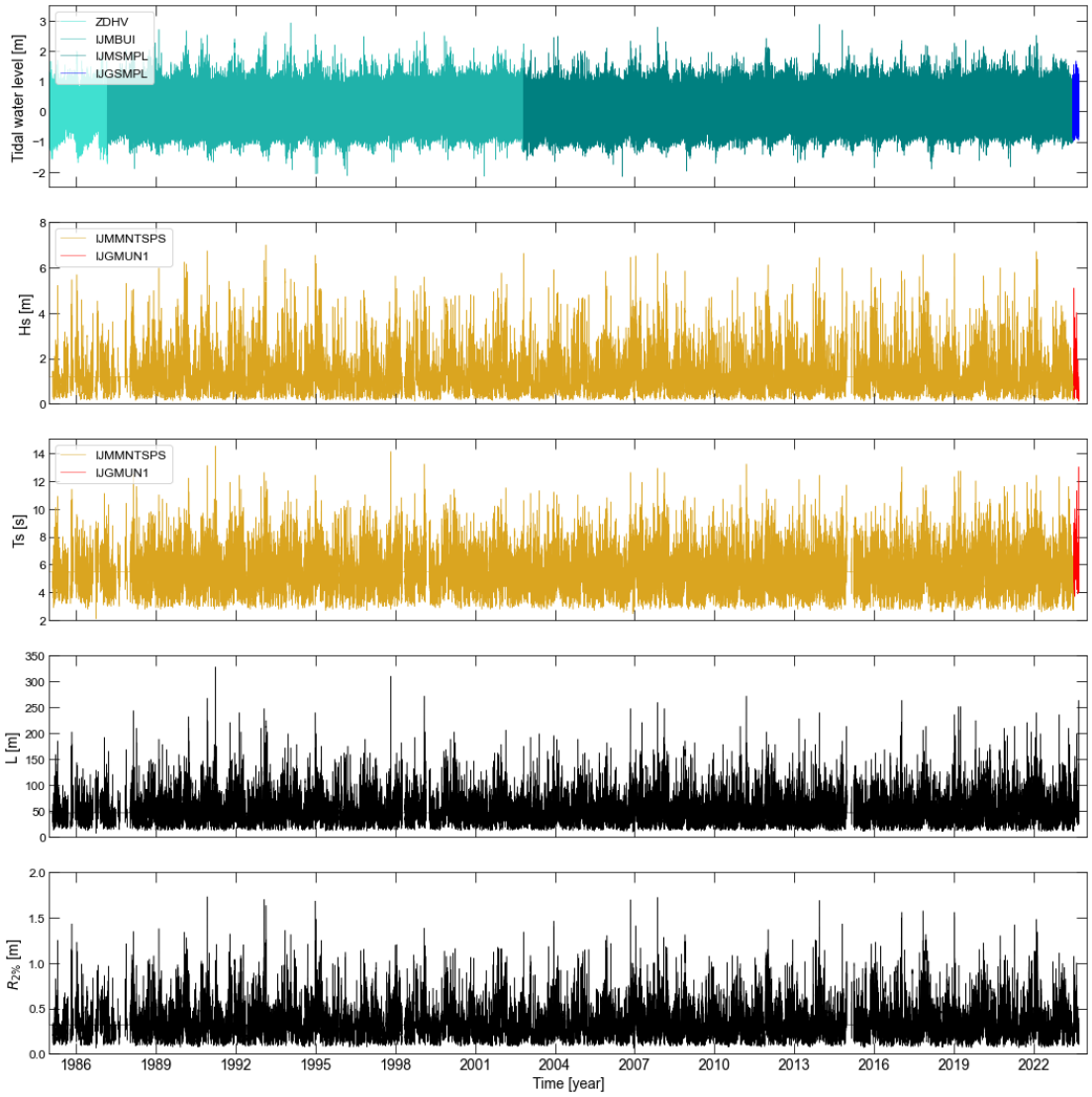

Figure 5.5: Offshore water levels, significant deep-water wave height Hs, the corresponding deep-water wave period Ts, the deep-water wavelength, and the runup elevation for the period between 1985-Sep 2023. For the water level, wave height and wave period the corresponding measurement locations are also indicated.

5.1.3 Dataset characteristics

To study the multi-temporal shoreline dynamics for the coast of Egmond and Bergen, shorelines were extracted from 1985 to September 2023. Every satellite image was extracted at a different stage of the tide and under different wave conditions. Therefore, all cross-shore positions of shorelines were corrected for the influence of storm surge, tidal elevation, and runup elevation on the detected shoreline positions. The sum of these different components yielded the total water level by which the shorelines were translated to a standard reference elevation. In Figure 5.6, the total water level between 1985-2023 is presented together with the water levels that corresponded to the time of image acquisition of the data points. Most detected shorelines were obtained during calmer weather conditions when wave height and runup elevation were relatively low. During higher-energy conditions, often too many clouds covered the satellite images, which made it difficult to extract shorelines during storm events.

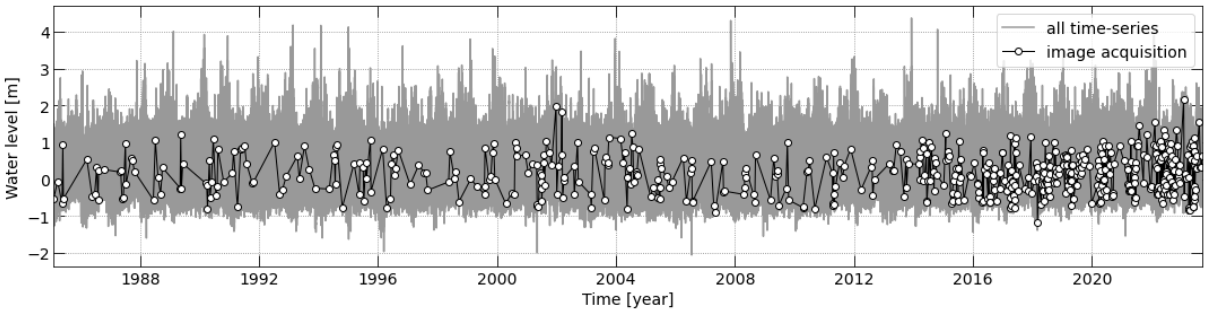

Figure 5.6: The total water level plotted against time and the water levels at the time of image acquisition. The total water level consists of measured tidal water levels, which also include storm surge, and the runup elevation $R_{2\%}$ approximated by the Stockdon parametrisation. Most images were acquired during calmer weather conditions.

5.2 Data-processing

To summarise and visualise all 271 transects along the study area with the acquired time-series of cross-shore shoreline change from 1985-2023, it was decided to make use of Hovmöller plots with the locations of the transects on the horizontal axis and time on the vertical axis. However, it has to be noted that the location and length of each transect were determined with respect to the locations of the RSP points. In Figure 5.7 the location of the RSP points and the line through it are depicted together with a satellite-derived shoreline from 03-1986 when the dynamic coastline preservation policy was not yet implemented and still no sand nourishments were carried out.

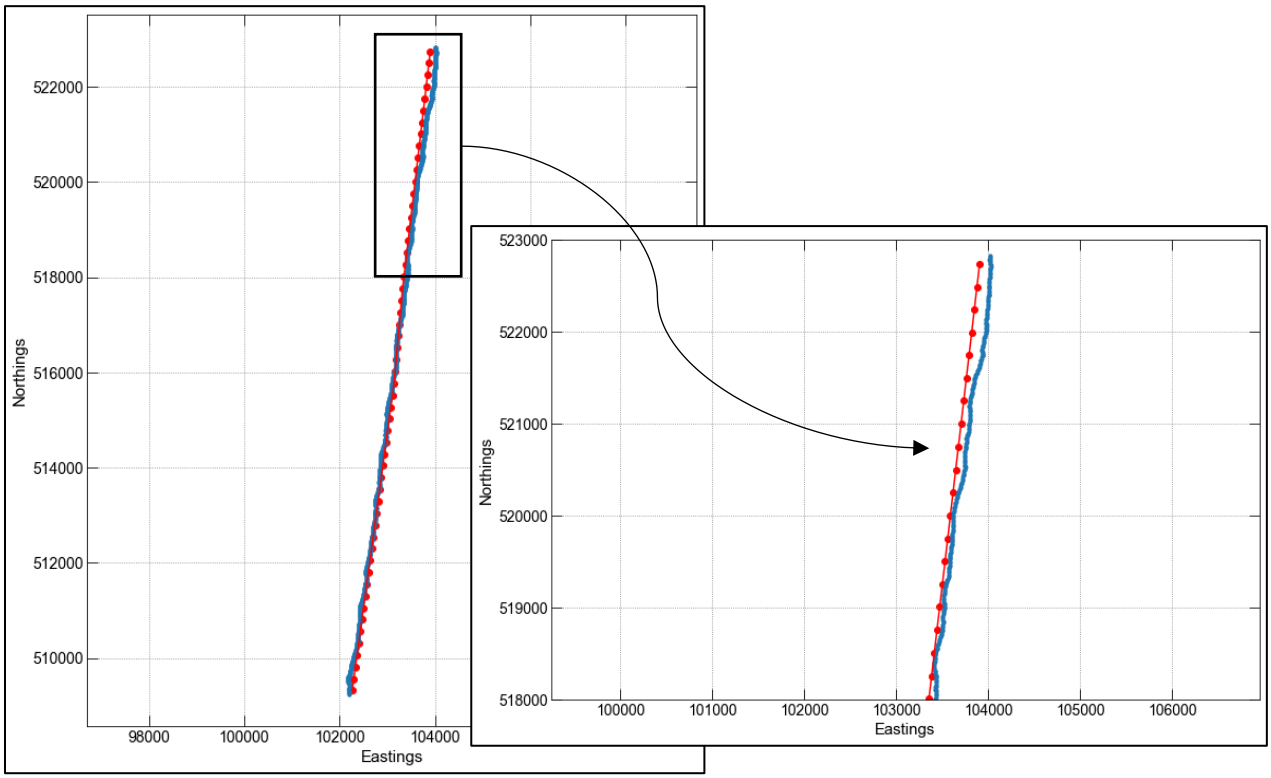

Figure 5.7: An individual satellite-derived shoreline from 19-03-1986 (indicated in blue) plotted with the location of the RSP line (indicated in red). The individual red points represent the locations of the RSP points.

This figure illustrates that along large parts of the shoreline a considerable offset existed between the RSP line and the actual shoreline positions derived from the satellite images. This offset can be attributed to the fact that the RSP points only represent an artificial reference line which was constructed in 1843. Since then, the coastline of the Netherlands has been subject to many changes and this RSP line cannot be seen as an accurate representation of the current shoreline position. Since the position and length of the transects were calculated using the location of the RSP points, a correction was needed to remove the influence of the location of the RSP points on the cross-shore positions of the shorelines. Therefore, a 'pre-nourishment profile' was computed based on the satellite-derived shorelines between 1985-1989. The shorelines acquired between 1985 and 1989 can be considered as 'unnourished' shorelines and therefore gave the most accurate representation of the shoreline position or shape of the coast without the presence of human influence. These five years of cross-shore positions were averaged over time to calculate an average cross-shore shoreline position for each transect over the period of 1985-1989, thus representing the pre-nourished profile. Subsequently, by subtracting the pre-nourishment profile from the original data, cross-shore positions with respect to the pre-nourishment profile could be obtained. This process is summarised in Equation 7. In the following equations, *t* represents time and *y* represents alongshore distance.

$$\boxed{\widetilde{D_{sh}}(y,t)} = \boxed{D_{sh}(y,t)} - \boxed{\widetilde{D}_{sh,t=1..5}(y)} \quad (7)$$

where $\widetilde{D_{sh}}(y,t)$ represents the cross-shore positions with respect to the pre-nourishment profile, $D_{sh}(y,t)$ represents the original cross-shore positions (=distance to the origin of the transect), and $\widetilde{D}_{sh,t=1..5}(y)$ represents the average cross-shore shoreline position for 1985-1989 and thus the pre-nourishment shape of the coast.

To centre the data around zero, the data was 'demeaned' both over time and over the alongshore axis. To demean the data in alongshore direction, the data already corrected for the RSP line was used, which is represented by $\widetilde{D_{sh}}(y,t)$ in Equation 7 & 8. Subsequently, the alongshore mean cross-shore position was calculated for each timestep, whereafter for each timestep this mean was subtracted from $\widetilde{D_{sh}}(y,t)$. This is represented by Equation 8.

$$\boxed{\widetilde{\widetilde{D_{sh,y}}}(y,t)} = \boxed{\widetilde{D_{sh}}(y,t)} - \boxed{\overline{D_y}(t)} \quad (8)$$

where $\widetilde{\widetilde{D_{sh,y}}}(y,t)$ represents the alongshore-demeaned cross-shore positions with respect to the pre-nourishment profile, and $\overline{D_y}(t)$ represents the mean alongshore cross-shore position for each timestep.

To demean the data over the time axis, the process was very similar and also used the cross-shore shoreline positions corrected with the pre-nourishment shape of the coast ($\widetilde{D_{sh}}(y,t)$). In this method, a mean cross-shore position over the entire time-series was calculated for each transect. The resulting mean value was then subtracted from all cross-shore positions per transect following Equation 9.

$$\boxed{\widetilde{\widetilde{D_{sh,t}}}(y,t)} = \boxed{\widetilde{D_{sh}}(y,t)} - \boxed{\overline{D_t}(y)} \quad (9)$$

where $\widetilde{\widetilde{D_{sh,t}}}(y,t)$ represents the time-demeaned cross-shore positions with respect to the pre-nourishment profile, $\overline{D_t}(y)$ represents the mean cross-shore position of each transect.

In essence, $\overline{D_y}(t)$ thus represents an overall mean shoreline position as a function of time, while $\overline{D_t}(y)$ is the mean shoreline position as a function of alongshore distance, and all shoreline positions were computed relative to these two mean shorelines.

By visualisation of all shoreline positions relative to a mean shoreline, positive values in the demeaned data should be interpreted as a more seaward located shoreline, while negative values represent a more landward situated shoreline. However, it has to be clear that the resulting negative or positive values in the demeaned data cannot be directly interpreted as erosion or seaward expansion of the beach but should be rather interpreted as an anomaly or perturbation from the computed mean value. 'Demeaning' the data results in the mean along the vertical or horizontal axis to be zero, thereby, strong seaward expansion of the beach may show up as very positive values but this also forces locations along the coast that did barely experience cross-shore change to falsely appear as negative values in the data. This then may be attributed to be erosion, while actually that is not the case.

5.3 Data analysis methods

5.3.1 Research question 1- Time-series decomposition

To study potential trends in the cross-shore shoreline position time-series, the statistical analysis of time-series decomposition was adopted. For the decomposition the cross-shore positions demeaned over the vertical time axis and corrected with the pre-nourishment profile were used ($\widetilde{\overline{D_{sh,t}}}(y,t)$ in Equation 9).

Before decomposing the time-series, the study area was divided into four sections. This was required because the study area had a large alongshore extent of about 13.5 km. In addition, this made it possible to study the trends separately for the coastal stretches in front of Bergen, Egmond and Castricum. A (smaller) section in between Egmond and Bergen, where fewer nourishments were carried out, was also defined to study the behaviour of this coastal stretch as well. Overall, this included the section between RSP 3000-3395 (Bergen), the section between RSP 3400-3595 (in between Egmond and Bergen), the section between RSP 3600-3995 (Egmond) and the section between RSP 4000-4350 (Castricum) (Figure 5.8). For each of the four coastal sections, the demeaned cross-shore shoreline positions were alongshore-averaged to obtain an average cross-shore position for each timestep. However, the data was unequally spaced and often contained large gaps of missing values. Therefore, the alongshore-average for each timestep was only computed if 50% or more data points were present in the data. In such a way, an additional check was carried out for quality control. The average variation around the alongshore-averages in each section was approximately between 15 and 20 m, approximated by the standard deviation around the alongshore-averaged values.

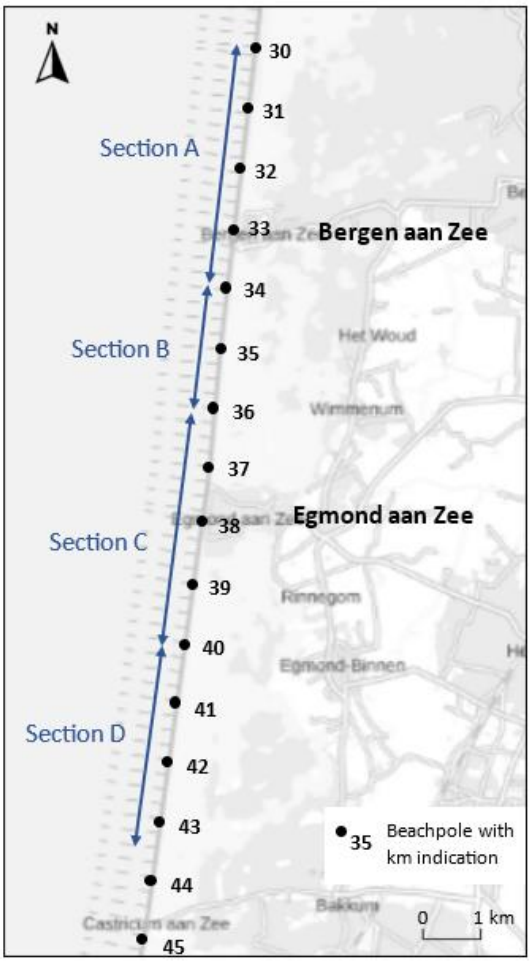

Figure 5.8: Map of the study area with the four sections for JUST decomposition. Section A: RSP 3000-3395. Section B: RSP 3400-3595. Section C: RSP 3600-3995. Section D: RSP 4000-4350.

To decompose the resulting time-series, the Jumps Upon Spectrum and Trend (JUST) software tool developed by E. Ghaderpour was utilised (Ghaderpour, 2021). The decomposition technique provided in this tool had the advantage that it could also work with nonstationary-unequally sampled time series. This is often the case with time-series acquired from satellite-imagery and this was also applicable to the obtained time-series of this study. In particular the addition of Sentinel-2 in the most recent years led to a difference in the number of observations between the first and final years, characterising the data as disproportionate regarding its sampling rate with more observations towards the end. JUST may also consider observational uncertainties in the satellite data. Although cross-shore shoreline position time-series were unequally sampled, there was thus no requirement to interpolate or to fill the gaps in the data which is often needed for other decomposition techniques (e.g. Awty-Carroll et al., 2019). Though, before decomposing the time-series, it was required to remove the timesteps with

missing values in the data, creating a continuous list of alongshore-averaged cross-shore shoreline positions.

JUST decomposes time-series into a trend component (Tr), a seasonal component (Se) and the remainder (Re):

$$\widetilde{\widetilde{D_{sh,t}}}(t) = Tr(t) + Se\ (t) + Re(t) \tag{10}$$

The decomposition of the data is grounded on spectral analysis, which finds statistically significant spectral components within the time-series. JUST makes use of the Anti-Leakage Least-Squares Spectral Analysis (ALLSSA) (Ghaderpour et al., 2018), which runs with a moving window with a fixed size of *M* observations. The ALLSSA season-trend model thereby establishes the best fit of sinusoids and trendlines for the time-series to estimate the trend and seasonal components. The temporal segmentation of the data by the application of successive windows takes seasonal variations and shifts in the trend into consideration and because the windows have a fixed size, this is very appropriate for data with missing values providing a more accurate approximation of the seasonal and trend components. For instance, a window with a fixed size may hold supplementary observations of adjacent seasons when only little data is available for one specific time period, improving the result of the decomposition (Ghaderpour et al., 2018; Ghaderpour & Vujadinovic, 2020).

Before running the decomposition, the user can specify several input parameters as described in Ghaderpour (2021), including the window size *R* and the translation step δ by which the window moves through the observations. For this study, the window size was chosen as the total number of data points in the last three years (Sep-2020 to Sep-2023) and the translation step amounted to the largest annual number of data points in these three years (Table 5.3). The year 2022 turned out to be the year with the most observations, therefore the translation step was determined based on the total number of data points in 2022. The decisions for these values were made based on the practical guidance for automation purposes provided in Ghaderpour & Vujadinovic (2020) and on an earlier study performed by Petrova et al. (2023) who used JUST decomposition with ALLSSA on NDVI time-series. A significance level α of 0.05 was chosen to determine the trends in the decomposition of the demeaned cross-shore shoreline positions. JUST decomposition also allows the user to select input parameters to detect potential jumps in the time-series caused by abrupt changes in the trend component, such as droughts, floods, and fires. However, in the present study the detection of jumps was excluded from the analysis because the time-series data presented itself to be somewhat noisy due to the nature of the data, which induced the detection of false jumps. Instead, other methods were deployed to study the shoreline response to storm events and nourishments. These will be described in the following sections.

Table 5.3: Input parameters for the JUST decomposition for each of the four defined coastal sections: the window size, the translation step, the significance level, and the cyclic frequencies.

Coastal section	Window size (*R*)	Translation step (δ)	Significance level (α)	Cyclic frequencies (ω)
RSP 3000-3395	118	59	0.05	[0.8, 1.0, 1.2, …, 3.8]
RSP 3400-3595	120	60	0.05	[0.8, 1.0, 1.2, …, 3.8]
RSP 3600-3995	125	64	0.05	[0.8, 1.0, 1.2, …, 3.8]
RSP 4000-4350	123	62	0.05	[0.8, 1.0, 1.2, …, 3.8]

After decomposing the alongshore-averaged cross-shore positions into a trend, seasonal and remainder, the strength and direction of the trend-series were evaluated by means of a Mann-Kendall

(MK) test (Kendall, 1975; Mann, 1945). The Mann-Kendall test is a non-parametric test, meaning that, in contrast to parametric tests, less assumptions about the data are made and the data does not have to be normally distributed. The only prerequisite that needs to be fulfilled before conducting the MK test is that the acquired time-series data are independent. For this reason and because this test is so widely-used for detecting potential trends in time-series data, it was chosen to employ the Mann-Kendall test to quantify the trend-series in the cross-shore shoreline data. Non-parametric tests are also considered to be robust in case there are outliers present in the data (Hamed & Ramachandra Rao, 1998). The MK test investigates if a trend is present in the data based on a chosen significance level (α). To test the significance of the trends detected in the decomposition of the alongshore-averaged cross-shore positions, a significance level of 0.01 was used. The null hypothesis (H_0) states that the data are independent and ordered in a random way, thus, the data do not follow a particular trend or possess serial correlation. If the alternative hypothesis (H_A) is true on the other hand, this implies the presence of a trend in the observations. Subsequently, the computed p-value by the MK test could be evaluated against the significance level. The null hypothesis was rejected if the p-value was equal or less than the significance level ($p \leq \alpha$). If the MK test indicated a statistically significant trend in the data, next, the slope or magnitude of change of the trend was analysed by applying the non-parametric Sen's slope estimator (Sen, 1968). Sen's slope estimator (and the MK-test) was applied to the trend component as this excludes the noise and seasonality that is present in the original time-series to improve the accuracy of the quantified slope.

Storm response

The remainder component resulting from the time-series decomposition contains all random occurrences of change in the cross-shore shoreline positions that cannot be attributed to seasonal effects or the general trend in the data. This component of the time-series thus contains the inaccuracies and outliers that exist within the data. For instance, this comprises of the errors caused by inaccurate shoreline detection during low tide and inaccurate georeferencing. However, the remainder component also includes the cross-shore shoreline change as a reaction to storm events, which can be considered as random occurrences of the weather. To study the effect and the relative importance of storms on the coast in front of Egmond and Bergen, both the instantaneous and the non-instantaneous response of the shoreline to storm events were investigated. The (instantaneous) response of the shoreline to individual storms was analysed by observing if large landward retreats of the shoreline coincided with high values of wave height, that is, a minimum significant wave height of 5 m. This first analysis was carried out solely between 2015-2023 because here the density of the data points was significantly higher than in the years before due to the addition of Sentinel-2 and Landsat 8. The reason being that the response of the shoreline to an individual storm cannot be accurately reviewed if the data points before and after the storm are timed too far from the actual moment of the storm.

The non-instantaneous response of the shoreline to storm events was investigated to see if more turbulent weather or multiple storms over a longer time period would lead to large shoreline retreat in comparison to a time period with calmer weather conditions. The non-instantaneous response was reviewed by means of computing the cumulative wave power based on hourly wave data and comparing that to cross-shore shoreline change in the remainder component in between two data points that were spaced apart for a fixed period of time. For this analysis, first monthly averages of the demeaned data ($\widetilde{\widetilde{D_{sh,t}}}(y,t)$) were computed to create equally spaced intervals between all data points. With the monthly averages again a JUST decomposition of the four alongshore-averaged time-series was done to attain the time-series of the remainder part on which this analysis is based. The results and the input parameters of the decomposition of monthly-averaged data are included in Appendix A.

The sum of the wave power serves as a measure of the amount of wave energy that was present within a certain period. Storm periods are characterised by a higher wave power. The wave power is approximated by Equation 11 (Price & Ruessink, 2011).

$$P = \frac{\rho g^2}{32\pi} * {H_{rms}}^2 * T_p \tag{11}$$

where P represents the wave power in kW m^{-1}, where ρ is the seawater density (1025 kg/m^3), g is the gravitational acceleration (9.81 m/s^2), H_{rms} is the root-mean-square wave height (m), T_p is the peak period (s). The H_{rms} was approximated by $H_s/\sqrt{2}$ and T_p was approximated by the significant wave period. Non-instantaneous storm response was evaluated for periods of 1 and 2 months between two data points. Because the decomposition was based on monthly-averaged data, a period of 1 month between data points equalled a total period of 2 months of data. Similarly, a period of 2 months between data points was based on 3 months of data.

To study if a possible relation existed between the cumulative wave power and the observed shoreline change, for instance within a time period of 2 months, all possible combinations of data points from the remainder component that were spaced 2 months apart were selected. Subsequently, for every two data points spaced two months apart, the shoreline change between the two data points was computed, as well as the sum of the wave power for that particular period. For an interval of 2 months, the wave power was calculated over a period of 3 months, as explained above. Another data point could exist between the interval of 2 months. However, including this data point by approximating a linear line through all three points and then quantifying its slope instead of computing only the shoreline change between the first and last point, barely influenced the results. Therefore, it was chosen to solely calculate the shoreline change between two points. The same was done for an interval of 1 month between data points. To visualise the results, the sum of the wave power was plotted against the shoreline change and a linear trendline was drawn through the points to assess a potential relation between the wave power and the shoreline change. It was expected that for a stormier period of time, a large negative shoreline change between two data points, indicating a considerable landward change in cross-shore shoreline position, would occur in combination with a large cumulative wave power.

5.3.2 Research question 2 - Effect of nourishments and their behaviour

Research question 2 aims to investigate the behaviour and spatial effects of beach and shoreface nourishments on the shoreline. To be able to study the effects of nourishments on the coast, detailed time-series graphs were made for each individual beach and shoreface nourishment. This included in total 23 beach nourishments and 10 shoreface nourishments. However, during this study the last shoreface nourishment was still under construction, therefore, this shoreface nourishment was not investigated.

The data used for this analysis comprised of the original data, thus the cross-shore positions with respect to the pre-nourishment shoreline, represented by the term $\widetilde{D_{sh}}(y,t)$ in Equation 7.

For each nourishment a subsection of the total dataset was extracted to take a closer look at the development of the coast over time as a response to one particular nourishment. The location and thus the total extent of each nourishment in longshore direction determined which transects were to be included in each subsection, so that the sides of a nourishment corresponded to the left- and right-hand side boundaries of a subsection. For beach nourishments it was decided to show the development of the shoreline 3 years before and 3 years after the construction period of the nourishment, since previous reports described a lifespan of 1 to 2 years for beach nourishments near

Egmond and Bergen (e.g. Boers, 1999) and beach nourishments along the Holland coast typically last for a maximum of 3 years (Brand et al., 2022). Therefore, each subsection including a beach nourishment contained about 6 years of data. For shoreface nourishments a longer time period was utilised because generally these have a longer lifespan. Quartel & Grasmeijer (2007) reported a lifespan of approximately 5 years for a shoreface nourishment in front of Egmond after which the beach volume returned 'back to normal'. Furthermore, the average recurrence time of shoreface nourishments for a regularly nourished location along the Holland coast is 5.2 years (Brand et al., 2022). Consequently, in case of shoreface nourishments it was determined to evaluate the development of the shoreline 5 years prior to and 5 years after the construction.

Subsequently, the transects within each subsection were used to calculate the alongshore-average cross-shore position of the shoreline for every timestep within the chosen time span. Again, because the data was alongshore-averaged, some variation existed around the alongshore-averaged time-series. Typically, the average variation (standard deviation) was between 10 and 15 m for shorter nourishments and on average between 15 and 20 m for longer nourishments. It is important to be aware of these variations around the mean when studying the results of this analysis. Timesteps for which no alongshore-average cross-shore shoreline position could be computed due to missing values were removed from the time-series as well as significant outliers, so that a continuous time-series without gaps remained. The alongshore-averaged time-series for each beach or shoreface nourishment could then be plotted over time. Logically, during a time period of about 6 or 10 years, besides the studied nourishment in a subsection, the other beach and shoreface nourishments also show up in the time-series. Their possible effect on a to-be-studied nourishment cannot be neglected, therefore, all other occurring nourishments within the chosen time span were also indicated in the graphs.

To further investigate the spatial effect and impact on nearby non-nourished beaches, a similar analysis was conducted but this time for the area adjacent to each beach and shoreface nourishment. In case of beach nourishments, the adjacent areas 500 m to the south and north of each nourishment were adopted. In case of shoreface nourishments, it was chosen to only look at the area 1000 m to the south and to the north of each shoreface nourishment. Therein the extent of the study area to the north was a limiting factor.

In addition to the methods described above, the standard deviation from the mean was used as a method to study the alongshore variability of the shoreline over time. To compare a nourished and unnourished coast in their behaviour and development, the study area was divided into two sections: the nourished coast between RSP 3000 and 3995 and the unnourished coast between RSP 4000 and 4350. The data used to compute the standard deviation also comprised of the time-series data contained in the term $\widetilde{D_{sh}}(y,t)$ of Equation 7, thus, the cross-shore positions with respect to the pre-nourishment profile. For both sections the alongshore average cross-shore shoreline position was computed for each timestep, whereafter the standard deviation could be determined from each alongshore-averaged position. Moreover, the nourishment analysis was supplemented with the Hovmöller plots and the satellite images to further study the (spatial) effects of beach and shoreface nourishments.

6. Results

In this chapter the most important results will be described that emerged from the analyses detailed in the preceding chapter. First, the general characteristics of the data will be portrayed with Hovmöller plots. Thereafter in Section 6.2, the results will be outlined regarding research question 1, including the results from the decomposition of the time-series and the analysis of the storm response. In Section 6.3 the results regarding the nourishment practices at the coast of Egmond-Bergen will be delineated based on Hovmöller plots, satellite images, and alongshore-averaged time-series graphs. There will be a focus on the spatial effects of the nourishments as well as the typical dynamics of beach nourishments.

6.1 Spatiotemporal shoreline evolution

In Figure 6.1, the original cross-shore shoreline positions for each transect ($D_{sh}(y,t)$) are presented within a Hovmöller plot with the alongshore distance on the x-axis and the time on the y-axis. As can be derived from this figure, the coast shows large alongshore variability. The figure implies that in the north (RSP 3000), the coastline is located relatively further landward than in the south (RSP 4350) with respect to the most landward point of each transect (zero-point). However, this considerable alongshore variation can for a large part be attributed to the fact that the location of the origin and extent of each transect were calculated based on the positions of the RSP points. As explained in Chapter 5.2, the RSP points only form an artificial reference line and do not give an accurate representation of the most recent position of the coastline in front of Egmond and Bergen. To exclude the influence of the RSP points on the result of the cross-shore shoreline positions, the average shoreline position calculated between 1985-1989 (pre-nourishment profile) was subtracted from the

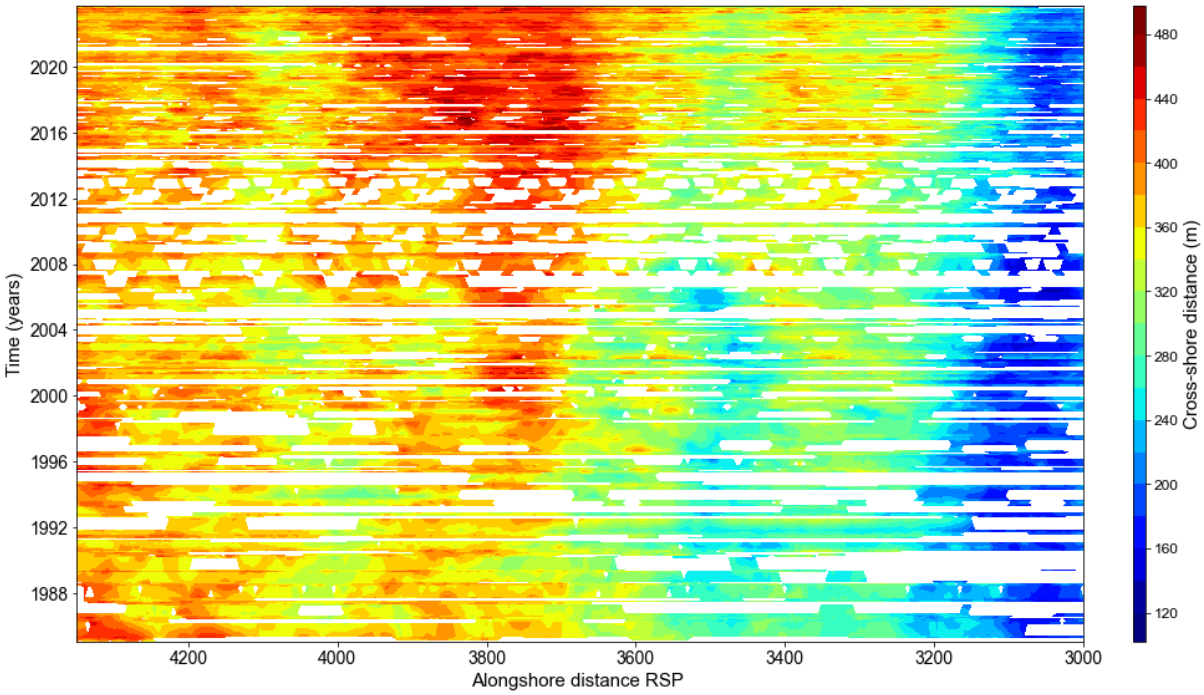

Figure 6.1: Hovmöller plot in which the entire evolution of shoreline ($D_{sh}(y,t)$) is visualised in time and in space, whereby the time is plotted on the vertical axis and the alongshore distance on the horizontal axis. The alongshore distance is expressed as beach pole distance (RSP) with one kilometre between beach poles 30.00 and 31.00 and so on. Therefore, the interval of 200 on the x-axis represents an interval of 2 km with 3000 corresponding to beach pole 30.00 in the study area. This same notation is used in all figures comparable to this one. North is to the right and south is to the left. The blank spaces between the data represent missing values.

data (Chapter 5.2, $\widetilde{D}_{sh,t=1..5}(y)$). This yielded Figure 6.2 ($\widetilde{D_{sh}}(y,t)$), giving a very different view of the development of the coast, in which the cross-shore distance is presented with respect to the pre-nourishment profile. The shoreline is situated more seaward with respect to the pre-nourishment profile when data points are represented by a warmer colour, whilst a cooler colour indicates a more landward situated shoreline.

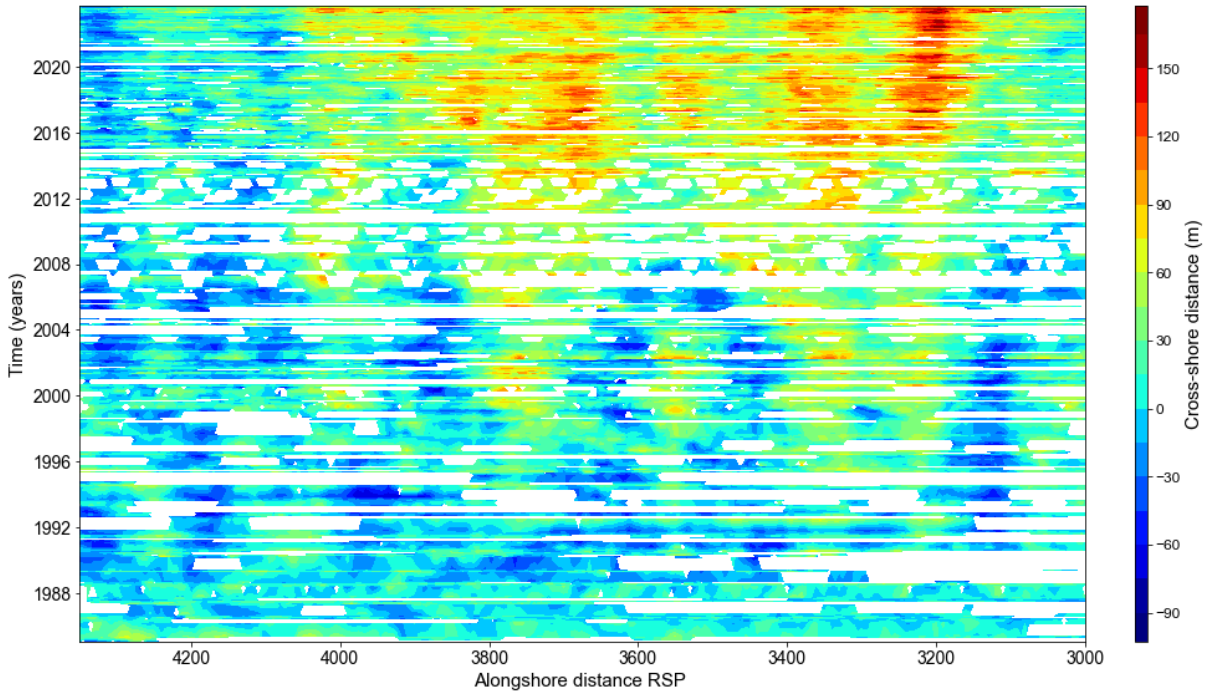

Figure 6.2: Hovmöller plot of the evolution of the shoreline relative to the pre-nourishment profile ($\widetilde{D_{sh}}(y,t)$). Time is plotted on the vertical axis and the alongshore distance (RSP) on the horizontal axis. North is to the right and south is to the left.

Although Figure 6.1 and Figure 6.2 look quite different, some similarities can still be found regarding the cross-shore change over the time axis. At first inspection, the coastal section between RSP 4000 and 4350 does not show considerable change over time, which can be recognised in both figures. On the contrary, the coast in front of Egmond (RSP 3800) and Bergen (RSP 3300) shows large variability over time with in some locations considerable seaward advance alternated with locations that experienced less or no shoreline progradation, especially in earlier years. This becomes very clear from Figure 6.2 but this is also apparent in Figure 6.1. At the end of 2023 can be observed that between RSP 3000-4000 most alongshore sections are situated approximately 50-80 m more seaward than the pre-nourishment profile, while some sections also show a seaward advance between 80-100 m (Figure 6.2).

To further analyse landward retreat/seaward expansion of the coastline and study the alongshore variability, the data was both 'demeaned' over the time axis and over the alongshore axis. In Figure 6.3, the data demeaned over the vertical or time axis is shown ($\widetilde{\widetilde{D_{sh,t}}}(y,t)$). The variation in cross-shore shoreline positions can be seen as perturbations or relative changes around the mean cross-shore position calculated for each transect. Positive values indicate a more seaward position, while negative values indicate a more landward position of the shoreline relative to the mean. Figure 6.3 clearly indicates seaward expansion of the shoreline, most prominent between RSP 3100 and 4000. Whereas in the first years of this section mostly values occurred between -30 and -120 m, in later years much more values can be observed between +30 and +90 m. Especially since 2012 all 'blue' parts in the graph

are almost completely replaced by more 'redder' values. Although this may seem the case, blue colours in the graph do not necessarily point to erosion of the beach, it solely indicates that in later years the shoreline is located more seaward in comparison to these earlier years.

In the south near Castricum aan Zee, RSP 4000-4350, the values fluctuate around 0, indicating no major change in cross-shore shoreline position over time.

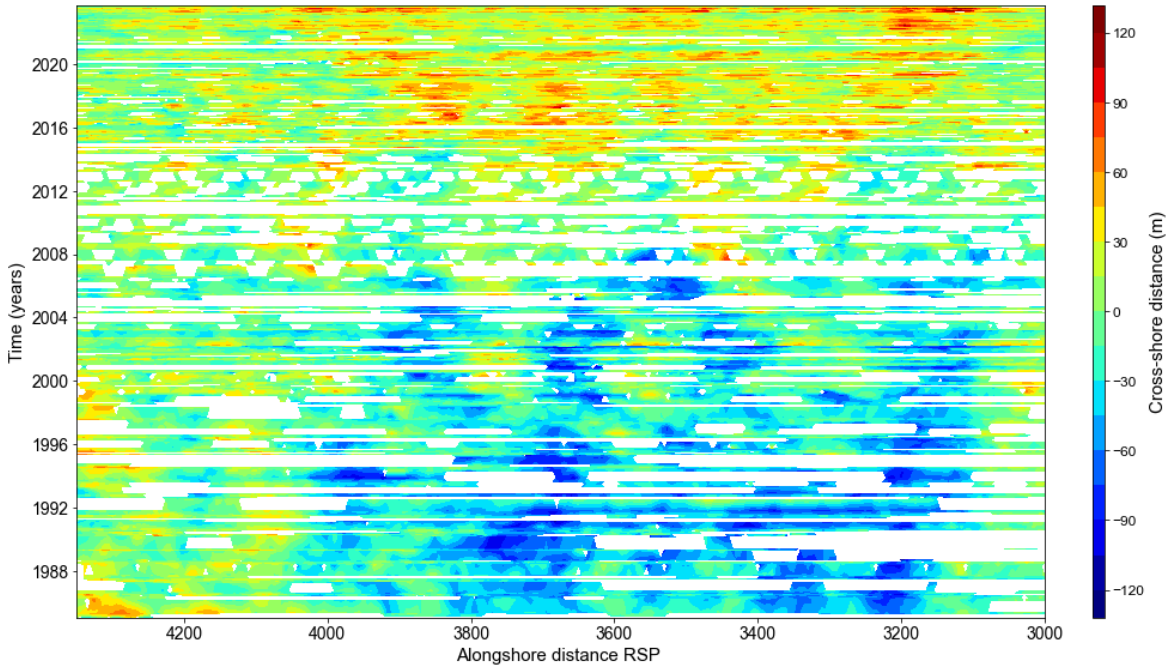

Figure 6.3: Hovmöller plot of the shoreline evolution relative to the average shoreline position calculated as a function of space ($\overline{D_t}(y)$). Time is plotted on the vertical axis and the alongshore distance (RSP) on the horizontal axis. North is to the right and south is to the left.

In Figure 6.4 the data demeaned over the alongshore axis is presented ($\widetilde{\overline{D_{sh,y}}}(y,t)$), whereby the mean alongshore position for each timestep was subtracted from every data point measured at that timestep. With this method, the alongshore variability over time is highlighted in contrast to the previous graph which was more aimed to display potential patterns in seaward expansion or landward retreat of the shoreline. An important finding is that initially the alongshore variability was limited until about 1996. Thereafter, the shoreline starts to show considerable variation over the alongshore axis. Especially around RSP 3300 (Bergen) and RSP 3800 (Egmond) bands of more red and warmer-coloured values can be detected, where the shoreline protrudes further seaward than the adjacent shoreline further north and south. These 'bands' characterised by positive values near Egmond and Bergen can also be recognised in Figure 6.3.

The results of Figures 6.2, 6.3 and 6.4 will be further elucidated in Sections 6.2 and 6.3.

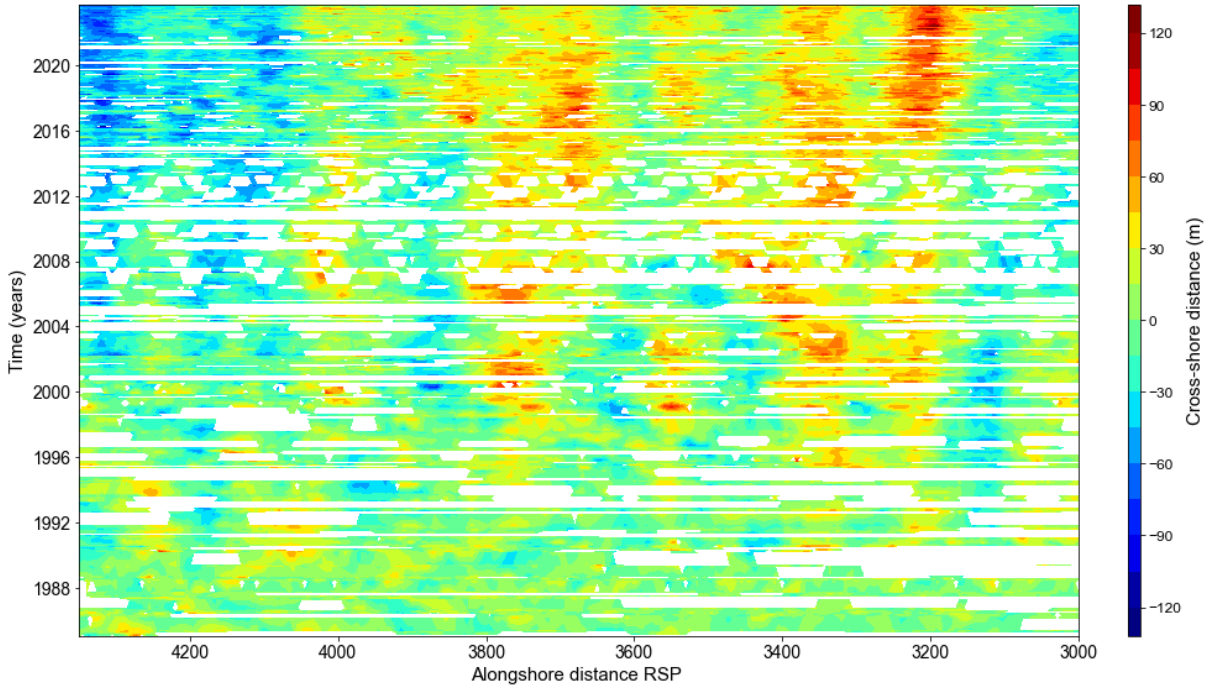

Figure 6.4: Hovmöller plot of the shoreline evolution relative to the average shoreline position calculated as a function of time ($\overline{D_y}(t)$). Time is plotted on the vertical axis and the alongshore distance (RSP) on the horizontal axis. North is to the right and south is to the left.

6.2 Time-series decomposition

6.2.1 Identification timescales of change

The decomposition in a trend, seasonal, and remainder component for each of the four coastal sections is presented in Figure 6.5, based on $\widetilde{\widetilde{D_{sh,t}}}(y,t)$. Section A corresponds to Bergen, Section B to the area between Bergen and Egmond, Section C to Egmond, and Section D to Castricum (Figure 5.8).

In the graphs of Figure 6.5, the interannual component is expressed by the trend recognised in the data by JUST, intra-annual fluctuations represent seasonality, and the remainder captures the short-term fluctuations caused by storm events but also includes the inaccuracies or so-called noise in the data. All three northern sections (A, B, C) that are affected by nourishments show an increasing interannual trend. The most southern unnourished section (D), on the other hand, exhibits no identifiable increasing or decreasing trend by first visual inspection. Furthermore, the magnitude of the seasonality is in all four cases rather small, the amplitude is typically around 10 m or less and varies over time and even between consecutive years. Sometimes relatively long periods occur with a temporary decrease in seasonality. In section B the amplitude of seasonal variation is smaller between approximately 2007 and 2015 than in the rest of the time-series. In section D also a decline in amplitude of seasonality can be seen between 2000 and 2015, whereafter it increases again. Sometimes seasonality is even completely lacking, indicated by the values of zero in section A during 2002-2010. It is possible that the shoreline during that time did not show a marked response to the seasonality that, on the other hand, does present itself in the wave climate of the Dutch Holland coast. However, it is important to note that between 2006 and 2012 less satellite images were retrieved with CoastSat, often only 6-9 images, in contrast to neighbouring years with more than 10 images. In addition, not all shorelines were always complete and an adequate number of images during the winter period was not always obtained, making it more difficult to capture seasonal cycles. This is likely to contribute to the absence of seasonality in the shoreline positions. Although the magnitude of the seasonality varies over time, a distinction of five negative peaks in autumn/winter and five positive peaks in spring/summer during a time period of 5 years (interval on the x-axis) is almost always visible. This is corroborated in Figure 6.6, where negative peaks occur simultaneously with larger wave heights, and positive peaks coexist with smaller wave heights during summer (Figure 6.6 will be discussed below in a more elaborate way). The negative peaks in the seasonality component typically have larger values than the positive peaks. While during winter peaks occur with values down to -15 m, in summer peaks at most are characterised by values of 10 m. This is most apparent from sections B, C and D. The shoreline thus seems to experience a larger retreat during winter in comparison to its seaward advance in summer. The decomposition of the four time-series was executed with a significance level α of 0.05. Setting the significance level to 0.01 (=default in JUST) was also attempted but this yielded even less seasonality with longer time periods where no seasonality could be defined by JUST. However, this does highlight the lack of dominance of seasonality in the time-series.

JUST decomposition was also performed on the time-series of significant wave height and the corresponding wave period for 1985-2023. The results of the decomposition are included in Appendix B. In contrast to the four coastal sections studied and as shortly mentioned above, the wave height and wave period do exhibit clearly recognisable seasonality in their time series. One distinct positive peak occurs in autumn/winter when the wave height and wave period are generally larger along the Dutch coast (storm season), while a negative peak occurs during spring/summer with smaller wave heights and periods coinciding with calmer weather conditions. The amplitude of seasonality for the wave height and period amounts to approximately 0.5 m and 0.7 s respectively. The mean wave height and period during the measurement time amounted to 1.18 m and 5.46 s.

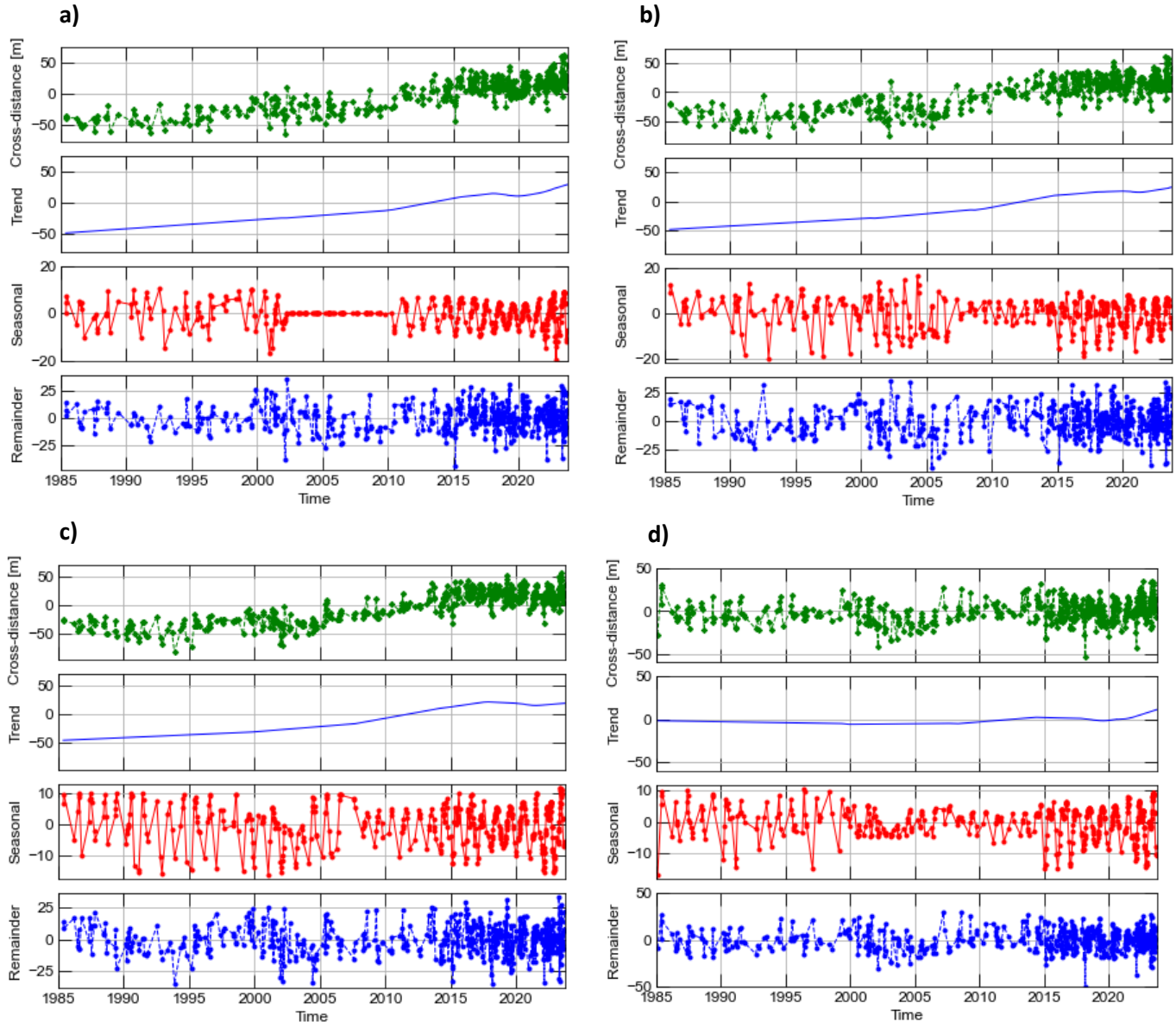

Figure 6.5: JUST decomposition of the four coastal sections defined: (a) corresponds to Section A in front of Bergen; (b) corresponds to Section B in between Bergen and Egmond; (c) corresponds to Section C in front of Egmond; and (d) corresponds to Section D in front of Castricum.

A comparison of the seasonality within the Dutch wave climate with the seasonality in the shoreline positions (Figure 6.6) visualises that seasonal shoreline retreat coincides with more energetic waves in the storm season (autumn/winter). And, at the same time, seasonal expansion of the shoreline coincides with the lower energetic waves in summer. The shoreline in front of Egmond and Bergen thus does possess some seasonality and follows the seasons in wave climate but only to a limited extent.

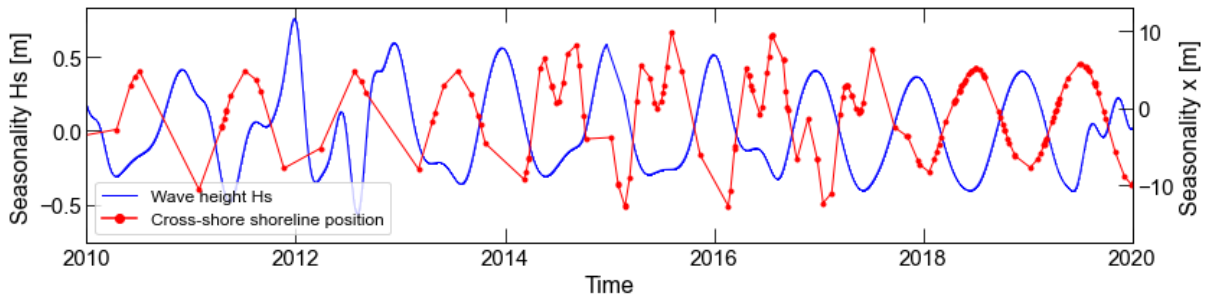

Figure 6.6: Combination plot of the seasonality that is present in the cross-shore shoreline positions (x) with the seasonality contained in the time-series of significant wave height (Hs). The seasonality in shoreline positions portrayed here was derived from section C (Egmond) and is the same time-series shown in Figure 6.5c. Note that a subset of the data was taken, this plot only considers 2010-2020 in order to provide enough detail.

With the Mann-Kendall test statistically significant trends in the four coastal sections were identified and quantified with Sen's slope estimator. The significance of a trend was tested against a significance level α of 0.01. A p-value less than 0.01 would indicate the presence of a significant trend. Table 6.1 gives the strength (p-value) and direction of the trend as well as the quantified slope for the four sections.

Table 6.1: Presence of a statistically significant trend, p-value, trend direction and Sen's slope given for all four coastal sections (A, B, C, D).

	Section A	**Section B**	**Section C**	**Section D**
Statistically significant trend (True/False)	True	True	True	True
p-value	0.0	0.0	0.0	0.0
Trend direction	increasing	increasing	increasing	increasing
Slope (m/year)	2.097	1.997	1.907	0.314

In all four sections an increasing long-term trend was determined, indicating a seaward expansion of the shoreline over time. For all four sections a strong trend was found with a p-value of zero or a p-value so small that it was presented by zero in the MK-test. In Figures 6.5a-c the increasing trends are visualised. The three trends all present a gradual advance of the shoreline, and in particular from 2010 an even more pronounced increase in the trend appears to be present in all three sections. Despite that, the trend in section C seems to stabilise near the end of the time-series, which to a lesser extent also seems to take place in section B. The three northern sections in the study area, all being affected by nourishments, exhibit a similar rate of change per year of approximately 2.00 m/year according to Sen's slope. Over the study period of almost 40 years this corresponds to a shoreline expansion between 70-80 m in the three nourished sections. For the section in the south in the neighbourhood of Castricum the MK-test also indicates a positively increasing trend. However, this is a rather slow increasing trend with a slope of only 0.31 m/year, which ultimately only results in less than 12 m shoreline expansion over almost 40 years of time. The trend in Figure 6.5d is almost constant over time and the shoreline thereby presents itself to be fairly stable. Interesting to observe is the sudden increase in the trend after 2020. This relatively large increase near the end of the time-series can also be recognised in section A.

Table 6.2: The contribution of each individual component (trend, seasonal, remainder) to the total variance, the latter being the sum of variance captured in the three components. This was performed for all four coastal sections (A, B, C, D).

Contribution to total variance	Section A	Section B	Section C	Section D
Trend	73.3%	70.3%	75.6%	10.7%
Seasonal	4.22%	5.99%	5.55%	15.9%
Remainder	22.5%	23.7%	18.9%	73.4%
Total	100%	100%	100%	100%

The relative contributions of the trend, seasonal and remainder component to the total variance contained in the time-series of the shoreline positions are presented in Table 6.2. The relative contributions are expressed as a percentage of the total sum of the variance captured in the three components. In the three northern sections, about 70% of the total variance is explained by the trend component. The results confirm the limited presence of seasonality in the time-series; the seasonality component only explains about 4-6% of the total variance contained in the time-series of sections A, B, C. This is in contrast to the distinct seasonality in the wave climate of the Netherlands with approximately a difference of 1 m in wave height between winter and summer (Appendix B). The remainder component contributes approximately 20% to the total variance. In section D a notable different distribution of the variance occurs. Only 10.7% is associated with the trend component, while the seasonal and remainder components explain 15.9% and 73.4% of the total variance respectively.

6.2.2 Storm response

The remainder component includes the inaccuracies that are present in the data but it also represents the short-term changes in the shoreline position caused by storm events for example. Shoreline change as a result of storms can also be captured by CoastSat because the magnitude of change typically exceeds the horizontal accuracy of ±10 m. The (instantaneous) response of the shoreline to individual storm events is shortly assessed below, whereafter the more non-instantaneous behaviour is reviewed with a second analysis.

Figure 6.7 gives an overview of storm events with Hs ≥ 5 m that were captured in the time-series of the significant wave height. It was decided to solely look at storm events with a significant wave height exceeding 5 m as these are heavier storms and are expected to cause the most shoreline change. Table 6.3 gives the approximate duration and the maximum significant wave height of the storms extracted from Figure 6.7 after 2015. Subsequently, the time period of each storm event was visualised in the graph of the remainder component for each of the four coastal sections. Figure 6.8 shows this graph for a nourished coast, section A, and Figure 6.9 shows it for section D, the unnourished coast. In Appendix C the results for all four sections are included. Figures 6.8 and 6.9 both do not portray a large retreat of the shoreline between two closely following data points in case of a large storm event. In most cases, only small-scale fluctuations occur and a considerable negative shoreline change cannot be inferred. Even if some shoreline regression occurs, the shoreline thereafter seems to quickly or immediately return to its pre-storm profile. For instance, the last storm of 2022 coincides with a more landward located shoreline but the closely following data point already shows a shoreline position similar to before the storm. The only years where the shoreline seems to have been more notably affected by a storm event include 2019 (multiple storms) and the first storm of 2022 whereby the shoreline temporarily shows a landward retreat. Furthermore, a difference in response between a nourished or unnourished coast cannot be distinguished (compare Figures 6.8 and 6.9). Important to take into account is the large presence of noise in the remainder part, which makes it difficult to locate

individual storm responses in the time-series. This gives some uncertainty in the results, but regardless of that, it can still be derived that the shoreline is barely affected by individual storms, especially considering the selection of relatively large storms.

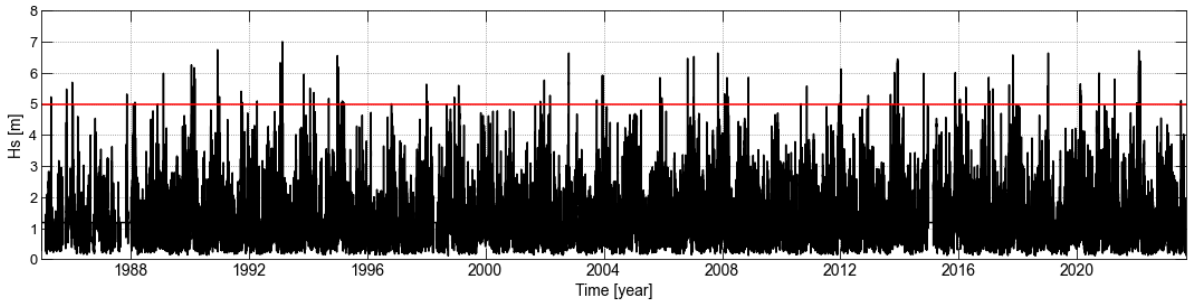

Figure 6.7: Significant wave height H_s measured at a 10-minute interval. This is the same time-series as shown in Figure 5.5. Storm events with a wave height $H_s \geq 5$ m are indicated by the horizontal red line.

Table 6.3: Additional information for the storm events indicated in Figure 6.7 with wave height $H_s \geq 5$ m. Both the duration of the storm and the maximum significant wave height are given.

Large storm events ($H_s \geq 5$ m)		
Event	**Approximate duration of storm (dd/mm/yy)**	**Maximum significant wave height H_s (m)**
1	18/11/2015 – 19/11/2015	6.00
2	16/01/2016	5.15
3	28/03/2016	5.53
4	03/01/2017 - 04/01/2017	5.25
5	13/01/2017 - 14/01/2017	5.41
6	23/02/2017 - 24/02/2017	5.40
7	12/09/2017 - 14/09/2017	5.61
8	28/10/2017 – 29/10/2017	6.57
9	01/01/2019 – 02/01/2019	5.57
10	08/01/2019 – 09/01/2019	6.63
11	09/02/2020 – 12/02/2020	5.64
12	26/09/2020 – 27/09/2020	5.99
13	05/04/2021 – 07/04/2021	5.79
14	01/05/2022	5.03
15	30/01/2022 – 31/01/2022	6.71
16	18/02/2022 – 21/02/2022	6.37
17	05/07/2023	5.10

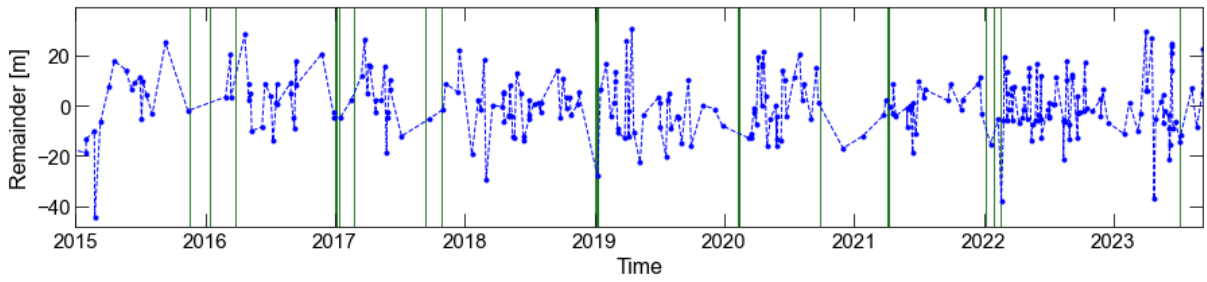

Figure 6.8: The remainder component resulting from the decomposition of the time-series of Section A (Bergen) between 2015-2023. The green lines represent the timing of the storm events that are included in Table 6.3. In some cases the green lines coincide (darker green lines) when storms occurred shortly after each other, therefore not all individual storms are clearly distinguishable.

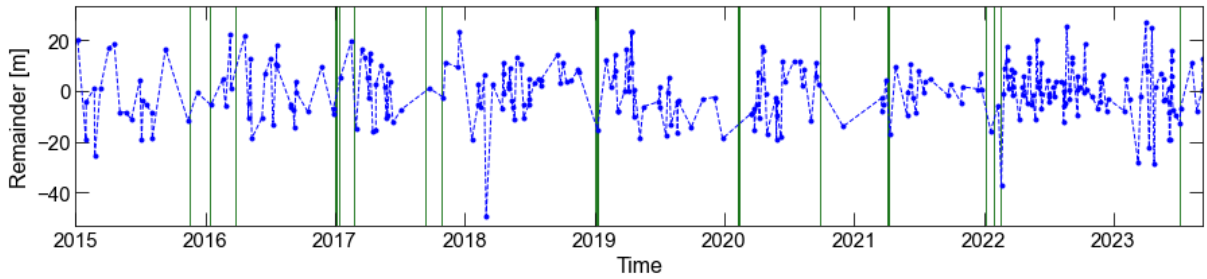

Figure 6.9: The remainder component resulting from the decomposition of the time-series of Section D (Castricum) between 2015-2023. The green lines represent the timing of the storm events that are included in Table 6.3. In some cases the green lines coincide (darker green lines) when storms occurred shortly after each other, therefore not all individual storms are clearly distinguishable.

An analysis of the influence of storm events on the coast was also carried out considering the non-instantaneous response of the shoreline. Figure 6.10 shows the results for two of the four coastal sections (A, D) considering an interval of 2 months, that is, 3 months in total. The results for the 1 month-interval (i.e. 2 months in total) are included in Appendix D. The graphs for both 1 and 2 month-intervals barely show a relation between the sum of the wave power and the shoreline change between two data points. A linear regression line was plotted through the data points but for all four coastal sections the R-squared value ended up being negligibly small, indicating no linear relationship. Additionally, the p-values were in all cases much larger (i.e. ranging from 0.28 to 0.99) than a significance level α of 0.05 ($p > 0.05$), meaning that the results were not statistically significant. The analysis performed for a 2-month interval does show that some data points with higher wave power were also characterised by a more negative shoreline change in Figure 6.10a. However, the other graphs do not portray the same and within the graphs regarding a 1-month interval (Appendix D) this pattern is even less visible. Overall, the results do not indicate that after a time period of 2 or 3 months with many storm events (high cumulative wave power), afterwards a substantial retreat of the shoreline can be observed.

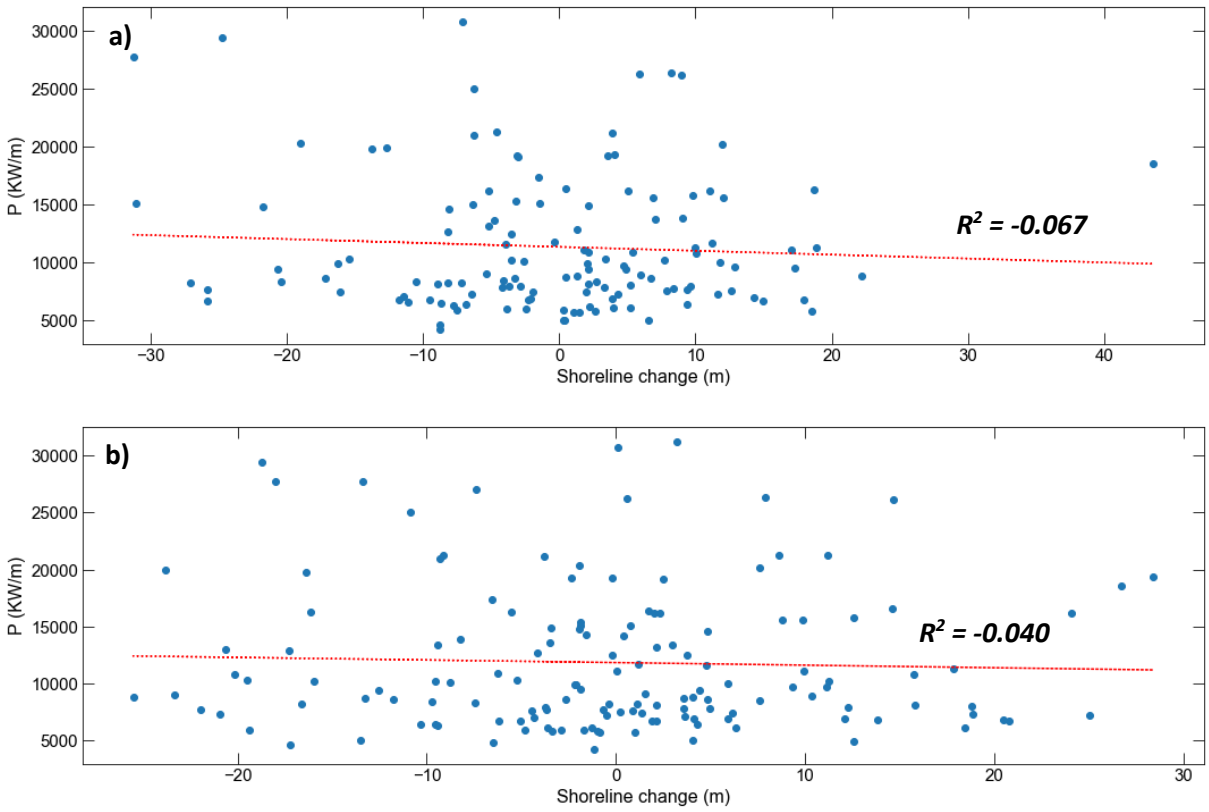

*Figure 6.10: The sum of the wave power P (H_{rms}^2 * T_p) plotted against the shoreline change between each two data points spaced 2 months apart, for: (a) Section A (Bergen); (b) Section D (Castricum).*

6.3 Nourishments

6.3.1 Hovmöller plots

Figure 6.11 shows the shoreline evolution relative to the pre-nourishment profile ($\widetilde{D_{sh}}(y,t)$) (a) and the shoreline evolution represented by $\widetilde{\widetilde{D_{sh,y}}}(y,t)$ (b) but now the timing, the alongshore extent, and the volume of the nourishments are also presented. Figure 6.11b is more aimed at showing the alongshore variability of the coastline to highlight the nourishments. In both graphs the influence of the nourishments can be seen when comparing the nourished section between RSP 3000-4000 and the unnourished section between 4000-4350. The shoreline underwent much more changes within the nourished section with, as aforementioned, in total a seaward shoreline expansion of roughly 60-80 m with respect to the pre-nourishment situation. In contrast, the unnourished section near Castricum seems to be fairly stable, confirming that nourishments in this part were not required. This was also noticeable in Figure 6.3. It is important to keep in mind that the values Figure 6.11b presents cannot be interpreted as absolute values of erosion and accretion since the data was demeaned. For instance, the blue part of Figure 6.11b in the south in later years is not caused by erosion but it is the result of the red values in the north for which the blue has to compensate to equate to zero over the alongshore axis.

Until 1999 only beach nourishments were placed at Egmond and Bergen. It turned out to be difficult to specifically locate the individual beach nourishments in these figures, the implementation of a beach nourishment does not lead to a localised region with considerable positive shoreline change (e.g. red peaks/clusters) in Figure 6.11a. At most, a local region with yellowish or greenish values instead of former blue values occurs after a beach nourishment. The beach nourishment, with a relatively large volume of 306 m^3/m, completed in 1995 and situated around RSP 3300 is an example where a small, localised area of greener values can be noticed. Though, it is difficult to say if these green areas can all be attributed to beach nourishments or that they are also the result of the natural variation of the shoreline. In Figure 6.11b beach nourishments appear to be a little bit more prominent, especially between RSP 3200 and 3400 a broad region of more positive values starts to make an appearance since approximately 1995. Near Egmond (RSP 3800) the same phenomenon takes place since 1995 but to a lesser extent. The absence of explicit visible beach nourishments in Figure 6.11b implies that the nourishments could not have largely protruded in seaward direction in comparison to the adjacent coastline.

Figure 6.11 indicates that the beach nourishments barely resulted in permanent accretion of the shoreline in the study area. The shoreline position roughly remained around the same cross-shore position (until the first shoreface nourishments), even though nourishments were carried out. Based on the figures it can be observed that the repeated beach nourishments resulted in less than about 10 m of shoreline advance over the time period from 1990-1999 when also considering the natural variation present in the coastline. The implementation of a new nourishment every one or two years was essential for the system to maintain the coastline, although it is hard to quantify the exact erosion from these graphs that would have taken place without nourishments.

In 1999 the first shoreface nourishment was constructed in front of Egmond. Interesting to notice is that the addition of shoreface nourishments leads to a more prominent response of the coastline. Only after the first shoreface nourishments were carried out in 1999 and 2000, the shoreline position started to show the first signs of sustainable shoreline progradation. The progradation expresses itself in a very localised manner in Figure 6.11a and Figure 6.11b. Specifically, in front of Egmond and Bergen some sort of ‘bands’ containing more positive values make an appearance. These bands correspond to the location of the nourishments and stay roughly in the same place over time and can be tracked all the

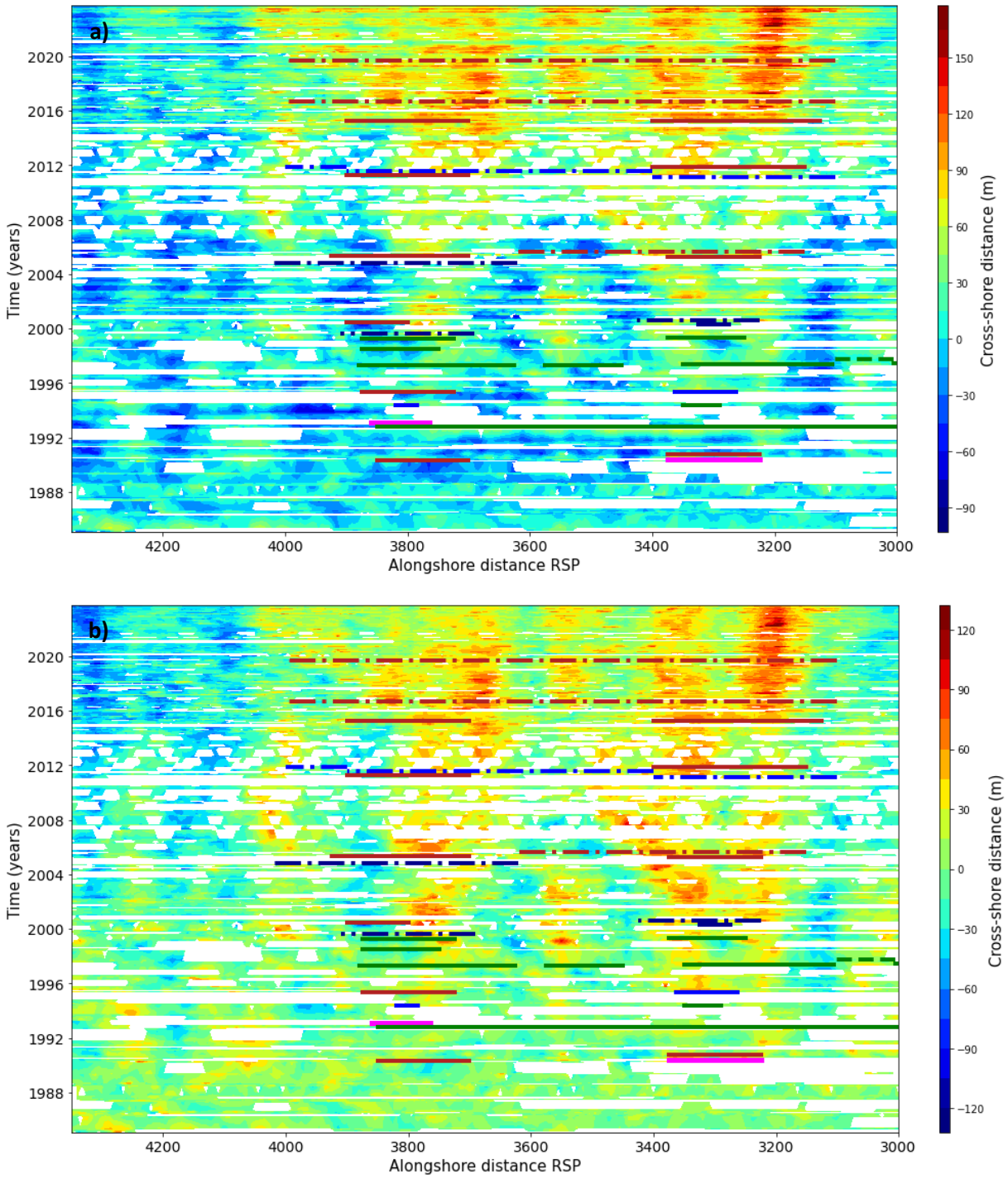

Figure 6.11: Shoreline evolution with the alongshore extent and timing of the nourishments: (a) relative to the pre-nourishment profile ($\widetilde{D_{sh}}(y,t)$); (b) demeaned over the alongshore axis ($\widetilde{\widetilde{D_{sh,y}}}(y,t)$). Important is that the nourishments are displayed by plotting the end of the construction. A distinction is made between beach, shoreface and 'other' types of nourishments. The volumes (m^3/m) of the nourishments are also presented and can be found in the corresponding legend.

way to 2023. These bands are plausibly the result of the nourishments amplifying the natural variation in the coastline. After a beach nourishment in 1997 that was placed in between Egmond and Bergen (RSP 3450-3575) such a band with shoreline expansion also occurs. Based on the Hovmöller plots alone it is difficult to say if this shoreline expansion can be attributed to this specific beach nourishment or that other processes also play a role, such as the influence of the adjacent beach and shoreface nourishments. Around 2005 and 2012 a beach nourishment is combined with a shoreface nourishment both at Egmond and Bergen. In 2015 the last beach nourishments were placed, whereafter a nourishment programme was initiated that introduced even larger shoreface nourishments extending over the whole area from RSP 3100-4000. In particular after 2012 and with the implementation of these larger shoreface nourishments, the most seaward expansion of the shoreline took place. After 2012 almost all blue negative parts in Figure 6.11a were replaced by positive values, with red and orange colours dominating the spectrum. Interesting is that Figure 6.11a thus displays a very gradual shoreline progradation over time ever since the continuous programme of shoreface nourishments was initiated. Taken together, the figures imply that most positive shoreline change is associated with repeated shoreface nourishments (in combination with beach nourishments) (~50 m), while beach nourishments only contribute a minor part (< 10 m). However, although the last two shoreface nourishments resulted in much shoreline accretion, the shoreline also seems to stabilise around these years. In contrast to what you would expect, the last shoreface nourishment in 2019 does not result in further progradation of the coast after the previous nourishment in 2016, it rather keeps the shoreline at the same level. Additionally, in more recent years the aforementioned repeating orange/red 'bands' are most visible, providing a good opportunity to determine the typical wavelength of these features. These bands present themselves with a longshore wavelength between approximately 1 and 2 km. An important observation includes that these bands do not appear to migrate over time but instead stay put at the same location.

Furthermore, it is remarkable that the repeated nourishments carried out in the study area barely seem to influence the shoreline adjacent to the nourished parts based on Figures 6.11a & b. In front of Bergen, some slight alongshore migration seems to be present, with 'greener' areas also adjacent to the initial extent of the nourishments. For beach nourishments, any effects are very difficult to observe since already they were hard to localise in the figures. Although, for shoreface nourishments alongshore migration of sand to adjacent coastal areas also seems to be limited. Only since 2016 the accretion of the shoreline starts to slightly flare out to both the northern and southern sides, becoming even more visible after 2019 whereby the sand also appears to migrate outside of the boundaries of the last shoreface nourishment (see also Figure 6.3).

Overall, the difference in the dynamics of the nourished and unnourished coast is striking. The southern part of the study area is characterised by almost no change in its behaviour, while the northern part of the study area shows much alongshore variability, strongly related to the anthropogenic impact on the beach. Figures 6.12a & b display the standard deviation around the alongshore-mean as a measure of the alongshore variability, for both the unnourished section (a) and the nourished section (b). In comparison with Figure 6.12b, the unnourished section exhibits a fairly constant progression of the standard deviation with at most a slight increase over time. On the contrary, the standard deviation calculated for the nourished area shows an unmistakable increase over time until the year 2000, whereafter the standard deviation stabilises around a more constant value. The stabilisation of the standard deviation coincides with the implementation of the first shoreface nourishments in 1999 and 2000. In recent years, the standard deviation even starts to decrease indicating the establishment of a more alongshore-uniform coastline, which takes place around the same time it was decided to implement the longer shoreface nourishments extending over the entire nourished area.

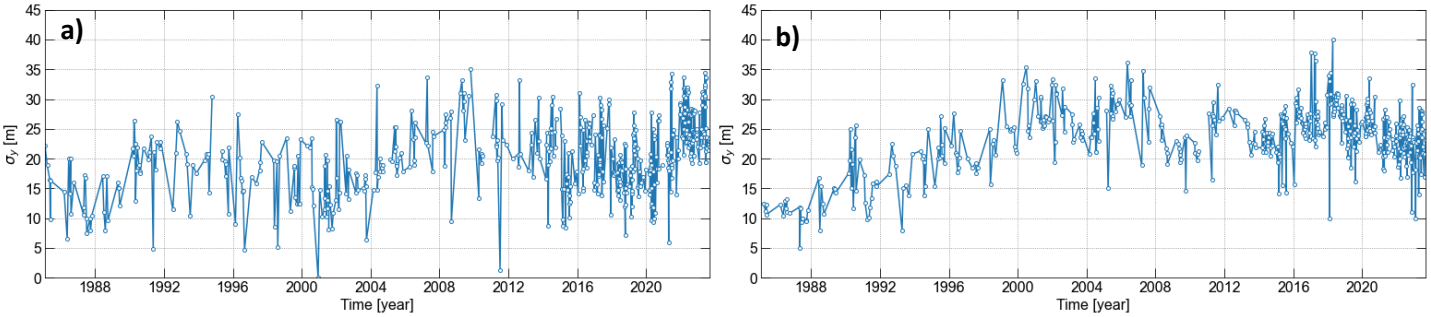

Figure 6.12: Standard deviation around the alongshore mean (σ_y) over time for: (a) the unnourished section of the study area between RSP 4000-4350; (b) and the nourished section of the study area between RSP 3000-4000. Gaps in the time-series represent years for which the alongshore mean could not be computed, for instance, because some years were removed with Otsu-thresholds outside of the range -0.5-0 (see Chapter 5.1).

6.3.2 Satellite images

Identifying beach nourishments in the satellite images proved to be challenging, which explains why they were barely visible in the Hovmöller plots as well. Figure 6.13 shows one satellite image prior and one satellite image after the implementation of two beach nourishments in April/May 1999 at Bergen and Egmond. This year was selected because it was one of the only years with satellite images acquired in the months shortly before the nourishment (e.g. on 12-02-1999). In general, most images acquired with CoastSat originated from spring/summer months and often the first image with a detected shoreline was collected in April or May. However, these are exactly the months in which often the construction works of nourishments are executed. Therefore, to be able to provide a satellite image of the situation before a beach nourishment, 1999 was selected. As can be observed, the satellite image taken on 06-08, two/three months afterwards, does not show an immediate visible sign of two beach nourishments. To better identify the potential perturbations in the shoreline, Figure 6.13b was exaggerated in its width. When carefully looking at Figure 6.13c, the beach does appear to be slightly wider in front of Egmond and Bergen in comparison with the adjacent coast. In front of Bergen, the coast even seems wider outside of the alongshore range of the beach nourishment, particularly to the north. Another, but cautious, observation may be that on 12-07-1999 the beach near Bergen appears

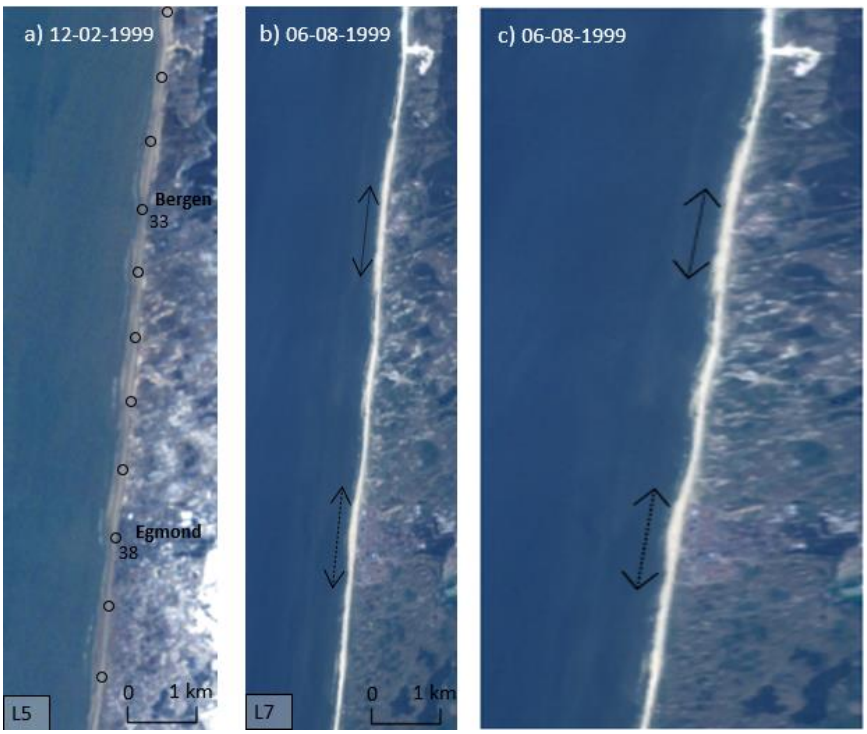

Figure 6.13: One satellite image prior to nourishing (in April/May-1999) and one satellite images afterwards: (a) Landsat 5 image taken on 12-02-1999; (b) Landsat 7 image taken on 06-08-1999; (c) same image as in (b), but the image is exaggerated in direction of the x-axis. In (a) the position of the beach poles is included, in total the images extend from RSP 30.00 to 40.50. The black arrows on the right images indicate the presumed alongshore extends of the two beach nourishments. Important to consider in the comparison is that (a) was probably taken at low tide, since some intertidal features are showing up on the image. However, this was the only image available prior to nourishing.

to be quite narrow, which seems to be resolved after nourishing. However, a large perturbation of the shoreline in seaward direction does not occur. The absence of a large seaward perturbation in the shoreline in 1999 is also representative of the other satellite images containing beach nourishments. However, in 2015 nourishments are a little bit more visible on the images and these are shown below.

Figure 6.14 presents five different satellite images before and after the implementation of two beach nourishments in April 2015 at Egmond (RSP 3700-3900) and Bergen (RSP 3125-3400). In contrast to the other beach nourishments, in these images more prominent features of the nourishments can be distinguished. The image taken on 20-04-2015 shows the nourishments while they are still partly under construction. Particularly, the beach nourishment in front of Bergen is not finished during this time, only a small extent has been constructed yet. On 07-06-2015 both beach nourishments are finished, noticeable is the large increase in longshore extent of the nourishment near Bergen. From the figures can be derived that both nourishments were probably placed relatively on a higher part of the beach, as they do not protrude very much seaward. In the areas adjacent to the nourishments the wet sand remaining from high tide is still visible, while this is less apparent in the areas of the nourishments, signifying the higher elevation of the beach after a nourishment. Both on 20-04 and 07-06 the edges of the nourishments can still be identified rather easily. Figure 6.15 provides a more detailed view of the beach nourishment carried out in front of Egmond. On 07-06, the nourishment already has had approximately 2 months to develop. Interesting to notice is that the northern edge of the nourishment shows small-scale spit formation during that time (indicated by the box). The southern edge on the

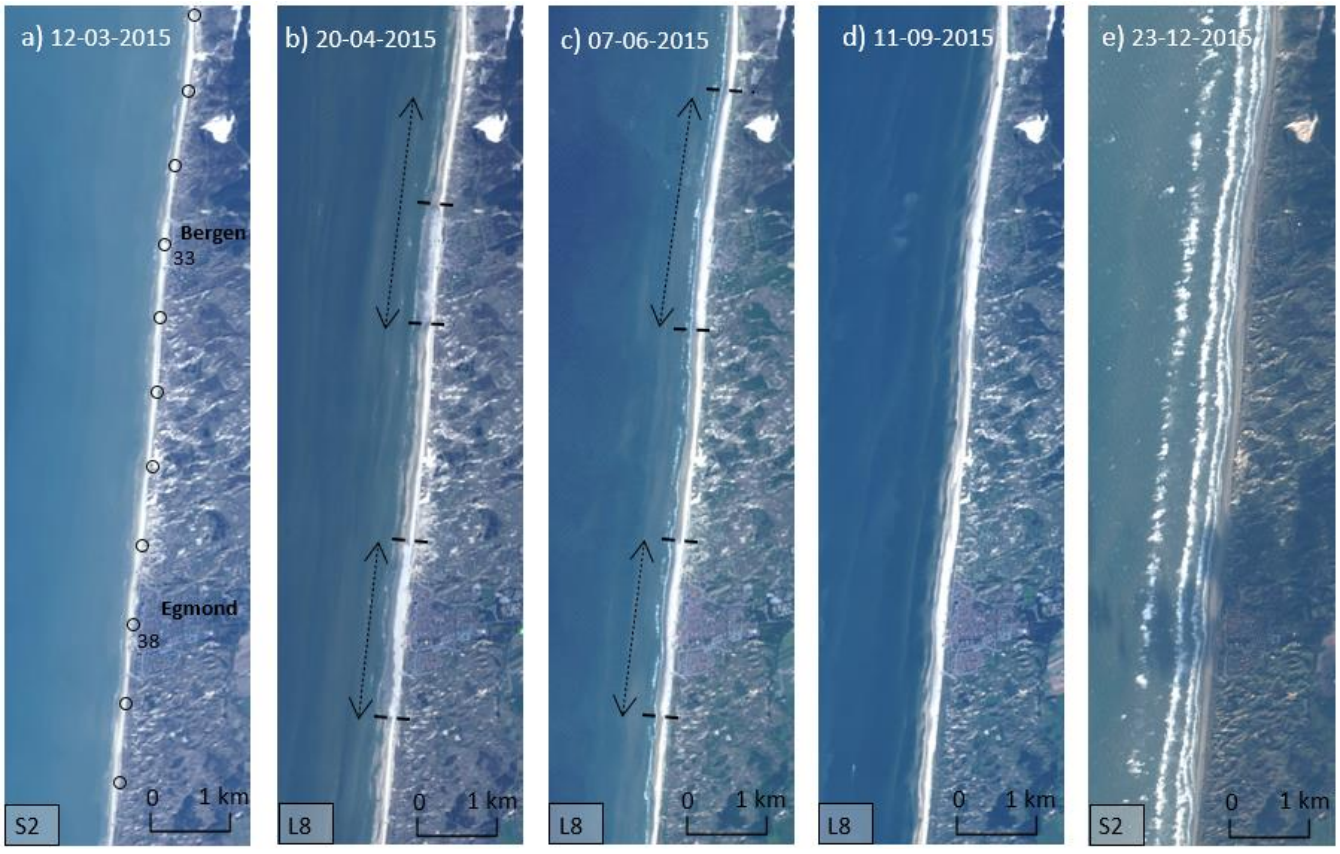

Figure 6.14: Five satellite images showing the progression of two beach nourishments performed in 04/2015 over time: (a) Sentinel-2 images of pre-nourishment shoreline on 12-03-2015; (b) Landsat 8 image on 20-04-2015 during which the construction of the beach nourishments was not finished yet; (c) Landsat 8 image on 07-06-2015; (d) Landsat 8 image on 11-09-2015; (e) Sentinel-2 image on 23-12-2015. In the left image the position of the beach poles is included, in total the images extend from RSP 30 to 40.5. In Figure (b) and (c) the edges of the nourishments were still distinguishable, consequently, the presumed extend and the edges of the nourishments are indicated by the black arrows and black dashed lines respectively.

other hand does not and solely shows a slightly protruding rounded edge. On 11-09-2015 the nourishments are already more difficult to recognise because they merged almost entirely with the shoreline. Alongshore migration again seems limited as far as the sand placed by the nourishments can still be tracked by visual inspection of the image; the sand could also have disappeared or been transported underwater. On 23-12-2015 wave conditions are more energetic, designated by the abundance of white-water. The beach appears narrower as a result of the higher water levels. Note that shoreface nourishments are constructed underwater and were not considered in this section.

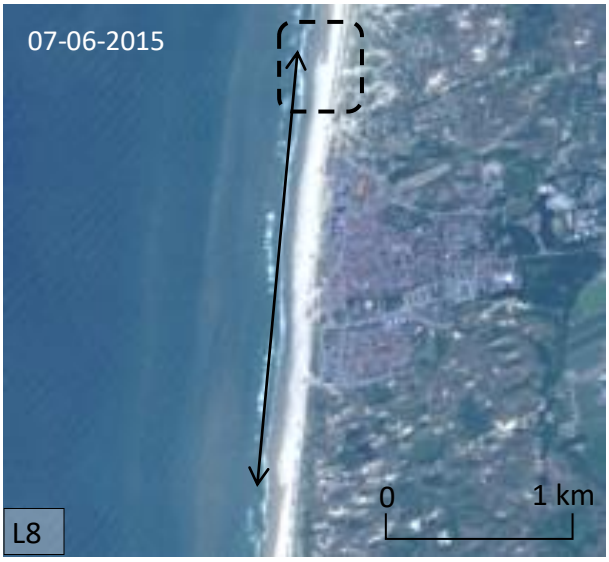

Figure 6.15: More detailed view of the beach nourishment in front of Egmond (RSP 37.00-39.00). The black arrow represents the alongshore extent of the nourishment. The spit formation at the northern edge of the nourishment is indicated in the box.

6.3.3 Nourishment analysis

Figure 6.16 shows the cross-shore time-series of the shoreline position corresponding to the nourishments carried out in 2015 (Figure 6.14). The time-series are alongshore-averaged over the longshore extent of the nourishments and the values on the y-axis are expressed relative to the pre-nourishment profile ($\widetilde{D_{sh}}(y,t)$). In both time-series positive shoreline change of approximately 30 m occurs during the implementation of the nourishments (highlighted grey areas).

The relatively large shoreline change might be attributed to the larger volumes of the two beach nourishments (216 m^3/m and 220 m^3/m). However, from 07-2015 until 09-2016 a shoreface nourishment was constructed (in the figures only the end date is indicated by the red line), therefore, the time-series of 2015 were not further used to study the typical dynamics of beach nourishments because the shoreface nourishment potentially influenced the results.

The following section presents the development of two beach nourishments and two shoreface nourishments. The areas 500 m north and south of the beach nourishments were also analysed to look at alongshore effects. For shoreface nourishments areas 1000 m north and south were determined. For three nourishments, two beach nourishments and one shoreface nourishment, the evolution of the adjacent areas is shown below. These three nourishments were selected because they were representative of the other nourishments but also allowed to examine the alongshore effects without too many limitations. For example, after the first shoreface nourishments, beach nourishments were

always implemented in combination with a shoreface nourishment, making it difficult to separate their effects. In 1997 three nourishments very near to each other were constructed, therefore, these also did not come in use to look at potential alongshore migration. The edge of the study area was also a limiting factor in some cases of shoreface nourishments. Besides the four nourishments presented in this chapter, the time-series of all other nourishments were also computed, as well as the development of the areas neighbouring the beach and shoreface nourishments for a few additional cases. These are included in Appendix E.

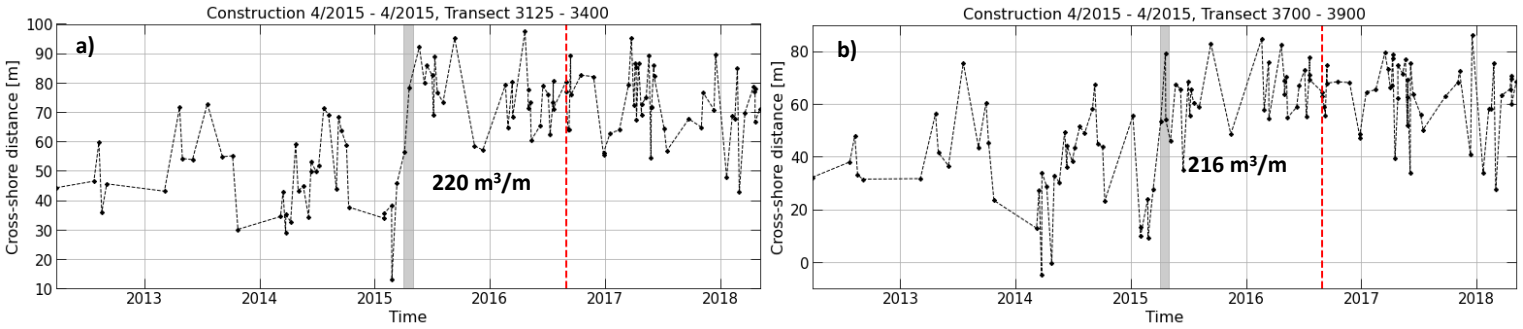

Figure 6.16: Alongshore-averaged time-series of the development of two beach nourishments in the grey highlighted areas: (a) beach nourishment carried out in front of Bergen in 4/2015 with a volume of 220 m^3/m; (b) beach nourishment carried out in front of Egmond in 4/2015 with a volume of 216 m^3/m. The red dashed lines represents the end of the construction of a shoreface nourishment in the same time period.

Figure 6.17a and Figure 6.18a show the development of a nourishment carried out in front of Bergen and Egmond. In both cases a distinct peak is visible after the sand has been placed on the beach. At Bergen the shoreline advances about 40 m seaward and at Egmond an expansion of the shoreline of almost 35 m can be seen. The shoreline exhibits the same behaviour regarding the other beach nourishments (included in Appendix E), in most cases a (steep) peak in shoreline expansion occurs during a beach nourishment with typically between 30 and 50 m of shoreline change. In approximately 18 of the total 23 beach nourishments a prominent peak in shoreline expansion is found. Sometimes the peak or a second peak occurs just after the construction period. It is difficult to say if this is caused by the actual beach nourishment or if it is related to noise but it is also possible that in those cases the sand was also placed higher up on the beach. Consequently, it took some time for the sand to be transported to the sand/water interface and affect the shoreline.

However, when comparing the shoreline change at the location of the beach nourishment to the adjacent areas (Figures 6.17c, d and Appendix E), in these neighbouring areas often also a peak occurs at the construction of the nourishment. In case of Figure 6.17, about 20 m of shoreline change takes place in the areas north- and southward. These peaks are smaller but still, this indicates that not in every case the 'entire peak' can be attributed to the presence of a nourishment. Seasonality is likely to also play a role. Beach nourishments are almost always placed during spring in April and May when the shoreline typically already shows some seaward advance, as appeared from the results of the time-series decomposition. When carefully looking at the graphs in Figures 6.17 and 6.18, some seasonality also does seem to come forth, with shoreline expansion in summer and retreat in winter. Despite that, it can still be said that a considerable part of a peak can be explained by nourishments because the graphs do show that the amplitude of a peak at the location of a nourishment is larger than in the adjacent areas (20 vs 40 m in Figure 6.17). When accounting for seasonality, it can be derived that typically between 10 and 40 m of positive shoreline change occurs during a beach nourishment.

Furthermore, the lifetime of beach nourishments at the coast of Egmond-Bergen appears to be very short. In Figure 6.18, a retreat of the shoreline within one year after the beach nourishment back to the pre-nourishment situation occurs, whereafter immediately a new beach nourishment is

implemented. Such as steep decrease after a nourishment is also portrayed in a few other figures contained in Appendix E. Figure 6.17 on the other hand, shows a more gradual redistribution of the nourishment, but after 2 years the shoreline has also largely returned to its original position. Important to keep in mind is the presence of the other beach and shoreface nourishments in the graphs (blue and red dashed lines respectively). For instance, in Figure 6.17 one year before the studied nourishment another was constructed as well. If this one was not entirely diffused before the new one was constructed, this could potentially have influenced the lifetime of this second nourishment.

It is difficult to draw conclusions on the effects of the volumes of the nourishments because the noise in the data is quite large. The nourishment in Figure 6.17 is a relatively larger one with a volume of 306 m^3/m and does show a considerable peak, but the peak does not necessarily have a larger amplitude than other beach nourishments with volumes around 200 m^3/m (e.g. Figure 6.18, Appendix E). Differences between larger and smaller nourishments regarding their volume were also not pronounced in the Hovmöller plots (Figure 6.11). Nevertheless, when looking at all beach nourishments in Appendix E, this does suggest that nourishments with a volume closer to 100 m^3/m result in less shoreline progradation and thus lower or even absent peaks. A sort of threshold seems to apply to 200 m^3/m, generally from this volume and larger it is safe to say that in every case a large amount of shoreline accretion took place.

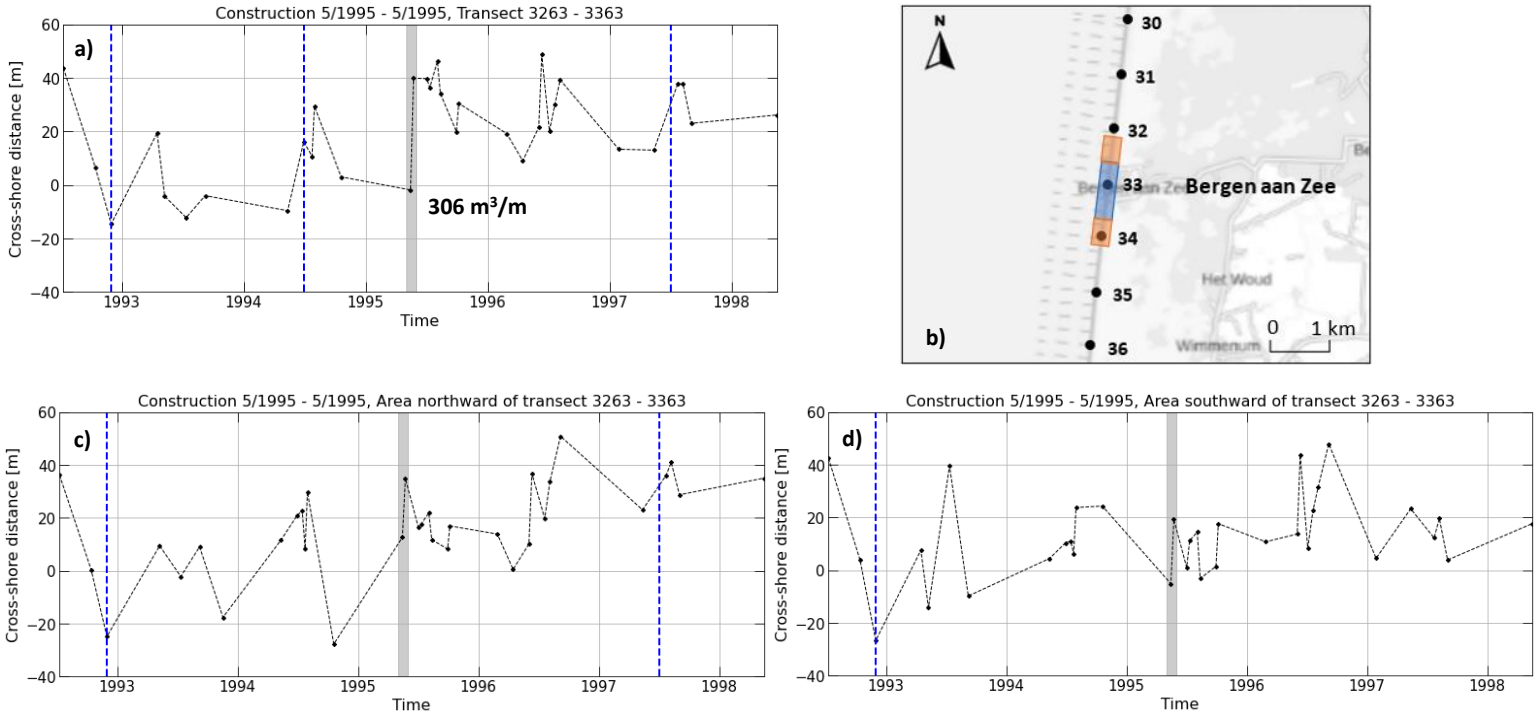

Figure 6.17: Alongshore-averaged time-series of the development of the beach nourishment (highlighted in grey) carried out in 5/1995 with a volume of 306 m^3/m: (a) alongshore-averaged time-series over the alongshore extent of the nourishment; (b) location of the nourishment highlighted in blue and the areas within 500 m adjacent to the nourishment highlighted in orange; (c) alongshore-averaged time-series of the area 500 m northward of the nourishment; (d) alongshore-averaged time-series of the area 500 m southward of the nourishment. In the figures the blue dashed lines represent the end of construction of other beach nourishments in the same time period. In (c) and (d) the other nourishments included in (a) did not always physically exist within the adjacent areas of 500 m (e.g. due to different lengths of nourishments), for clarity only the nourishments that (sometimes partly) were actually present are indicated here.

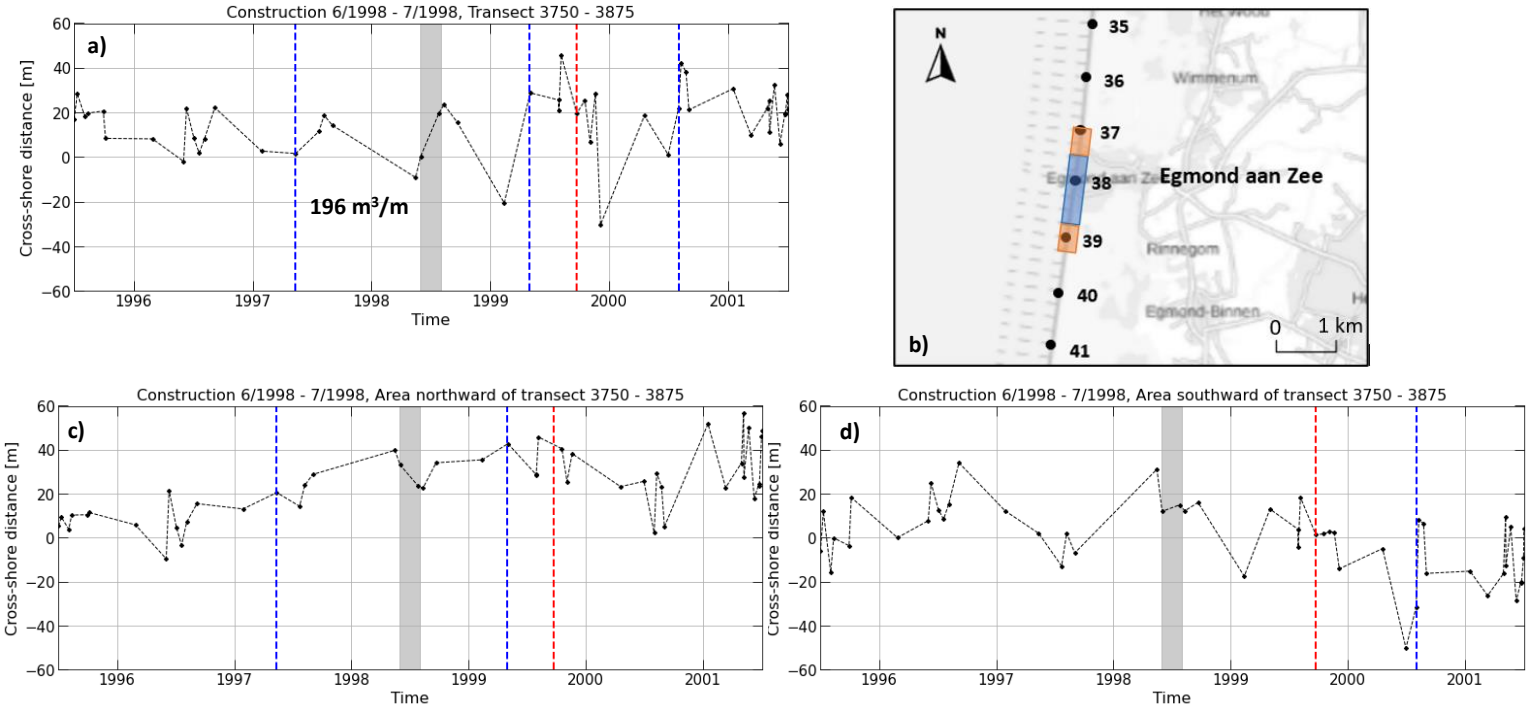

Figure 6.18: Alongshore-averaged time-series of the development of the beach nourishment (highlighted in grey) performed between 6/1998 and 7/1998 with a volume of 196 m³/m: (a) alongshore-averaged time-series over the alongshore extent of the nourishment; (b) location of the nourishment highlighted in blue and the areas within 500 m adjacent to the nourishment highlighted in orange; (c) alongshore-averaged time-series of the area 500 m northward of the nourishment; (d) alongshore-averaged time-series of the area 500 m southward of the nourishment. In the figures the blue dashed lines represent the end of construction of other beach nourishments and the red dashed line represents the end of construction of a shoreface nourishment. In (c) and (d) the other nourishments included in (a) did not always exist within the adjacent areas of 500 m (e.g. due to different alongshore extents of nourishments), for clarity only the nourishments that (sometimes partly) were actually present within the adjacent areas are indicated here.

Inspection of the development of the shoreline in the areas adjacent to the nourished sections makes clear that a pronounced alongshore effect of a beach nourishment on the neighbouring coastline is lacking. It is expected that any alongshore effects would translate into a delayed, but muted peak in the alongshore-averaged time-series since it would take some time for the sand to gradually migrate or diffuse along the coast, creating a delayed effect in the adjacent areas. In addition, the net alongshore transport is to the north along the Holland coast, suggesting that migration of the nourishment should be more dominant to the north. However, Figure 6.17c, the area northward of the beach nourishment in front of Bergen, shows the same evolution over time as the actual nourishment. Both locations show a shoreline retreat of about 30 m over the same time span after implementation of the nourishment. In the area southward of the nourishment (Figure 6.17d) there does seem to be some slight influence of the nourishment, but this is hard to quantify. Namely, the shoreline in this area already appeared to be more stable before the nourishment and the second peak that occurs near the end of 1996 is also present, although smaller, in Figure 6.17a. Therefore, this second peak cannot directly be related to the occurrence of a delayed peak due to alongshore migration. In the neighbouring areas to the beach nourishment near Egmond (Figure 6.18) the time-series do include a second peak, suggesting some alongshore migration of the sand. When looking at the other nourishments for which the adjacent areas were investigated (Appendix E), most of them barely show any indication of alongshore effects. Often the time-series of the adjacent areas are similar to the time-series for the location of the actual nourishment. This is confirmed by the results earlier described for the Hovmöller plots, whereby mainly at the alongshore extents of the beach nourishments some

shoreline progradation could be observed. Lastly, the areas 1000 m north and south of the beach nourishments were also studied in this analysis, however, these results were not included here because already for the adjacent areas of 500 m almost no effects of longshore migration were visible. Appendix E does contain two examples, solely for Figures 6.17 and 6.18. The time-series of the 1000 m areas were also very similar to the 500 m areas, this may suggest that the alongshore effects reach as far as 1000 m, for instance in case of Figure 6.18. On the other hand, it may also invalidate the presence of alongshore effects for the nourishment in Figure 6.18. Large alongshore effects reaching as far as 1000 m is very unlikely for this coast, especially considering the limited alongshore effects depicted in the Hovmöller plots. If the latter is true, the time-series for the 1000 m areas would have to show a muted version of the secondary peaks that were located in Figures 6.18c & d after the nourishment. But this is not the case. Therefore, this suggests that the secondary peaks are more likely to be related to the natural occurring variation in the shoreline or noise in the data. The same can be applied to the other beach nourishments.

On the whole, beach nourishments appeared to have a very short lifetime but a distinct peak occurred in shoreline change at the same moment they were constructed, while these 'peaks' were not as visible in the Hovmöller plots. Alongshore effects seemed to be limited, with sand not diffusing to the adjacent coast.

Alongshore-averaged time-series of shoreface nourishments were also investigated. Figure 6.19 presents a shoreface nourishment carried out at Bergen between 4/2000 and 8/2000 with a volume of 497 m^3/m. Figure 6.20 displays a second one near Egmond between 8/2010 and 8/2011 with a volume of 343 m^3/m. In Appendix E the rest of the shoreface nourishments are also included. Shoreface nourishments are placed underwater and therefore do not display a peak in shoreline change right after construction. Figure 6.19 visualises the development of one of the first nourishments implemented at the Egmond-Bergen coast. Based on only this figure, effects of a shoreface nourishment are not directly visible. The shoreface nourishment in Figure 6.20 is part of the third round of shoreface nourishments carried out in the study area. In this graph, the shoreline already shows progradation before the 343 m^3/m nourishment, probably related to the preceding shoreface nourishments, which is also advocated with the Hovmöller plots. The 343 m^3/m nourishment seems to contribute further to the shoreline accretion continuing the positive increasing trend. With the first visualisation of the entire dataset in the Hovmöller plots it was already derived that effects of continuous shoreface nourishments at an interval of approximately 5 years became more and more apparent over time, suggesting a sort of cumulative effect. This would also explain why in Figure 6.19 effects were still difficult to see but in Figure 6.20 noticeable progradation of the shoreline takes place. It is safe to say that the effects of shoreface nourishments on the shoreline are very gradual and can best be considered by studying the Hovmöller plots.

Effects of shoreface nourishments on the adjacent coast due to alongshore sand transport are difficult to deduce from these time-series graphs. Figures 6.19c & d show the alongshore-averaged time-series for the areas 1000 m adjacent to the shoreface nourishment in the year 2000. However, the presence of alongshore effects does not become apparent from these figures. The 343 m^3/m nourishment was situated between two other shoreface nourishments in the same time period, consequently, the areas 1000 m to the north and south were not determined. In Appendix E, the results for a few other shoreface nourishments are included but often the edge of the study area or the presence of other neighbouring shoreface nourishments was a limiting factor. Over time, the figures in Appendix E do seem to show a slight increase in alongshore effects, similar to the cumulative effect of the shoreface nourishments. Generally, the alongshore effects can better be quantified from the Hovmöller plots, providing the bigger picture of the data. Because the alongshore effects of shoreface nourishments

appear to be rather small, the unnourished coast of Castricum barely experienced positive influences of the nourishments. Though, the Hovmöller plots (Figure 6.11) as well as the shoreface nourishment from 2019 in Appendix E do seem to indicate that near the end of the time-series in 2022 and 2023 the shoreface nourishments did start to spread more to the adjacent coastlines. This could also explain the relatively steep increase in the trend of the time-series decomposition for the most northern and southern sections after 2021 (Figure 6.5).

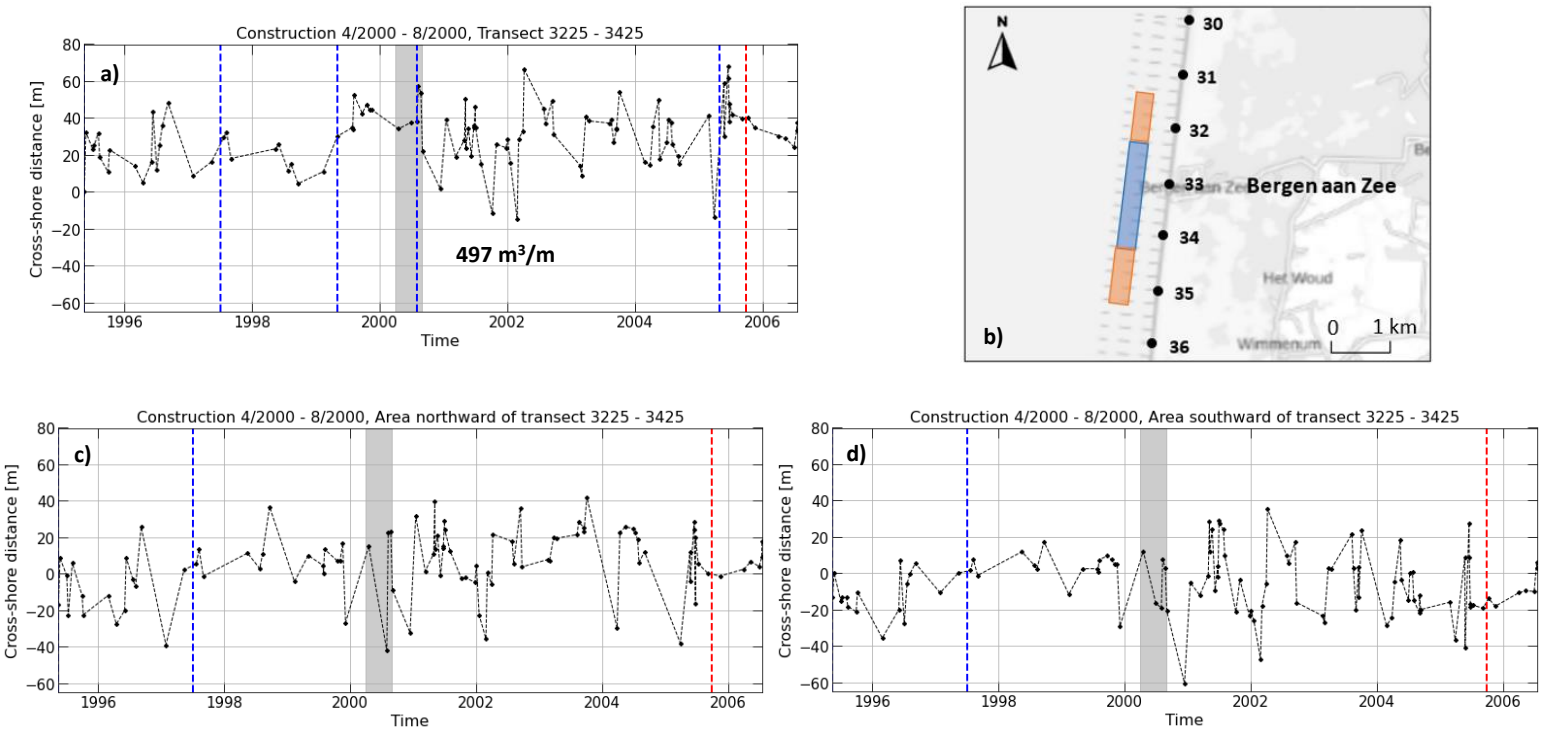

Figure 6.19: Alongshore-averaged time-series of the development of the shoreface nourishment (highlighted in grey) performed between 4/2000 and 8/2000 with a volume of 497 m³/m: (a) alongshore-averaged time-series over the alongshore extent of the nourishment; (b) location of the nourishment highlighted in blue and the areas within 1000 m adjacent to the nourishment highlighted in orange; (c) alongshore-averaged time-series of the area 1000 m northward of the nourishment; (d) alongshore-averaged time-series of the area 1000 m southward of the nourishment. In the figures the blue dashed lines represent the end of construction of other beach nourishments and the red dashed line represents the end of construction of another shoreface nourishment. In (c) and (d) the other nourishments included in (a) did not always exist within the adjacent areas of 1000 m (e.g. due to different alongshore extents of nourishments), for clarity only the nourishments that (sometimes partly) were actually present within the adjacent areas are indicated here.

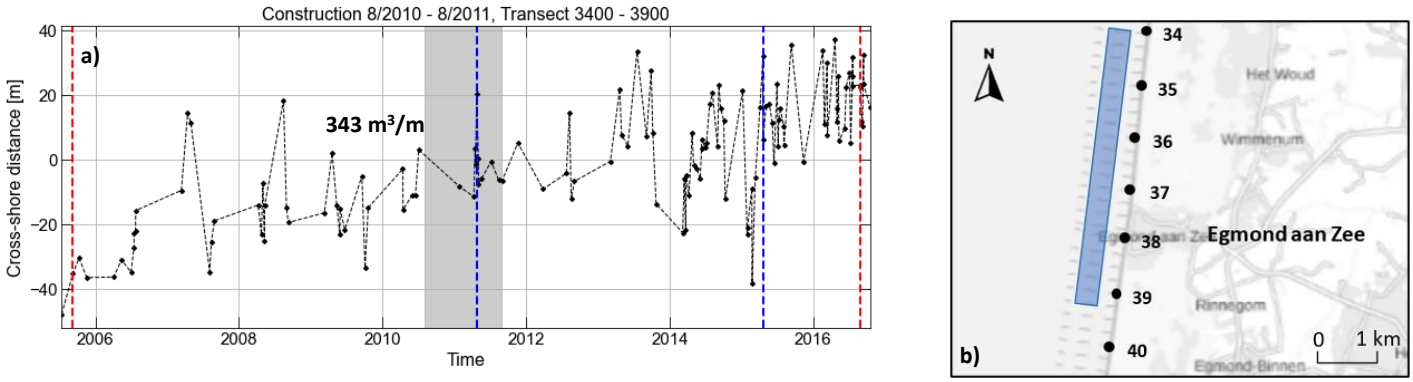

Figure 6.20: Alongshore-averaged time-series of the development of the shoreface nourishment (highlighted in grey) constructed between 8/2010 and 8/2011 with a volume of 343 m³/m: (a) alongshore-averaged time-series over the alongshore extent of the nourishment; (b) location of the nourishment highlighted in blue.

7. Discussion

With an eye on climate change and its effect on present-day coastlines, for instance, climate change is likely to exacerbate beach erosion, it is important to quantify the present-day dynamics of the shoreline and understand the drivers of change. This thesis focused on a nourished stretch of coast in front of Egmond-Bergen, a high-energy coast characterised by low-sloping beaches. Shoreline dynamics were investigated over a period of 1985-2023. The first part of this chapter will discuss the results regarding the temporal trends found in the shoreline positions. Thereafter, the spatial effects and dynamics of nourishments at the Egmond-Bergen coast will be evaluated. The discussion finishes with the limitations and uncertainties of the study and gives a recommendation and outlook for future coastal management.

7.1 Temporal variability in the shoreline

The shoreline in front of Egmond-Bergen was investigated with regard to the presence of three potential temporal trends in the time-series. A positively increasing interannual trend of approximately 2.00 m/year was found for the three coastal sections that receive regular nourishments. On the other hand, the unnourished coast in the south in front of Castricum displays much more stable behaviour with an almost constant interannual trend. This indicates that the anthropogenic forcing in the form of repeated nourishments had a large influence on the shoreline and is responsible for the large accretion of the coast at Egmond and Bergen. In the three nourished sections the interannual trend component explained about 70% of the variation in the data, implying that these nourished sections are very trend-dominated. For Castricum the trend only explained approximately 10%. A previous study by Turner (2006) already indicated that nourishments can have a considerable influence on shoreline variability.

In general, seasonality in the shoreline position is related to the incident wave conditions. Low-energy waves lead to beach accretion, while high-energy waves are responsible for beach retreat through the generation of offshore currents (Quartel et al., 2008). For the Egmond-Bergen coast, seasonality was found to be minor. This is in contrast to other studies conducted at varying sites across the world. At Truc Vert, a gently-sloping sandy meso-macro tidal beach in France, temporal variability was also investigated with CoastSat (Castelle et al., 2021; Vos et al., 2019a). They found the presence of strong seasonal cycles in the evolution of the shoreline, approximately 90% of all variability was found to occur at a timescale of 6 months (seasonal) (Vos et al., 2019a). Castelle et al. (2021) further reported an amplitude of about 30-40 m for the seasonal cycles at Truc Vert, while for Egmond-Bergen the seasonal component only described less than 10% of the total variability with an amplitude of c. 10 m. For the coast of Castricum also an amplitude of 10 m for seasonality was found, implying that repeated nourishments did not affect the seasonal cycles in shoreline position at Egmond and Bergen. Other examples of coastal sites that exhibit seasonal variability in their shoreline which were assessed with CoastSat include the storm-dominated beach of Narrabeen-Collaroy in Australia (Vos et al., 2019a), and two beaches at the southwest coast of England, Perranporth beach and Slapton Sands. For the latter strong intra-annual cycles in shoreline positions were derived, however, due to the low availability of satellite data especially during winter their results had limited accuracy. The same problem but to a lesser extent was also the case for the obtained satellite data at Egmond-Bergen. Particularly, until 2015 fewer images (5-10 per year) were collected with CoastSat, whereafter Sentinel-2 became available in 2015, increasing the density of the images (>20 per year). In combination with the relatively small number of images acquired during winter (November to March), this made it more difficult to capture seasonal variability in the time-series. Though, enough images were available after 2015 and by setting the significance level α to 0.05 (default is 0.01), JUST decomposition captured the seasonality in the shoreline reasonably well. The results further demonstrate that the seasonality observed in the time-series of shoreline positions did correspond to the seasonality in the incident wave conditions of the

Holland coast. Beach accretion was found in summer, while shoreline retreat took place during the storm season. Nonetheless, seasonality in the Dutch wave climate is quite strong as indicated by the time-series decomposition of wave height and wave period (Appendix B) but this large seasonality, thus, does not translate itself into a large intra-annual signal in the shoreline positions of Egmond-Bergen. Other studies investigating the seasonality in the shoreline position along the Dutch coast are scarce. A paper by Quartel et al. (2008) explored seasonal patterns at the storm-dominated coast of Noordwijk, the Netherlands, with monthly measurements of beach elevation and daily ARGUS images for a time period of 3 years. They did not specifically study the cross-shore shoreline position but rather looked at the width and the volume of the beach, in which they did recognise seasonal patterns. During low-energy conditions in summer a narrow, reflective beach profile was detected with a relatively large volume of the beach. On the other hand, in winter they noticed a more dissipative beach with a smaller beach volume and wider beach. They appointed the variation in beach width and volume between the seasons to cross-shore sediment transport between the lower-intertidal and supratidal sections of the beach. Furthermore, in winter a flatter beach profile was found than in summer, which coincides with the theory described for a storm-dominated beach in Chapter 2.1. Also, once a year and only during summer, an intertidal bar merged with the beach. The Noordwijk coast showed a better correspondence to the 'storm-post storm' model than to the classical swell-profile (Chapter 2.1). As this is likely to be also the case for Egmond-Bergen, since the entire Holland coast can be referred to as storm-dominated (Quartel & Grasmeijer, 2007), this might (partly) explain the limited seasonality found in the shoreline positions of this study, lacking the classical large accretion and erosion of the shoreline embedded in the swell-profile. Moreover, at Noordwijk ~ 150 m^3/m of sediment was observed to be stationary on the beach, not contributing to seasonal exchange, and only ~ 19 m^3/m was related to actual sediment loss or gain. For swell-dominated beaches the 'active' sediment participating typically amounts to ~ 50 m^3/m, with approximately the same amount being stationary (Quartel et al., 2008). This demonstrates the robust nature of storm-dominated and microtidal coastlines, shielded by the presence of subtidal bars (Guillén et al., 1999; Quartel et al., 2008), therefore being not so susceptible to storms and seasonality in wave conditions, as the results of this study show. However, important to note is that this research did not specifically look at the seasonality in shoreline position and they did not investigate the contribution of the seasonality to the total temporal variability present, complicating the comparison between the two coastal sites. For example, beach width cannot be directly related to the cross-shore shoreline position since beach width is determined by both the cross-shore positions of the dune foot and the low water line. Another study by Cohen & Brière (2007) looked at seasonal patterns present in the coast of Egmond by making use of JARKUS and ARGUS data. In particular, they focused on the intertidal beach volume. The coast was characterised by a smaller intertidal beach volume during winter and by a larger intertidal volume during summer, which seems to support the results found in Quartel et al. (2008). An important finding of Cohen & Brière (2007) includes that they established a strong positive correlation between intertidal beach volume and shoreline position. A larger intertidal beach volume coincides with a more seaward located shoreline and vice versa. This confirms the results of this work, where, although to a limited extent, a more seaward position of the shoreline coexisted with lower-energy wave conditions in summer. And, according to the abovementioned studies, this would coincide with a larger (intertidal) beach volume, however, the nature of the data in this thesis did not allow for investigation of beach volumes. Moreover, the research of Cohen & Brière revealed that a winter season with multiple intense storms resulted in stronger erosion than a winter season with relatively minor storms at Egmond. It is very plausible that the variations in amplitude of the seasonality found in the shoreline positions of the current study are related to the latter.

In addition to the relatively small variability found on the seasonal timescale, a direct or even indirect response of the shoreline to storm events also appeared to be limited for all four coastal sections considered (Figure 5.8). It was expected that the presence of individual large storms ($H_s \geq 5$ m) in the time-series would coincide with a considerable retreat of the shoreline between two closely following data points. However, this hypothesis was not necessarily always supported by the results from Figures 6.8 and 6.9. A response of the shoreline to one relatively large storm was barely visible, in most cases they were only responsible for some small fluctuations not bigger than the rest of the fluctuations incorporated in the remainder part of the time-series decomposition. Furthermore, a more non-instantaneous response of the shoreline to a longer period (2 or 3 months) with multiple storms, thus a higher wave power, was also not found. The R-squared values in all cases did not indicate a relationship between the cumulative wave power and the observed shoreline change within 2 or 3 months. It was expected that a higher cumulative wave power over the 2 or 3 months would correspond to a larger negative shoreline change between those 2 or 3 months, while calmer periods would match to a lower cumulative wave power, but this could not be proven. A possible reason for the absence of a direct reaction of the shoreline position to a storm event is related to the sediment transport during a storm. A storm often leads to erosion of the supratidal zone as well as of the dunes. It is very plausible that the eroded sand is first deposited on the lower (intertidal) beach or close to the waterline before it is transported elsewhere, explaining why direct landward retreat of the shoreline cannot be seen right after a storm. This hypothesis is consistent with the results reported in Quartel & Grasmeijer (2007) where they found a relatively higher intertidal beach volume after two storms. This transport from the supratidal zone to the lower intertidal zone was also mentioned in Quartel et al. (2008).

Aagaard et al. (2005) researched the effect of storms on intertidal beach change at Egmond. First of all, they already mention that at times (intertidal) beaches can be very resilient against storms, with in particular gently-sloping, more dissipative beaches such as Egmond-Bergen. In their study, they distinguished both protruding horns and landward bays occurring along the coast of Egmond for which they observed a different response of the shoreline to a sequence of storms. At the generally steeper sloping embayments significant erosion was found accompanied by a change in the beach face slope from $\beta = 0.043$ to $\beta = 0.033$. On the other hand, at the gentler-sloping horns erosion was a factor 5 smaller and the intertidal slope only decreased from $\beta = 0.026$ to $\beta = 0.024$, implying a 'quasi-equilibrium slope' on the timescale of storms. This lack of erosion is likely to be related to the already gentle beach slope prior to the storms. They hypothesise that gentler beach slopes thereby could strengthen the stability of a beach. This is also in accordance with the model of Wright (1980). In this thesis, the presence of horns and bays was not considered since the time-series were alongshore-averaged prior to the storm-analysis. In addition, the shoreline positions were adjusted based on a water level correction executed with a beach slope of ~0.0277, a more dissipative slope. This might explain why along the entire coast of Bergen-Egmond almost no storm erosion was noticed. Despite that, the paper by Aagaard et al. (2005) does seem to support the results discerned in this research.

Furthermore, in the work of Quartel et al. (2008) no correlation or at most a very weak correlation was discovered between the daily to weekly averaged offshore wave conditions and the monthly values of beach volume and beach width. Consequently, the wave conditions were not strongly related to the monthly changes of the beach, which is confirmed by the results of this thesis. However, they consider the timing of a beach survey with respect to a storm to be an important factor in the lack of a correlation. If a monthly measurement is based on a survey spaced 3 or 4 weeks apart from the storm event, the effects of the storm may be less evident if the beach is already recovering. This is a very important limitation to consider and also applies to the storm analyses carried out in the current study. First, the storm response was investigated by looking at individual storms with a significant wave height

larger than 5 m. However, the shoreline positions were not equally distributed, sometimes data points were spaced a few days apart but in other cases a relatively long time period occurred between two consecutive data points during which a storm took place. This time period may even consist of a few weeks. By only selecting the higher density data between 2015 and 2023 it was tried to avoid this as much as possible. Still, there is uncertainty in the actual shoreline change resulting from the storms (Figure 6.7). As a result, the shoreline change after a storm cannot always be called an instantaneous response in Figures 6.8 and 6.9 and the abovementioned explanation of transport of the supratidal to intertidal zone certainly should not always be used to clarify the results. Furthermore, in the remainder part of the time-series decomposition not only storm response is included, but it also consists of all uncertainties present in the total time-series. This so-called noise had a fairly large share in the data, for Castricum more than 70% of the total variability was explained by the remainder part. This large share of noise introduced considerable uncertainty in the method for determining the influence of storms on the shoreline. The second analysis regarding the cumulative wave power and shoreline change in the remainder part over a period of 2 or 3 months also had its limitations. This analysis was based on monthly-averaged shoreline positions as this allowed for more accurate extraction of the desired time periods of exactly 1 and 2 months between two data points, which is equal to a total period of 2 and 3 months respectively in the case of monthly averages. Subsequently, the cumulative wave power was computed over these 2 or 3 months. However, because of the nature of monthly-averaged data, it is important to keep in mind that in the case a relatively large cumulative wave power is computed over the entire time period, implying the occurrence of multiple storms, one or even both of the selected monthly-averages could have been influenced by these storms and not necessarily solely the shoreline change between them. This, of course, also applies to other situations with lower values of cumulative wave power. The same analysis for the individual data points, so without first calculating monthly-averages was also performed. However, this method had the problem that the shoreline-positions were randomly sampled in time with sometimes a few months between data points and in other cases only 2 or 3 days between consecutive data points. This made it difficult to extract time periods of 1 or 2 months between data points without considerable deviations from these time periods or duplicates (two sets of data points covering the same time period). To allow for equal comparisons of the cumulative wave power, it was necessary that two data points did not deviate too much from the 1-month or 2-month time period. Despite of these uncertainties, still the R-squared values and p-values for this method were computed but it showed similar results to the method with the monthly-averaged data, with results not being statistically significant ($p > 0.05$). R-squared values in the same order as the R-squared values for the monthly-averages were found. Again, this suggests a poor correlation between offshore wave conditions and shoreline change.

To conclude, the coast studied in this thesis showed increasing trends in shoreline position in front of Egmond and Bergen, while near Castricum a stable trend was found. Seasonality and a response to storm events appears to be very small, implying that the shoreline responds barely or very slowly to changes in offshore conditions. Although, important to consider are the large uncertainties associated with the storm analysis.

7.2 Effect of nourishments

A heavy nourishment campaign was implemented at the coast of Egmond-Bergen ever since the Dutch dynamic preservation policy came into practice in 1990. These repeated nourishments have had a considerable influence on the shoreline position and alongshore variability in the shoreline. In total the repeated nourishments resulted in roughly 60-80 m of seaward shoreline expansion over almost 40 years. This value also takes into account the natural variation and wave-like features of the coastline that became amplified by the nourishments, which will be explained in the text below. Alongshore variability increased until approximately 2000 but decreased again in most recent years. This decrease

is most likely related to the implementation of the longer shoreface nourishments, resulting in a more uniform coast. In particular, the repeated shoreface nourishments seem to have contributed a great deal to the progradation of the shoreline as is illustrated in Figure 6.11a. Beach nourishments (without combination with a shoreface nourishment), on the other hand, only resulted in a temporary and relatively small expansion of the shoreline. Although beach nourishments did lead to local accretion of the shoreline, this was not sustainable and every 1 to 2 years a new one had to be placed to prevent subsequent erosion. Figures such as 6.17 and 6.18 also indicate that in general between 1 and 2 years the effect of a beach nourishment on the shoreline was gone and all or almost all of the placed sand was eroded. In total about 10 m of total shoreline change between 1990 and 1999 can be attributed to the repeated beach nourishments. The lack of some sort of cumulative, sustainable effect in combination with the results of these figures points to a typical lifetime of 1 or 2 years for beach nourishments in front of Egmond-Bergen. A more precise lifetime cannot be determined based on this data alone because there is quite some noise in the data and seasonal variations also play their part. This makes it also difficult to recognise the so-called sawtooth concept in the time-series. For some beach nourishments, such as in Figure 6.17, the shoreline evolution does approach a sort of saw-tooth shape, with a clear peak and more gradual erosion afterwards. In other cases such as Figure 6.18, a peak in sedimentation is seen but it is followed by immediate erosion after nourishing. However, previous literature on nourishments in front of Egmond do confirm these statements (e.g. Boers, 1999). Earlier it has already been found that smaller nourishments (0<400 m^3/m) do not automatically always result in a positive shoreline change and strong sedimentation following the saw-tooth concept (Cohen & Brière, 2007; Van Koningsveld & Lescinski, 2006). Van Koningsveld & Lescinski (2006) further computed the effectiveness of nourishments from 1990-2005 at the central transect of Egmond (RSP 3800). They came to the conclusion that after a total amount of 2500 m^3/m was nourished, only a total volume increase of 500 m^3/m could be seen. This suggests that the continuous nourishment efforts were only effective for 20 percent in enlarging the sand volumes. Although this calculation also involved two shoreface nourishments, the low efficiency does agree with the relatively minor effects with regard to beach nourishments in this study.

Additionally, in the satellite images, beach nourishments were difficult to detect and they did not protrude very much seaward. A possible reason for the limited visibility of the beach nourishments could be related to the placement of the sand. A nourishment can be placed mainly on the upper parts of the beach or also extend to lower parts of the beach underwater (De Schipper et al., 2020). If the beach nourishments in front of Egmond and Bergen were predominantly placed on the higher sections of the beach, this might explain their limited appearance in the satellite images. After a beach nourishment, the beach is steeper and wider than before. If the sand is mostly placed on the above-water beach, this causes an even more unnatural steep slope of the beach, enhancing large offshore directed sand transports and narrowing of the beach (De Schipper et al., 2020). If the above is true, this could contribute to the rapid disappearance of beach nourishments at Egmond-Bergen.

Only after the first shoreface nourishments were carried out, a large positive cumulative effect on the position of the shoreline was noticeable over time. Often these shoreface nourishments were combined with a beach nourishment. Although at the scale of an individual shoreface nourishment no pronounced effect on the shoreline occurred (e.g. Figure 6.19), over time with the repeated shoreface nourishments a much larger effect on the shoreline was seen. This indicates that especially the repetition of the shoreface nourishments contributed to the large shoreline advance. Taking into account the natural variation in the coastline, about 50 m of cumulative shoreline advance could be seen in response to repeated shoreface nourishments (in combination with beach nourishments).

Quartel & Grasmeijer (2007) also investigated shoreface nourishments near Egmond, in particular the two constructed in 1999 and 2004. They considered the width of the (intertidal) beach, the (intertidal) beach volume, and the volume of the inner breaker zone in their analysis. They argue that the combination of eight beach nourishments at Egmond with one relatively small shoreface nourishment (1990-1999) has a similar effect as one beach nourishment combined with one relatively large shoreface nourishment (2004-2005). Cohen & Brière (2007) also denote that the second shoreface nourishment with the beach nourishment in front of Egmond resulted in a higher stabilisation of the beach than the first one in 1999, for which they state that positive effects already disappeared in June 2001. They attribute this difference to the possibility of a milder wave climate around 2004 and similar to Quartel & Grasmeijer (2007), also to the different geometries of the two shoreface nourishments. Furthermore, Quartel & Grasmeijer (2007) note that shoreface nourishments mainly have a protective influence on the beach, and to a lesser extent, a feeding or nourishing one. This suggests that the combination of a shoreface nourishment with a beach nourishment was essential to generate the large amount of cumulative shoreline accretion that took place in the study area. Though, in the research of Van Duin et al. (2004) they did report sedimentation, but in the surf zone shoreward of the shoreface nourishment of 1999, probably related to the 'lee' and 'feeder' effect (Figure 2.10) which their modelling results confirmed. Their study also confirms the very limited influence of the first shoreface nourishment at Egmond on the beach, however, they do hypothesise that maintaining the shoreface nourishments will most likely result in the sediment to also reach the beach in the long run. With the repeated shoreface nourishments after the one in 1999, this assertion very well applies to the coast of Egmond and Bergen.

Especially in the more recent years (2012-2023) accretion of the shoreline is most pronounced. However, after the shoreface nourishment of 2016, the one constructed in 2019 does not seem to further contribute much to expansion of the shoreline. The shoreline rather stays put at the same cross-shore location. This might be related to the fact that after the repeated shoreface nourishments so much sand accumulated in the system that the entire system became saturated. Potential onshore transport of sand must have continued at the same pace as after the nourishment of 2016, with the waves and currents not being able to transport the extra amount of sand that was nourished in 2019. It is very probable that this phenomenon was also accompanied by a stop in the net offshore subtidal sandbar migration, since the repeated shoreface nourishments must have had a large impact on the subtidal bars as well. Previous studies on bar behaviour documented a temporal stop in the net seaward migration of the subtidal bars after the implementation of a shoreface nourishment (e.g. Grunnet & Ruessink, 2005; Ojeda et al., 2008), while in some cases the seaward migration was even reversed in net onshore movement (e.g. Van der Spek et al., 2007; Radermacher et al., 2018). The latter effect was also observed at Egmond already after the first shoreface nourishment of 1999 (Van Duin et al., 2004). However, another possible reason for the absence of additional advance of the shoreline after 2019 is the lack of a beach nourishment. In contrast to all other shoreface nourishments, the shoreface nourishment of 2019 was not combined with a beach nourishment. If it is true that shoreface nourishments rather have a protective function than a feeding one, as mentioned above, then a beach nourishment would have been necessary to result in visible shoreline expansion. Future studies that may include the last, but still unfinished shoreface nourishment in 2023/2024 might shed more light on this topic. Taken together, it is very plausible that both the protective function of a shoreface nourishment on a beach nourishment and sedimentation of the beach related to the repeated shoreface nourishments themselves (e.g. due to the 'lee' and 'feeder' effect), resulted in the large amount of shoreline progradation that was observed.

In the Hovmöller plots longshore features are present with a typical wavelength between 1 and 2 km. These features were present over the whole time period 1985-2023 but became amplified by the

implementation of the nourishments. These features can be attributed to sand waves that occur along the entire Dutch coast with typical wavelengths in the order of 1 km (Quartel & Grasmeijer, 2007; Ruessink & Jeuken, 2002). Quartel & Grasmeijer (2007) reported a wavelength of 500-1000 m for a sand wave in front of Egmond and Van Duin et al. (2004) indicated rhythmic features with an interval of 2 km. Wijnberg et al. (2007) studied the response of a shoreline sand wave after the construction of a beach and shoreface nourishment in 1999 at Egmond. This study confirms that the input of extra sand through nourishments enhances the growth of the amplitude of a sand wave, even to the point that the addition of sand can locally lead to more problems. Namely, the added sand enhances both the crest and the trough of a sand wave. The beach nourishment carried out in 2000 in front of Egmond is an example of an additional nourishment that had to be placed in the trough of a sand wave to counteract the erosion in the trough. Its placement in the trough of the sand wave can also be recognised in the Hovmöller plots. The presence of these sand waves does make it more difficult to see how much the beach and shoreface nourishments contributed to the total shoreline change as the shoreline in some locations may already have been located further seaward than in other locations. Furthermore, the shoreline sand waves that become apparent from the Hovmöller plots do not seem to migrate over time. Ruessink & Jeuken (2002) investigated sand wave patterns in dune foot behaviour along the Dutch coastline based on annual data from as early as 1850. These sand waves in the dune foot can be interpreted as the seaward extensions of the sand waves that occur along the beach. They found that sand waves typically migrate northward along the Delta and Holland coast with migration speeds varying between 80 m/year (Delta coast) and 200 m/year (Holland coast), except for one region, the coast between Petten and IJmuiden. This is exactly the region in which Egmond and Bergen are located. In this coastal section sand waves stay fixed at the same place, sometimes for even more than a century. Cohen & Brière (2007) report similar but also slightly contradicting findings. Only in recent years a stabilisation of the shoreline sand waves at Egmond was found, while they state that in earlier years still migration of the sand waves took place. They reason that the large anthropogenic influence expressed through the nourishments may have been responsible for this stabilisation, with a sand wave crest in front of Egmond and a trough just south of Egmond. Lastly, Guillén et al. (1999) also reported findings on sand waves based on dunefoot mobility but these are for the most part contradictory to this study but also to other studies. In their research they suggested a periodicity of (dunefoot) sand waves of 10-15 years for the northern part of the Holland coast with a migration rate of 150-200 m/yr to the south. This periodicity of 10-15 years coincides with the period of the offshore bar cycle at Egmond-Bergen, which implies a possible relation between the two. However, these findings cannot be confirmed by this thesis.

Alongshore effects of the beach and shoreface nourishments were barely visible at the shoreline, especially in earlier years. Shoreline expansion seems to be very local and predominantly occurs at the pre-determined alongshore extents of the nourishments. In front of Bergen, slight alongshore migration seemed to occur. In case of the 2015 beach nourishment in front of Egmond, there was some small spit formation on the lateral ends of the nourishment indicating the presence of alongshore processes that distribute the nourishment. However, overall the alongshore migration of nourished sand seems to be very limited. This could be (partly) related to the fact that waves approach the Dutch Holland coast from both the south-westerly and north-westerly directions, which roughly keep the nourished sand in a similar location without pronounced alongshore migration in one direction. The lack of migration also corresponds to the stationary behaviour of the sand waves along the coast which also remained in place. Additionally, the beach nourishments did not protrude very much seaward and showed roughly between 10 and 40 m of positive shoreline change after nourishing. Typically, larger-scale coastline perturbations induce larger gradients in alongshore transport, distributing the sand over a wider region than for smaller-scale coastline perturbations (De Schipper et al., 2020). The latter seems

to be the case for Egmond-Bergen. Boers et al. (1999) studied the processes responsible for the short lifetime of beach nourishments in the study area. From their research they suspect that the short lifetime is mainly related to wave-driven alongshore sand transport, which is contradictory to the results in this study. They do also attribute a part of the problem to cross-shore processes, including rip currents and sand transport after dune scarping, creating large mobility of the sand on the beach and on the shoreface. Van Duin et al. (2004) confirms the latter by explaining that the Egmond-Bergen coast is very prone to develop rip currents and horizontal circulations due to its bathymetric longshore irregularities. These rip currents can transport substantial amounts of (nourished) sand seaward. However, this thesis did not look at cross-shore processes, therefore, these findings cannot be confirmed by this thesis.

Entirely different was the response to the mega-nourishment implemented at the southern Holland coast, called the 'Sand Engine'. This nourishment was of a completely different scale with a volume of 17 Mm^3 (~ 10.000 m^3/m) and protruded about 1 km seaward. In this case, rapid and primarily alongshore redistribution of the sand to the northern and southern adjacent coastal sections was observed. Up to 200 m of shoreline expansion was seen in the adjacent sections with an increase in the alongshore extent of the nourishment of 1200 m in the first 18 months (De Schipper et al., 2016). This difference in the importance of alongshore processes between the sand engine and the smaller nourishments near Egmond-Bergen is striking but it is very likely related to the degree of seaward protrusion of the nourishments.

In the case of shoreface nourishments, limited alongshore effects were found as well. Though, the Hovmöller plots do indicate an increase in alongshore effects over time for the shoreface nourishments. In the most recent years (e.g. 2020-2023), the nourished sand also visibly spreads to a maximum 1 km north and south of the shoreface nourishment. Alongshore effects probably became more pronounced due to the large cumulative amount of sand available in the system after years of repeated shoreface nourishments combined with beach nourishments. The alongshore spread in the most recent years also explains the increase in the trend found in the coastal section of Bergen and Castricum (Figures 6.5a, d) after 2020. However, for the rest of the years, the most southern unnourished section near Castricum seems to be barely influenced by the repeated nourishments in the section northward of it. Limited alongshore transport regarding 19 shoreface nourishments along the Dutch coast was also reported by a study of Huisman et al. (2019). In this research 60 to 85% of the erosion from the shoreface nourishments was due to onshore transport, while only 15 to 40% of sand was eroded by alongshore transport predominantly during storm conditions. Impact on neighbouring shorelines was also difficult to distinguish, supporting the results of this thesis. In the research of Cohen & Brière (2007) they did report that the shoreface nourishment at Egmond in 2004 affected the bars 2 km south of the nourished area. However, in this thesis an influence of this particular shoreface nourishment but then on the adjacent shoreline was not observed. Any effects of nourishments on subtidal bars were not considered in this study.

Important to note is that this thesis only investigated the spatial development of the shoreline positions, not considering the alongshore and cross-processes underwater and the sand that accumulates underwater. A large part of nourished sand may also end up in the shallow nearshore zone, in particular for shoreface nourishments (Huisman et al., 2019). Furthermore, CoastSat has a limited horizontal accuracy of approximately 10 m. It is possible that the beach and shoreface nourishments only resulted in very gradual and small-scale alongshore transport which could not be captured and visualised with CoastSat. If, for instance, the adjacent coast accreted only by a few metres in case of a beach nourishment, CoastSat could not capture this minor change because the accuracy of 10 m largely exceeds this. To summarise, alongshore processes only seem to have a minor influence on

the nourishments, though, it is not known how the sand is distributed underwater and which processes are responsible for that. Given the limited impact of alongshore processes, this would suggest that cross-shore processes are more important for the distribution of the nourished sand. However, this study did not investigate the importance of cross-shore processes and therefore no conclusions can be drawn on this subject.

7.3 Limitations and recommendations

This study looked into the dynamics of the coast of Egmond and Bergen on both a temporal and spatial scale under the influence of sand nourishments. However, it also involves some limitations and recommendations for further study. First of all, the toolkit used to determine the shorelines, CoastSat, has a limited horizontal accuracy of approximately 10 m. This error is not only related to the pixel size of the satellite images but also to inaccuracy in the georeferencing of the images. An important uncertainty in this study includes the georeferencing of the satellite images between 1991 and 1997. In these years the geoaccuracy was almost always above 10 m, while generally the threshold for inaccurate georeferencing is set to 10 m in CoastSat. However, this was a time period in which a large number of beach nourishments was carried out. Consequently, the georeferencing threshold for removal was set to 12 m to retain these images but this does pose larger uncertainty in the results between 1991 and 1997. Almonacid-Caballer et al. (2017) show that the georeferencing can be improved according to the method described in their research which also includes high-resolution orthophotos, which might be a recommendation for future studies.

Furthermore, the water level correction was performed with an average, space- and time-invariant beach slope representative for the entire study site instead of a space- and time-varying beach slope. The latter may be better suited because the beach slope is not stationary and varies over space but also over time as a result of variations in incident wave conditions. However, a recent study by Castelle et al. (2021) for Truc Vert in France did not report an improvement in the accuracy of the derived shorelines when a time- and space-varying beach slope was used. This advocates for the average beach slope, but further research on this subject, in particular for high-energy low-sloping beaches will have to reveal if this is also true for the shoreline of Egmond and Bergen.

Another limitation follows from the fact that the acquired shoreline positions were not validated with in-situ measurements of the shoreline. Therefore, no quality control was performed on the dataset to see if the results corresponded to the actual measured shoreline position from beach surveys. A more exact horizontal accuracy than the standard ~10 m for CoastSat can thus not be given. Though, the shoreline positions were both corrected for tidal influence and for wave runup which in other studies generally resulted in good agreement between CoastSat and in-situ data (e.g. Castelle et al., 2021; Graffin et al., 2023). For CoastSat to accurately capture the temporal shoreline variability, the magnitude of typical shoreline change on a certain timescale must exceed this error of ~10 m. In the case of this study, shoreline change on a seasonal timescale mostly ranged between 10 and 20 m, with shoreline change after a beach nourishment also typically exceeding the horizontal error.

Moreover, CoastSat's ability to detect shorelines proved to be more difficult during low-tide conditions. During low tide intertidal features emerged at the beach, distorting the continuity of the shoreline. By manual adjustment of the MNDWI threshold these fluctuations in the shoreline were avoided as much as possible, but only selecting images at higher stages of the tide may prove to be a better solution. The only downside of this method is that this drastically reduces the number of images available for shoreline detection. Another problem affecting the satellite images consisted of a problem with the cloud mask algorithm CFMASK (Chapter 5.1). Multiple images were influenced by masked pixels, making them not useful. CoastSat did provide a setting to remove the masked pixels but due to an

unresolved flaw in this setting for Landsat Collection 2 (C02) satellite images the masked pixels could not be removed. Still, the better quality Landsat Collection 2 was preferred over the older Collection 1, which did not have this issue. Future development in the toolkit CoastSat will very likely resolve this issue.

Time-series of wave heights and wave periods were obtained from Rijkswaterstaat. However, these time-series also contained gaps. Gaps were partly filled through linear interpolation but in case data gaps were too large, the average wave height or period was used to fill in the missing values. Particularly, this is important to consider in the storm analysis in which the wave power was calculated based on these time-series. Additionally, quantifying the effects of storms on the position of the shoreline appeared to be difficult as the data was characterised by quite some noise, obscuring potential storm response. For further studies on storm response it is also recommended to adopt a measuring technique that measures both right before a storm and directly after a storm to accurately determine the influence of storms on the beach. In the current study, the period between the storm and a previous or subsequent data point was sometimes too long to accurately observe the direct effects on the shoreline.

Lastly, this research solely examined the two-dimensional (2D) position of the shoreline and the resulting shoreline change. Including measurements of sand volumes of different cross-shore coastal sections, for instance volumes of the dunes, nearshore zone, beach, or the MKL-zone, can provide valuable additional insights into the redistribution and development of beach and shoreface nourishments.

7.4 Outlook

This study shows that the beach and shoreface nourishments carried out at the coast of Egmond and Bergen had a remarkable influence on the development of the shoreline. Especially after the first shoreface nourishments were placed shoreline expansion really started to kick off. Shoreface nourishments combined with beach nourishments seemed to have been an optimal strategy. As shoreface nourishments are also more cost-effective and have to be constructed less often, either with or without a beach nourishment, this proves to be a good solution to counteract the erosion at Egmond and Bergen, also in the future. These results on the effects of beach and shoreface nourishments in this study can also aid in future nourishment projects in determining the optimal strategies to maintain the coastline. In most recent years, shoreline progradation mostly stabilised but future research will have to tell whether this trend continues under the influence of repeated shoreface nourishments. In an ideal situation, the current shoreline position will only need to be maintained at this level. Additionally, the last shoreface nourishment was not combined with beach nourishments and if this will also not be the case in 2023/2024 this might provide more insight into the actual contribution of a beach nourishment to a shoreface nourishment. In the south near Castricum the shoreline position can be considered stable without the need for nourishments. However, with global change and rising sea levels, beach erosion is likely to exacerbate in the future. Therefore, nourishment efforts will almost certainly have to be increased in the Netherlands. With regard to the technical aspect, satellite remote sensing techniques are under continuous development and in the previous decades already the optical image resolution and satellite revisit period have been largely improved. These are only two examples but in the future it is very plausible that even smaller temporal and spatial scales can be resolved beyond the ones investigated in this research, with high-resolution satellite data becoming vital for monitoring the present-day shorelines worldwide.

8. Conclusion

With the use of satellite images from 1985-present and the shoreline mapping tool CoastSat both the temporal and spatial variability in the shoreline of Bergen-Egmond was investigated, including the effects of repeated sand nourishments. Overall, this thesis aimed to increase the understanding of shoreline dynamics for highly energetic, low-sloping, repeatedly nourished beaches.

The temporal variability in the shoreline revealed that for a repeatedly nourished coast the interannual trend component is very dominant, while for the unnourished coast the interannual trend only explained a minor part of the total variability. For the latter, most of the variation was explained by the remainder component, which contained the random variations in the shoreline (e.g. storms) but also the inaccuracies present in the data. The nourished Egmond-Bergen coast showed an increasing trend of approximately 2.00 m/year, while along the unnourished coast of Castricum a relatively stable interannual trend was found (0.31 m/year). A very small contribution of seasonality became apparent for the whole study area, indicating that these low-sloping beaches do not possess large seasonal cycles with beach accretion in summer and large retreats in winter following the incident wave conditions. This is in line with previous research which already reported the more robust nature of storm-dominated (dissipative), microtidal coastlines, protected by subtidal bars that are often present. A clear response of the shoreline to large storm events was also barely observed. The lack of a distinct storm response together with the limited seasonality designates the robust character and very gradual dynamics of this coast in comparison to other coasts across the world (e.g. Truc Vert, France; Narrabeen, Australia).

With regard to spatial changes in shoreline position and dynamics after the implementation of a nourishment, the following conclusions can be drawn. From the results can be derived that the coast of Egmond and Bergen underwent considerable changes due to the placement of the repeated sand nourishments, signified by the large changes in alongshore variability found for the nourished area in comparison to the unnourished section. The beach nourishments constructed between 1990 and 2000 only resulted in relatively small but not sustainable progradation of the shoreline (< 10 m). At the scale of only one shoreface nourishment limited shoreline advance was seen as well. However, in particular the repetition of the shoreface nourishments was responsible for the shoreline expansion over time, creating a sort of cumulative effect on the shoreline with in total about 50 m of seaward advance. Consequently, shoreface nourishments (in combination with beach nourishments) were essential to generate the large amount of shoreline progradation (in total ~60-80m), which is illustrated both in the Hovmöller plots and in the increasing interannual trend. The shoreline advance probably resulted from beach sedimentation induced by the repeated shoreface nourishments themselves but was also likely the result of the protective function of a shoreface nourishment on a beach nourishment.

Both types of nourishments showed relatively limited alongshore migration of sediment, thereby not considerably influencing nearby non-nourished beaches. Only in recent years alongshore effects of shoreface nourishments became more prominent on the adjacent shorelines, probably related to the cumulative effect of the shoreface nourishments. Though, important to keep in mind is that this study only looked at shoreline changes above water and not how the sand is redistributed below water, for example in the nearshore zone. The minor alongshore effects do coincide with the stationary behaviour of the shoreline sand waves that came forth from the Hovmöller plots. Moreover, the nourishments noticeably enhanced the amplitude of the sand waves in the study area. Beach nourishments only had a lifetime of 1 to 2 years in the study area before they were (almost) completely redistributed. Some beach nourishments followed the ‘saw-tooth’ concept with a marked peak after nourishing followed by gradual erosion, but in other cases the peak was immediately succeeded by steep erosion.

Alongshore distribution of beach nourishments appeared to be limited, however, no conclusions can be drawn on the importance of cross-shore processes.

This study demonstrates that the current nourishment strategy employed at Egmond and Bergen is without any doubt effective, evidenced by the considerable sedimentation of the shoreline in the last decade. Especially the combination of a shoreface nourishment with a beach nourishment seemed to be successful, whereby it is very plausible that the repeated shoreface nourishments had a protective function resulting in an elongation of the lifetime of the beach nourishments. Furthermore, the insights gained from this research hold valuable implications for the design and execution of future nourishment projects and can aid in the development of new coastal policies, particularly in the context of climate change. Lastly, with the limited seasonality found and the results on the effect of repeated nourishments on long-term trends in shoreline position, this study also can serve as a starting point for better understanding of low-sloping and wave-dominated coasts in future studies.

References

Aagaard, T., Kroon, A., Andersen, S., Møller Sørensen, R., Quartel, S., & Vinther, N. (2005). Intertidal beach change during storm conditions; Egmond, The Netherlands. *Marine Geology*, *218*(1–4), 65–80. https://doi.org/10.1016/j.margeo.2005.04.001

Almonacid-Caballer, J., Pardo-Pascual, J., & Ruiz, L. (2017). Evaluating Fourier Cross-Correlation Sub-Pixel Registration in Landsat Images. *Remote Sensing*, *9*(10), 1051. https://doi.org/10.3390/rs9101051

Awty-Carroll, K., Bunting, P., Hardy, A., & Bell, G. (2019). An Evaluation and Comparison of Four Dense Time Series Change Detection Methods Using Simulated Data. *Remote Sensing*, *11*(23), 2779. https://doi.org/10.3390/rs11232779

Boers, M. (1999). Suppleties bij Egmond en Bergen. *RIKZ - 99.030*. http://resolver.tudelft.nl/uuid:7c65b12a-33f8-4709-93be-09bada9d32b1

Bosboom, J., & Stive, M. J. F. (2022). *Coastal dynamics* (1.1). Delft University of Technology, Civil Engineering and Geosciences. https://doi.org/10.5074/T.2021.001

Brand, E., Ramaekers, G., & Lodder, Q. (2022). Dutch experience with sand nourishments for dynamic coastline conservation – An operational overview. *Ocean & Coastal Management*, *217*, 106008. https://doi.org/10.1016/j.ocecoaman.2021.106008

Briere, C., Ormondt, M., & Walstra, D.-J. (2008). Morphodynamic modelling of a shoreface nourishment at Egmond-aan-Zee, The Netherlands. *Xèmes Journée Nationales Génie Côtier–Génie Civil, Sophia Antipolis*, 38. https://doi.org/10.5150/jngcgc.2008.003-B

Bruins, R. J. (2016). Morphological behaviour of shoreface nourishments along the Dutch coast: Data analysis of historical shoreface nourishments for a better understanding and design. M.Sc. Report. Delft University of Technology, Delft. http://resolver.tudelft.nl/uuid:e7585706-571d-4b97-8b89-d7c7abd9730c

Castelle, B., Masselink, G., Scott, T., Stokes, C., Konstantinou, A., Marieu, V., & Bujan, S. (2021). Satellite-derived shoreline detection at a high-energy meso-macrotidal beach. *Geomorphology*, *383*, 107707. https://doi.org/10.1016/j.geomorph.2021.107707

Chander, G., Markham, B. L., & Helder, D. L. (2009). Summary of current radiometric calibration coefficients for Landsat MSS, TM, ETM+, and EO-1 ALI sensors. *Remote Sensing of Environment*, *113*(5), 893–903. https://doi.org/10.1016/j.rse.2009.01.007

Cipolletti, M. P., Delrieux, C. A., Perillo, G. M. E., & Cintia Piccolo, M. (2012). Superresolution border segmentation and measurement in remote sensing images. *Computers & Geosciences*, *40*, 87–96. https://doi.org/10.1016/j.cageo.2011.07.015

Cohen, A. B., & Brière, C. (2007). Evaluatie van de uitgevoerde suppleties bij Egmond op basis van Argus video waarnemingen. *Deltares (WL) report Z4212*. http://resolver.tudelft.nl/uuid:008d440d-6535-4bd9-b100-00206bce3881

De Ronde, J. G. (2008). Toekomstige langjarige suppletiebehoefte. *Deltares (WL) report Z4582.24*, Delft. http://resolver.tudelft.nl/uuid:5fa41e3f-007b-468d-a963-b531e4974af9

De Ruig, J. H. M., & Hillen, R. (1997). Developments in Dutch Coastline Management: Conclusions from the Second Governmental Coastal Report. *Journal of Coastal Conservation*, *3*(2), 203–210. https://www.jstor.org/stable/25098269

De Schipper, M. A., De Vries, S., Ruessink, G., De Zeeuw, R. C., Rutten, J., Van Gelder-Maas, C., & Stive, M. J. F. (2016). Initial spreading of a mega feeder nourishment: Observations of the Sand Engine pilot project. *Coastal Engineering*, *111*, 23–38. https://doi.org/10.1016/j.coastaleng.2015.10.011

De Schipper, M. A., Ludka, B. C., Raubenheimer, B., Luijendijk, A. P., & Schlacher, Thomas. A. (2020). Beach nourishment has complex implications for the future of sandy shores. *Nature Reviews Earth & Environment*, *2*(1), 70–84. https://doi.org/10.1038/s43017-020-00109-9

De Sonneville, B., & Van der Spek, A. J. F. (2012). Sediment- and morphodynamics of shoreface nourishments along the North-Holland coast. *ICCE 2012: Proceedings of the 33rd International Conference on Coastal Engineering, Santander, Spain*. http://resolver.tudelft.nl/uuid:c96bb814-811f-4858-b1d8-a48f552904de

Dean, R. G. (2002). *Beach Nourishment: Theory and Practice*. World Scientific.

Dean, R. G., & Campbell, T. J. (2016). Springer Handbook of Ocean Engineering. *Journal of Ocean Engineering and Marine Energy*, *3*(3), 635–652. https://doi.org/10.1007/s40722-017-0083-9

Deltacommissie. (2008). *Samen Werken met water: Een land dat leeft, bouwt aan zijn toekomst*. http://resolver.tudelft.nl/uuid:6bb16d66-94c6-44eb-bb6b-e389283c1e82

El Fellah, S., Rziza, M., & El Haziti, M. (2017). An Efficient Approach for Filling Gaps in Landsat 7 Satellite Images. *IEEE Geoscience and Remote Sensing Letters*, *14*(1), 62–66. https://doi.org/10.1109/LGRS.2016.2626138

Elko, N. A., Holman, R. A., & Gelfenbaum, G. (2005). Quantifying the Rapid Evolution of a Nourishment Project with Video Imagery. *Journal of Coastal Research*, *214*, 633–645. https://doi.org/10.2112/04-0280.1

Elko, N. A., & Wang, P. (2007). Immediate profile and planform evolution of a beach nourishment project with hurricane influences. *Coastal Engineering*, *54*(1), 49–66. https://doi.org/10.1016/j.coastaleng.2006.08.001

Ghaderpour, E. (2021). JUST: MATLAB and python software for change detection and time series analysis. *GPS Solutions*, *25*(3), 85. https://doi.org/10.1007/s10291-021-01118-x

Ghaderpour, E., Liao, W., & Lamoureux, M. P. (2018). Antileakage least-squares spectral analysis for seismic data regularization and random noise attenuation. *GEOPHYSICS*, *83*(3), V157–V170. https://doi.org/10.1190/geo2017-0284.1

Ghaderpour, E., & Vujadinovic, T. (2020). Change Detection within Remotely Sensed Satellite Image Time Series via Spectral Analysis. *Remote Sensing*, *12*(23), 4001. https://doi.org/10.3390/rs12234001

Graffin, M., Taherkhani, M., Leung, M., Vitousek, Sean. F., Kaminsky, G., & Ruggiero, P. (2023). Monitoring interdecadal coastal change along dissipative beaches via satellite imagery at regional scale. *Cambridge Prisms: Coastal Futures*, 1–22. https://doi.org/10.1017/cft.2023.30

Grunnet, N. M., & Ruessink, B. G. (2005). Morphodynamic response of nearshore bars to a shoreface nourishment. *Coastal Engineering*, *52*(2), 119–137. https://doi.org/10.1016/j.coastaleng.2004.09.006

Guillén, J., Stive, M. J. F., & Capobianco, M. (1999). Shoreline evolution of the Holland coast on a decadal scale. *Earth Surface Processes and Landforms*, *24*(6), 517–536. https://doi.org/10.1002/(SICI)1096-9837(199906)24:6<517::AID-ESP974>3.0.CO;2-A

Hamed, K. H., & Ramachandra Rao, A. (1998). A modified Mann-Kendall trend test for autocorrelated data. *Journal of Hydrology*, *204*(1–4), 182–196. https://doi.org/10.1016/S0022-1694(97)00125-X

Hamm, L., Capobianco, M., Dette, H. H., Lechuga, A., Spanhoff, R., & Stive, M. J. F. (2002). A summary of European experience with shore nourishment. *Coastal Engineering*, *47*(2), 237–264. https://doi.org/10.1016/S0378-3839(02)00127-8

Hanson, H., Brampton, A., Capobianco, M., Dette, H. H., Hamm, L., Laustrup, C., Lechuga, A., & Spanhoff, R. (2002). Beach nourishment projects, practices, and objectives—A European overview. *Coastal Engineering*, *47*(2), 81–111. https://doi.org/10.1016/S0378-3839(02)00122-9

Heuvel, T. V., De Kruik, H., & Ebbing, H. (1996). Coastline management. *National Institute for Coastal and Marine Management/RIKZ report C12318 RWS*. https://edepot.wur.nl/177625

Hillen, R., & Roelse, P. (1995). Dynamic preservation of the coastline in the Netherlands. *Journal of Coastal Conservation, 1*(1), 17–28. https://doi.org/10.1007/BF02835558

Hoefel, F., & Elgar, S. (2003). Wave-induced sediment transport and sandbar migration. *Science*, *299*(5614), 1885–1888. https://doi-org.proxy.library.uu.nl/10.1126/science.1081448

Huisman, B. J. A., Walstra, D.-J. R., Radermacher, M., de Schipper, M. A., & Ruessink, B. G. (2019). Observations and Modelling of Shoreface Nourishment Behaviour. *Journal of Marine Science and Engineering*, *7*(3), Article 3. https://doi.org/10.3390/jmse7030059

Kendall, M. (1975). Rank correlation measures. *Charles Griffin, London*, *202*(15).

Konstantinou, A., Scott, T., Masselink, G., Stokes, K., Conley, D., & Castelle, B. (2023). Satellite-based shoreline detection along high-energy macrotidal coasts and influence of beach state. *Marine Geology*, *462*, 107082. https://doi.org/10.1016/j.margeo.2023.107082

Liu, Q., Trinder, J., & Turner, I. L. (2017). Automatic super-resolution shoreline change monitoring using Landsat archival data: A case study at Narrabeen–Collaroy Beach, Australia. *Journal of Applied Remote Sensing*, *11*(1), 016036. https://doi.org/10.1117/1.JRS.11.016036

Lodder, Q., & Slinger, J. (2022). The 'Research for Policy' cycle in Dutch coastal flood risk management: The Coastal Genesis 2 research programme. *Ocean & Coastal Management*, *219*, 106066. https://doi.org/10.1016/j.ocecoaman.2022.106066

Mann, H. B. (1945). Nonparametric Tests Against Trend. *Econometrica*, *13*(3), 245. https://doi.org/10.2307/1907187

Meulen, F. V. D., Van Der Valk, B., Baars, L., Schoor, E., & Van Woerden, H. (2014). Development of new dunes in the Dutch Delta: Nature compensation and 'building with nature'. *Journal of Coastal Conservation*, *18*(5), 505–513. https://doi.org/10.1007/s11852-014-0315-2

Ministerie van Verkeer en Waterstaat. (2000). *3e Kustnota, Traditie, Trends en Toekomst*. Ministerie van Verkeer en Waterstaat. https://stive51.home.xs4all.nl/deltalinks/3ekustnota.pdf

Mulder, J. P. M. (2000). Zandverliezen in het Nederlandse kustsysteem: Advies voor dynamisch handhaven in de 21e eeuw. *Rapport RIKZ/2000.36*. http://resolver.tudelft.nl/uuid:25fec7e4-91d2-44c2-b60e-503149dd9893

Mulder, J. P. M., Hommes, S., & Horstman, E. M. (2011). Implementation of coastal erosion management in the Netherlands. *Ocean & Coastal Management*, *54*(12), 888–897. https://doi.org/10.1016/j.ocecoaman.2011.06.009

Mulder, J. P. M., Nederbragt, G., Steetzel, H. J., Van Koningsveld, M., & Wang, Z. B. (2007). DIFFERENT IMPLEMENTATION SCENARIOS FOR THE LARGE SCALE COASTAL POLICY OF THE NETHERLANDS. *Coastal Engineering 2006*, 1705–1717. https://doi.org/10.1142/9789812709554_0144

Mulder, J. P. M., & Tonnon, P. K. (2011). " SAND ENGINE ": BACKGROUND AND DESIGN OF A MEGA-NOURISHMENT PILOT IN THE NETHERLANDS. *Coastal Engineering Proceedings*, *32*, 35. https://doi.org/10.9753/icce.v32.management.35

Ojeda, E., Ruessink, B. G., & Guillen, J. (2008). Morphodynamic response of a two-barred beach to a shoreface nourishment. *Coastal Engineering*, *55*(12), 1185–1196. https://doi.org/10.1016/j.coastaleng.2008.05.006

Otsu, N. (1979). A Threshold Selection Method from Gray-Level Histograms. *IEEE Transactions on Systems, Man, and Cybernetics*, *9*(1), 62–66. https://doi.org/10.1109/TSMC.1979.4310076

Pedregosa, F., Varoquaux, G., Gramfort, A., Michel, V., Thirion, B., Grisel, O., Blondel, M., Prettenhofer, P., Weiss, R., Dubourg, V., Vanderplas, J., Passos, A., Cournapeau, D., Brucher, M., Perrot, M., & Duchesnay, E. (2011). Scikit-learn: Machine Learning in Python. *Journal of Machine Learning Research*, *12*, 2825–2830. https://www.jmlr.org/papers/volume12/pedregosa11a/pedregosa11a.pdf

Petrova, P. G., Jong, S. M. D., & Ruessink, G. (2023). A Global Remote-Sensing Assessment of the Intersite Variability in the Greening of Coastal Dunes. *Remote Sensing*, *15*(6), 1491. https://doi.org/10.3390/rs15061491

Pilarczyk, K. W. (2007). FLOOD PROTECTION AND MANAGEMENT IN THE NETHERLANDS. In O. F. Vasiliev, P. H. A. J. M. Van Gelder, E. J. Plate, & M. V. Bolgov (Eds.), *Extreme Hydrological Events: New Concepts for Security* (Vol. 78, pp. 385–407). Springer Netherlands. https://doi.org/10.1007/978-1-4020-5741-0_26

Price, T. D., & Ruessink, B. G. (2011). State dynamics of a double sandbar system. *Continental Shelf Research*, *31*(6), 659–674. https://doi.org/10.1016/j.csr.2010.12.018

Pwa, S. T., & Nieboer, H. E. (2006). Evaluatie onderwatersuppleties Noord-en Zuid-Holland. *RIKZ-06355*. http://resolver.tudelft.nl/uuid:eb12d812-e0f2-4fd6-aeb8-a67a5a2c3f26

Quartel, S., & Grasmeijer, B. T. (2007). Dynamiek van het strand bij Noordwijk aan Zee en Egmond aan Zee en het effect van suppleties. *Rijksinstituut Voor Kust En Zee (RIKZ). Opdracht RKZ-1667*. http://resolver.tudelft.nl/uuid:b3c98ba0-f81e-443f-b982-d17fda17e264

Quartel, S., Kroon, A., & Ruessink, B. G. (2008). Seasonal accretion and erosion patterns of a microtidal sandy beach. *Marine Geology*, *250*(1–2), 19–33. https://doi.org/10.1016/j.margeo.2007.11.003

Radermacher, M., De Schipper, M. A., Price, T. D., Huisman, B. J. A., Aarninkhof, S. G. J., & Reniers, A. J. H. M. (2018). Behaviour of subtidal sandbars in response to nourishments. *Geomorphology*, *313*, 1–12. https://doi.org/10.1016/j.geomorph.2018.04.005

Roelse, P. (1996). Evaluatie van zandsuppleties aan de Nederlandse kust 1975-1994. *RIKZ-96.028*. http://resolver.tudelft.nl/uuid:124344c6-151c-4e31-bb5b-95eb2e63f5c5

Ruessink, B. G., Holman, R. A., Kuriyama, Y., Van Enckevort, I. M. J., & Wijnberg, K. M. (2003). Intersite comparison of interannual nearshore bar behavior. *Journal of Geophysical Research: Oceans*, *108*(C8). https://doi.org/10.1029/2002JC001505

Ruessink, B. G., & Jeuken, M. C. J. L. (2002). Dunefoot dynamics along the Dutch coast. *Earth Surface Processes and Landforms*, *27*(10), 1043–1056. https://doi.org/10.1002/esp.391

Ruessink, B. G., & Kroon, A. (1994). The behaviour of a multiple bar system in the nearshore zone of Terschelling, the Netherlands: 1965–1993. *Marine Geology*, *121*(3), 187–197. https://doi.org/10.1016/0025-3227(94)90030-2

Ruessink, G., Schwarz, C. S., Price, T. D., & Donker, J. J. A. (2019). A Multi-Year Data Set of Beach-Foredune Topography and Environmental Forcing Conditions at Egmond aan Zee, The Netherlands. *Data*, *4*(2), 73. https://doi.org/10.3390/data4020073

Sen, P. K. (1968). Estimates of the Regression Coefficient Based on Kendall's Tau. *Journal of the American Statistical Association*, *63*(324), 1379–1389. https://doi.org/10.1080/01621459.1968.10480934

Short, A. D., & Aagaard, T. (1993). Single and Multi-Bar Beach Change Models. Journal of Coastal Research, 141–157. http://www.jstor.org/stable/25735727

Shand, R. D., Bailey, D. G., & Shepherd, M. J. (1999). An Inter-Site Comparison of Net Offshore Bar Migration Characteristics and Environmental Conditions. *Journal of Coastal Research*, *15*(3), 750–765. https://www.jstor.org/stable/4298989

Spanhoff, R., De Keijzer, S., Walburg, A. M., & Biegel, E. J. (2004). Evaluatie onderwatersuppleties Egmond en Bergen. *RIKZ/OS/2004/112W*. http://resolver.tudelft.nl/uuid:c17162db-fa79-440f-bb3d-fc5f778c865b

Spanhoff, R., & van de Graaff, J. (2007). Towards a better understanding and design of shoreface nourishments. In *Coastal Engineering 2006* (pp. 4141–4153). World Scientific Publishing Company. https://doi.org/10.1142/9789812709554_0348

Stive, M. J. F., Aarninkhof, S. G. J., Hamm, L., Hanson, H., Larson, M., Wijnberg, K. M., Nicholls, R. J., & Capobianco, M. (2002). Variability of shore and shoreline evolution. *Coastal Engineering*, *47*(2), 211–235. https://doi.org/10.1016/S0378-3839(02)00126-6

Stive, M. J. F., De Schipper, M. A., Luijendijk, A. P., Aarninkhof, S. G. J., Van Gelder-Maas, C., Van Thiel de Vries, J. S. M., De Vries, S., Henriquez, M., Marx, S., & Ranasinghe, R. (2013). A New Alternative to Saving Our Beaches from Sea-Level Rise: The Sand Engine. *Journal of Coastal Research*, *290*, 1001–1008. https://doi.org/10.2112/JCOASTRES-D-13-00070.1

Stockdon, H. F., Holman, R. A., Howd, P. A., & Sallenger, A. H. (2006). Empirical parameterization of setup, swash, and runup. *Coastal Engineering*, *53*(7), 573–588. https://doi.org/10.1016/j.coastaleng.2005.12.005

Stolk, A. (1989). Kustverdediging na 1990 (Kustnota 1990): Technisch rapport 1: Zandsysteem Kust. *TR-01, Rapport Geopro 1989.02 van Rijksuniversiteit Utrecht, Vakgroep Fysische Geografie*. http://resolver.tudelft.nl/uuid:1953f7f6-c0e5-45aa-824d-6dfb0ccb9585

Tu, T.-M., Su, S.-C., Shyu, H.-C., & Huang, P. S. (2001). A new look at IHS-like image fusion methods. *Information Fusion*, *2*(3), 177–186. https://doi.org/10.1016/S1566-2535(01)00036-7

Turner, I. L. (2006). Discriminating Modes of Shoreline Response to Offshore-Detached Structures. *Journal of Waterway, Port, Coastal, and Ocean Engineering*, *132*(3), 180–191. https://doi.org/10.1061/(ASCE)0733-950X(2006)132:3(180)

Van Alphen, J. (2016). The Delta Programme and updated flood risk management policies in the Netherlands. *Journal of Flood Risk Management*, *9*(4), 310–319. https://doi.org/10.1111/jfr3.12183

Van der Grinten, R. M., & Ruessink, B. G. (2012). Evaluatie van de kustversterking bij Noordwijk aan Zee—De invloed van de versterking op de zandbanken. *Deltares report 437842.* https://dspace.library.uu.nl/handle/1874/281743

Van der Spek, A. J. F., Kruif, A. C., & Spanhoff, R. (2007). Richtlijnen Onderwatersuppleties. *RIKZ-2007.012*. http://resolver.tudelft.nl/uuid:f310d329-c75a-409a-8422-f8041601d95a

Van der Wal, D. (2004). Beach-Dune Interactions in Nourishment Areas along the Dutch Coast. *Journal of Coastal Research*, *201*, 317–325. https://doi.org/10.2112/1551-5036(2004)20[317:BIINAA]2.0.CO;2

Van der Walt, S., Schönberger, J. L., Nunez-Iglesias, J., Boulogne, F., Warner, J. D., Yager, N., Gouillart, E., & Yu, T. (2014). scikit-image: Image processing in Python. *PeerJ*, *2*, e453. https://doi.org/10.7717/peerj.453

Van Duin, M. J. P., Wiersma, N. R., Walstra, D. J. R., Van Rijn, L. C., & Stive, M. J. F. (2004). Nourishing the shoreface: Observations and hindcasting of the Egmond case, The Netherlands. *Coastal Engineering*, *51*(8–9), 813–837. https://doi.org/10.1016/j.coastaleng.2004.07.011

Van Koningsveld, M., & Lescinski, J. (2006). Decadal scale performance of coastal maintenance in the Netherlands. *Shore & Beach*, *75*(1), 1–17. https://www.researchgate.net/publication/256297002_Decadal_scale_performance_of_coastal_maintenance_in_the_Netherlands

Van Rijn, L. C. (1995). Sand budget and coastline changes of the central coast of Holland between Den Helder and Hoek van Holland, period 1964-2040. *Deltares (WL) Report H2129*. http://resolver.tudelft.nl/uuid:6837af90-6f12-4f14-ac73-4d6978f72f47

Verhagen, H. J. (1989). Sand waves along the Dutch coast. *Coastal Engineering*, *13*(2), 129–147. https://doi.org/10.1016/0378-3839(89)90020-3

Verhagen, H. J. (1992). Method for artificial beach nourishment. *Proc. of the 23rd International Conference on Coastal Engineering, ICCE '92, Venice, Italy, 1992*. http://resolver.tudelft.nl/uuid:5d24ef34-1698-4860-9d78-8884269f79b2

Vermaas, T., Boersen, S., Wilmink, R., & Lodder, Q. (2021). National analysis of nourishments; Coastal state indicators and driving forces for Bergen-Egmond, the Netherlands. *Rijkswaterstaat & Deltares.* https://northsearegion.eu/media/18020/national-analysis_bergen_rws-deltares_20210713-final.pdf

Vermaas, T., Elias, E. P. L., & Vonhögen-Peeters, L. M. (2013). Ontwikkeling gefaseerde suppletie Ameland 2010-2011. *Deltares report 1207724-002*. https://www.deltares.nl/expertise/publicaties/ontwikkeling-gefaseerde-suppletie-ameland-2010-2011

Vos, K., Harley, M. D., Splinter, K. D., Simmons, J. A., & Turner, I. L. (2019a). Sub-annual to multi-decadal shoreline variability from publicly available satellite imagery. *Coastal Engineering*, *150*, 160–174. https://doi.org/10.1016/j.coastaleng.2019.04.004

Vos, K., Splinter, K. D., Harley, M. D., Simmons, J. A., & Turner, I. L. (2019b). CoastSat: A Google Earth Engine-enabled Python toolkit to extract shorelines from publicly available satellite imagery. *Environmental Modelling & Software*, *122*, 104528. https://doi.org/10.1016/j.envsoft.2019.104528

Walstra, D. J. R., Reniers, A. J. H. M., Ranasinghe, R., Roelvink, J. A., & Ruessink, B. G. (2012). On bar growth and decay during interannual net offshore migration. *Coastal Engineering*, *60*, 190–200. https://doi.org/10.1016/j.coastaleng.2011.10.002

Wijnberg, K. M. (2002). Environmental controls on decadal morphologic behaviour of the Holland coast. *Marine Geology*, *189*(3), 227–247. https://doi.org/10.1016/S0025-3227(02)00480-2

Wijnberg, K. M., Aarninkhof, S., & Spanhoff, R. (2007). Response of a shoreline sand wave to beach nourishment. *Proceedings of the Coastal Engineering Conference* (pp. 4205–4217). https://doi.org/10.1142/9789812709554_0353

Wittebrood, M., De Vries, S., Goessen, P., & Aarninkhof, S. (2018). AEOLIAN SEDIMENT TRANSPORT AT A MAN-MADE DUNE SYSTEM; BUILDING WITH NATURE AT THE HONDSBOSSCHE DUNES. *Coastal Engineering Proceedings, 1*(36), papers.83. https://doi.org/10.9753/icce.v36.papers.83

Wright, L. D. (1980). BEACH CUT IN RELATION TO SURF ZONE MORPHODYNAMICS. *Coastal Engineering Proceedings*, *17*, 60. https://doi.org/10.9753/icce.v17.60

Wright, L. D., & Short, A. D. (1984). Morphodynamic variability of surf zones and beaches: A synthesis. *Marine Geology*, *56*(1), 93–118. https://doi.org/10.1016/0025-3227(84)90008-2

Appendices

Appendix A

Decomposition of the alongshore-averaged time-series for the four coastal sections, but in this case the demeaned data ($\widetilde{\widetilde{D_{sh,t}}}(y,t)$) was also monthly-averaged. The decomposition was done based on the same method described in Chapter 5.3.1, with the same motivation for the input parameters. In the following figures, (a) represents RSP 3000-3395; (b) represents RSP 3400-3595; (c) represents RSP 3600-3995; (d) represents RSP 4000-4350.

a)

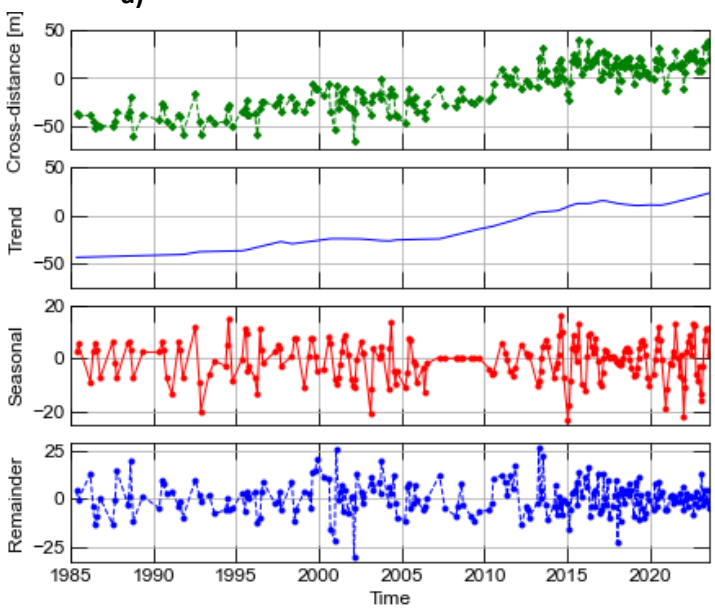

b)

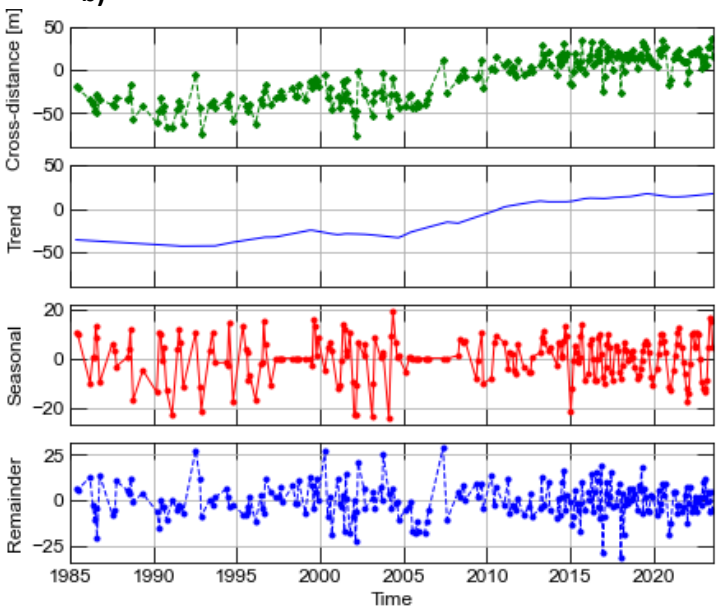

c)

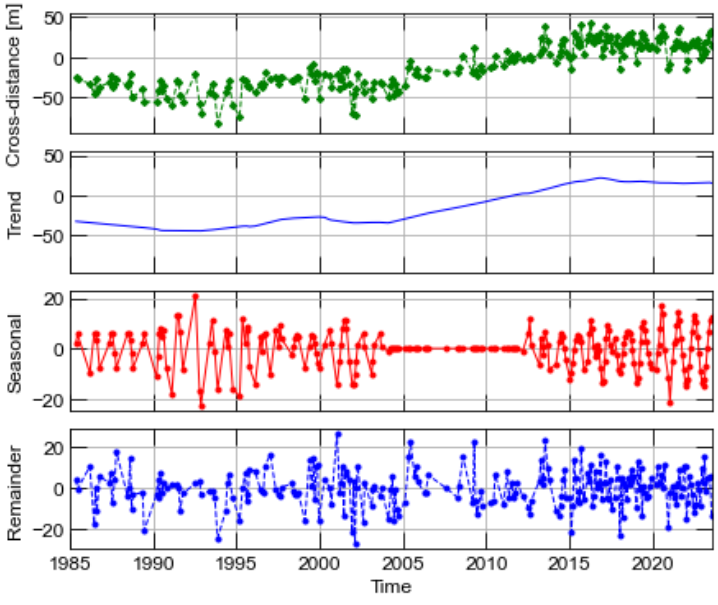

d)

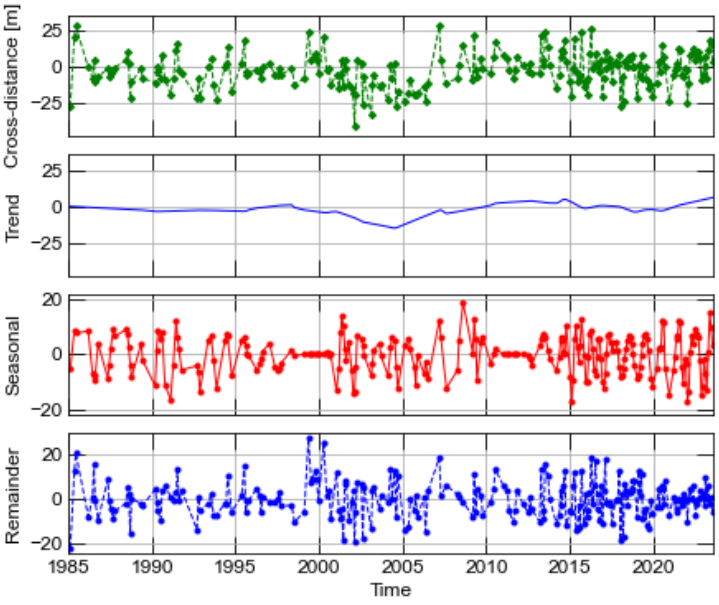

Input parameters for the JUST decomposition for each of the four defined coastal sections: the window size, the translation step, the significance level, and the cyclic frequencies.

Coastal section	Window size (*R*)	Translation step (δ)	Significance level (α)	Cyclic frequencies (ω)
RSP 3000-3395	33	12	0.05	[0.8, 1.0, 1.2, …, 3.8]
RSP 3400-3595	33	12	0.05	[0.8, 1.0, 1.2, …, 3.8]
RSP 3600-3995	34	12	0.05	[0.8, 1.0, 1.2, …, 3.8]
RSP 4000-4350	33	12	0.05	[0.8, 1.0, 1.2, …, 3.8]

Appendix B

Time series decomposition of wave height (above) and wave period (below).

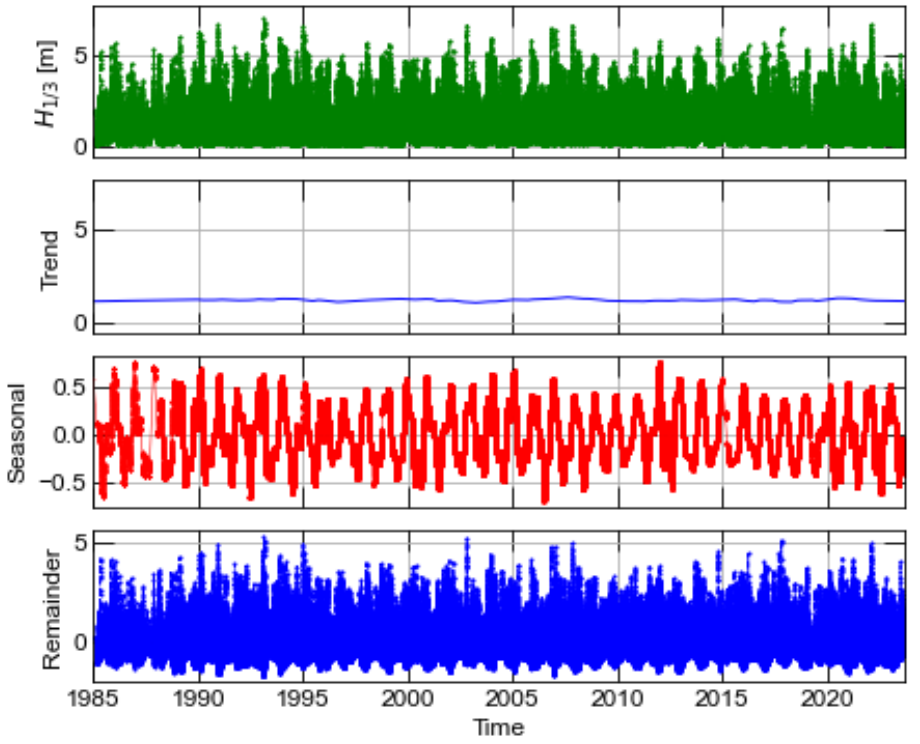

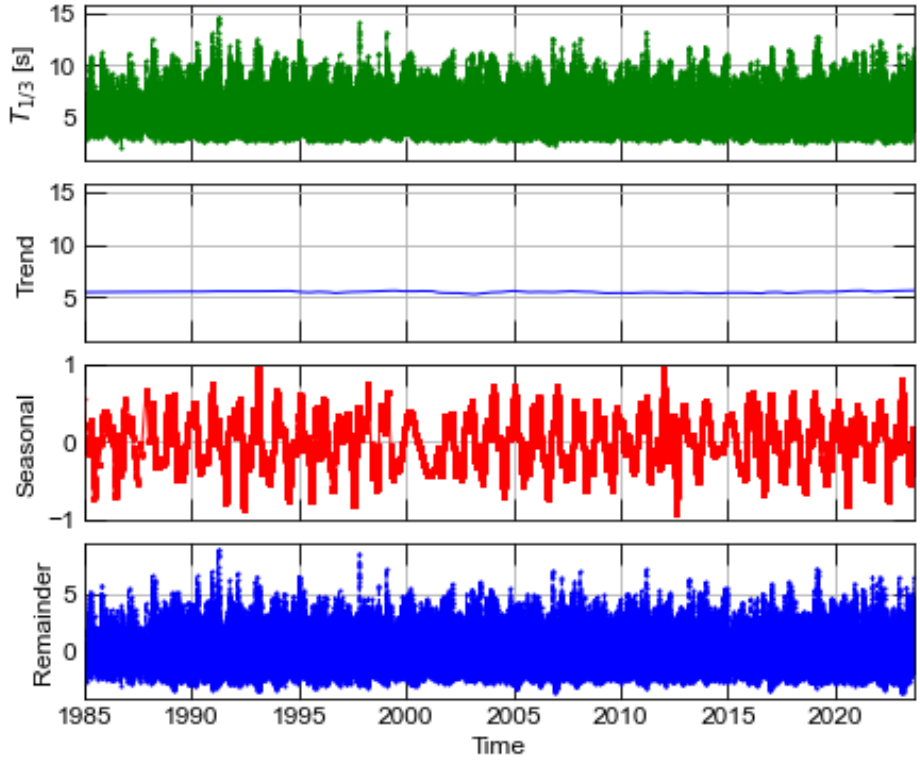

Appendix C

The remainder component resulting from the decomposition of the time-series of all coastal sections defined in Chapter 6.2.1. The graphs include the remainder components from 2015-2023. The dark green lines represent the timing of the storm events that are included in Table 6.3. In some cases the green lines coincide when storms occurred shortly after each other, therefore not all individual storms are clearly distinguishable.

Section A:

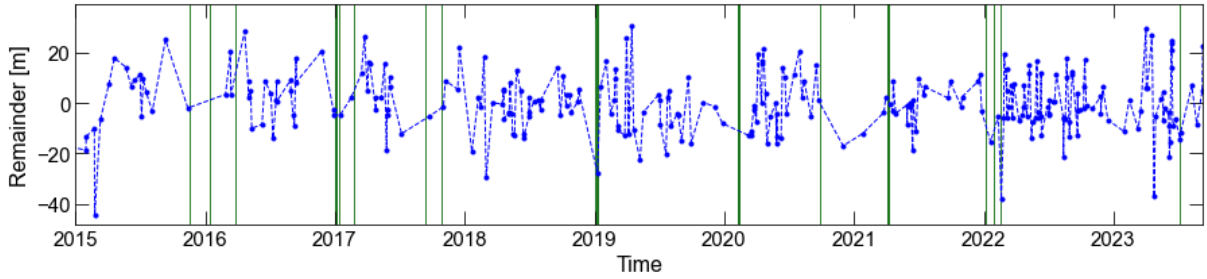

Section B:

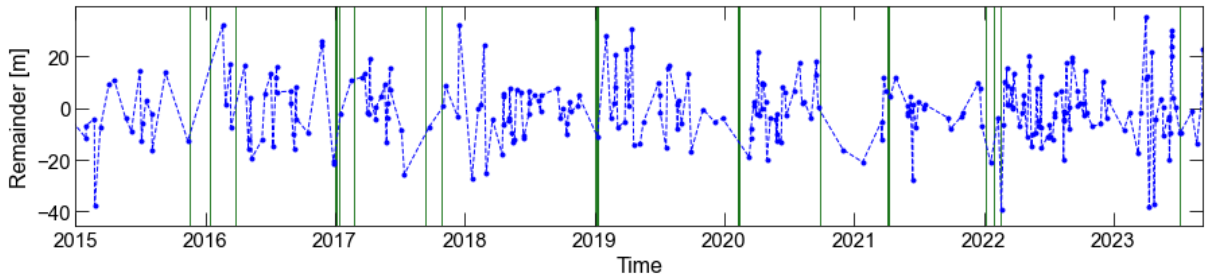

Section C:

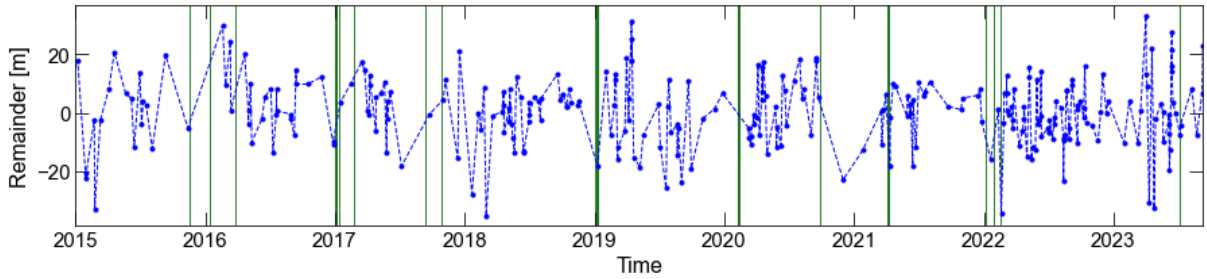

Section D:

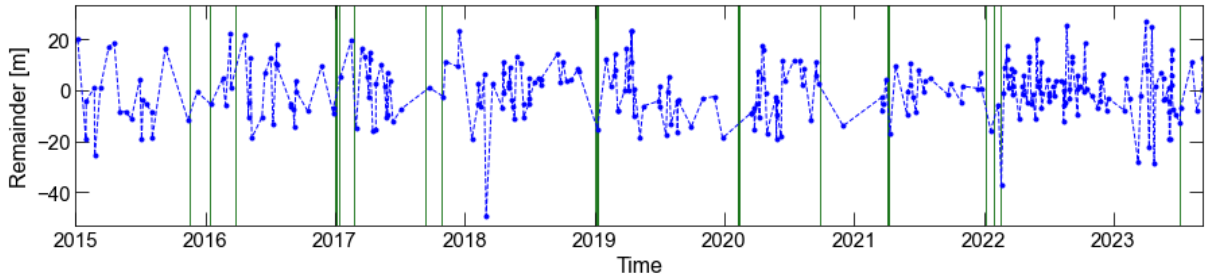

Appendix D

The sum of the wave power P plotted against the shoreline change between each two data points spaced 1 month apart for all four coastal sections to study the non-instantaneous response of the shoreline position to storm events. Two monthly-averaged data points spaced 1 month apart thus equals a total time period of 2 months for which the sum of the wave power was calculated.

Section A:

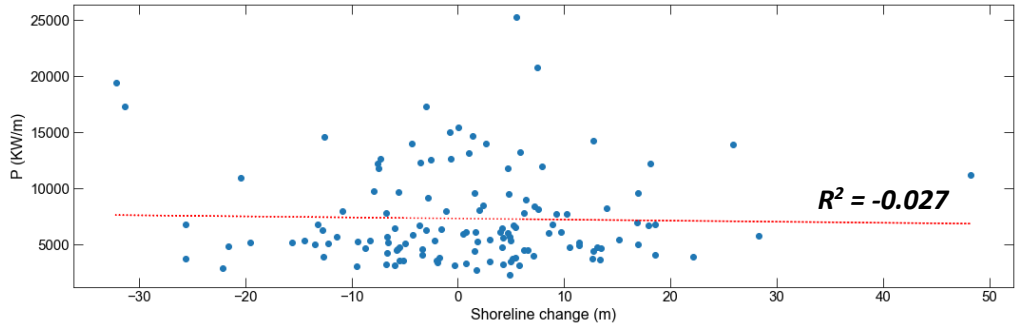

Section B:

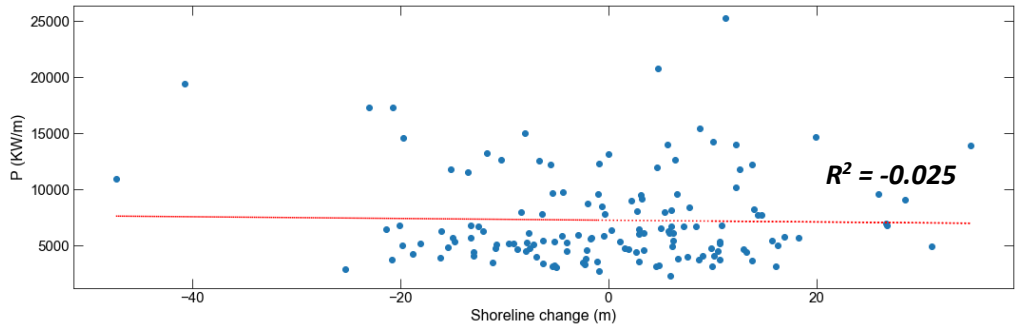

Section C:

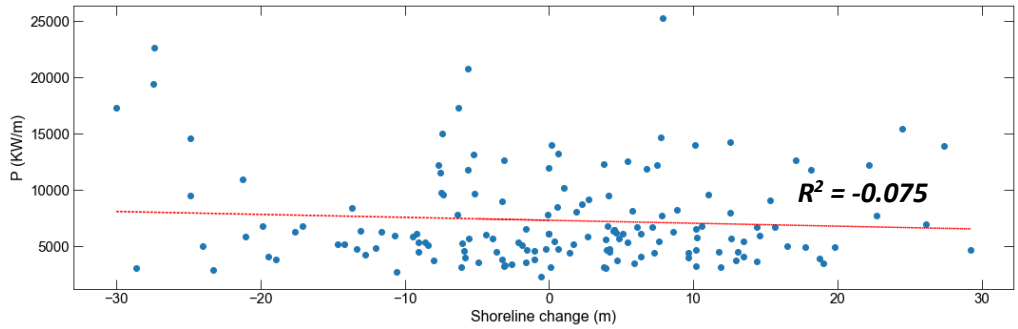

Section D:

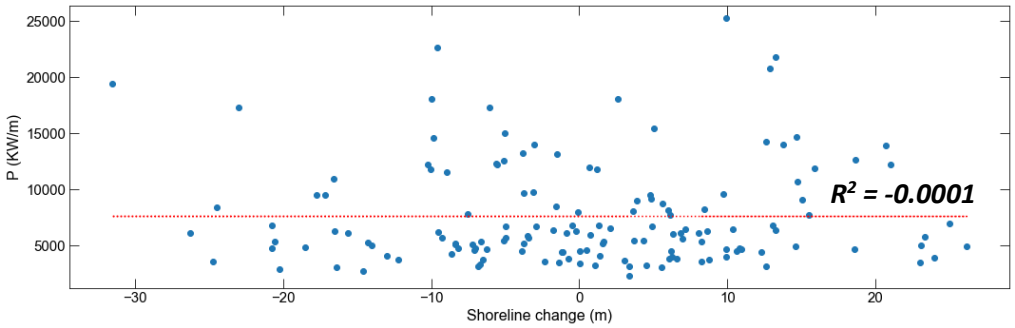

The same analysis was carried out for the four coastal sections but this time with an interval of 2 months between two monthly-averaged data points. Two monthly-averaged data points spaced 2 months apart thus equals a total time period of 3 months for which the sum of the wave power was calculated.

Section A:

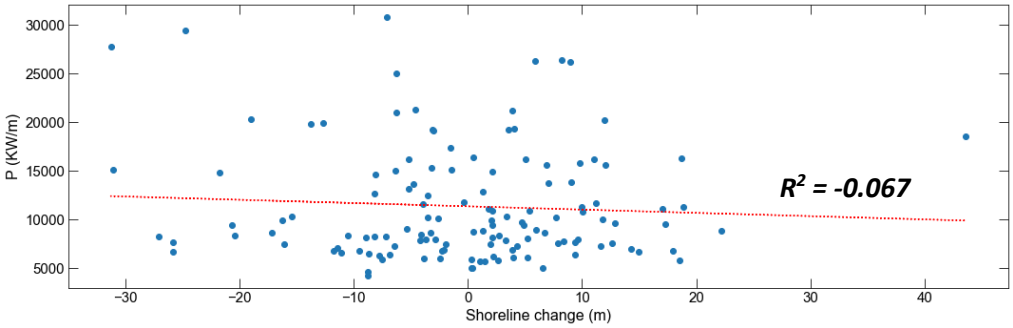

Section B:

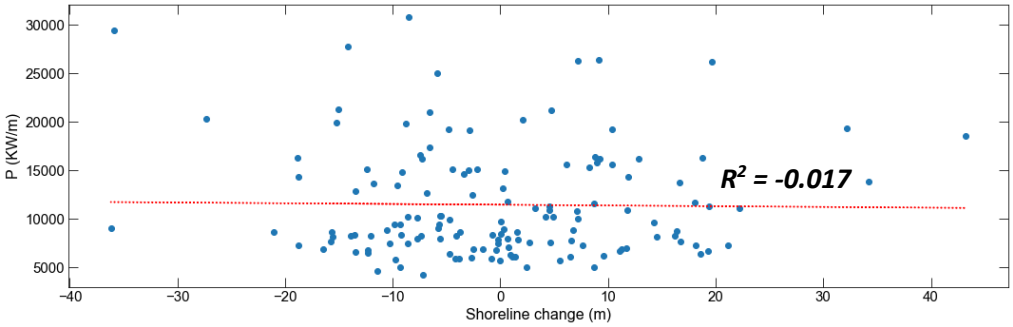

Section C:

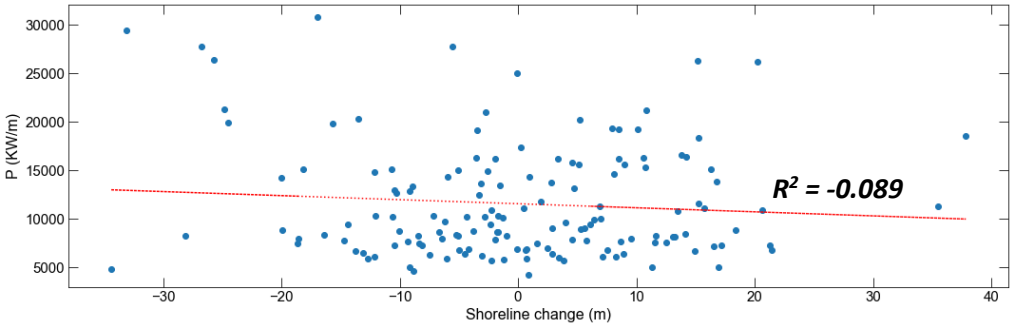

Section D:

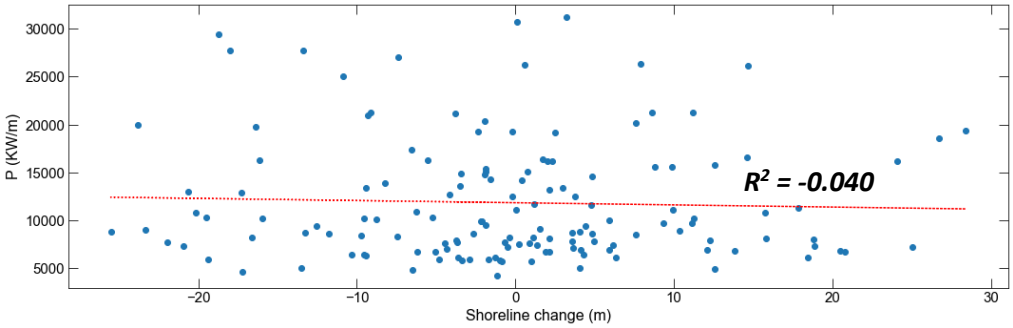

Appendix E

The following text gives a description of the figures included in this appendix.

E.1: Beach nourishments. Alongshore-averaged time-series of beach nourishments, based on $\widetilde{D_{sh}}(y,t)$. For every nourishment the time of construction is highlighted in grey and the volume (m^3/m) is indicated. The number in the left upper corner corresponds to the numbers in Table 4.1. Beach nourishment 1 and 3 are displayed together in one graph because they were implemented during the same month, making it impossible to separate them. In the figures, the blue dashed lines represent the end of construction of other beach nourishments and the red dashed lines represent the end of construction of other shoreface nourishments to give an indication of the presence of other nourishments. The unfinished nourishment (35 in Table 4.1) is also presented in some graphs where relevant because its construction was already in progress, therefore its possible influence could not be excluded.

E.2 Areas 500 m northward (left figures) and southward (right figures) of the beach nourishments. For a few nourishments, the longshore-averaged time-series of the area 500 m northward and southward of the beach nourishments were also investigated. Not all beach nourishments were studied, as explained in Chapter 6.3.3. Particularly, the beach nourishments which resulted in a clear peak in shoreline change were selected to evaluate the alongshore effects, since these were expected to have the most influence on the adjacent areas 500 m north and south. Again, the number in the left upper corner corresponds to the numbers in Table 4.1 and to the numbers in E.1. The y-axes of each three graphs containing the actual beach nourishment, the area northward, and the area southward, were set to the same range of values to be able to compare them more easily. Lastly, for clarity only the nourishments that (sometimes partly) were actually present within the adjacent areas are indicated here with the dashed blue and red lines. This section also includes two examples of areas 1000 m northward and southward of two beach nourishments.

E.3 Shoreface nourishments. This section includes the same as described in E.1, but now in the case of shoreface nourishments.

E.4 Areas 1000 m northward (left figures) and southward (right figures) of the shoreface nourishments. Same as delineated for E.2, but now for shoreface nourishments with areas of 1000 m adjacent to each shoreface nourishment.

E.1 Beach nourishments

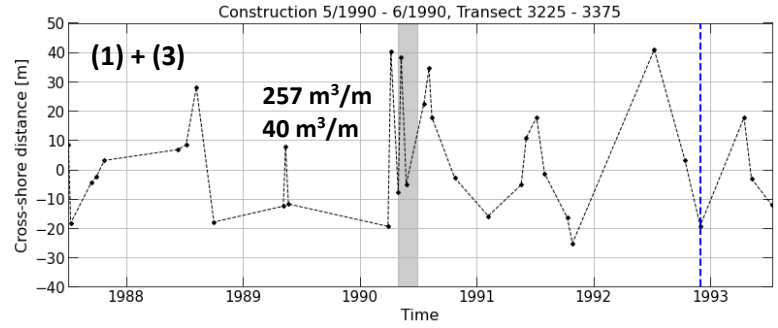

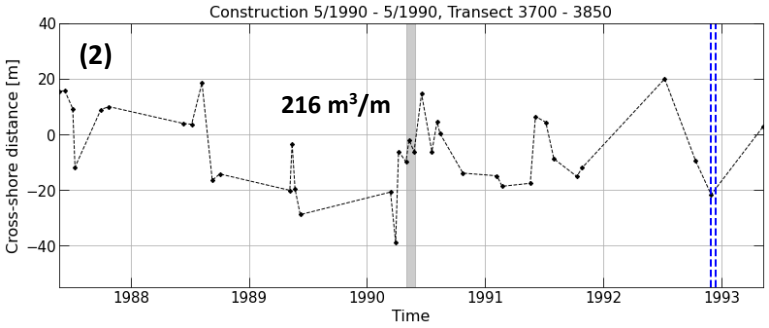

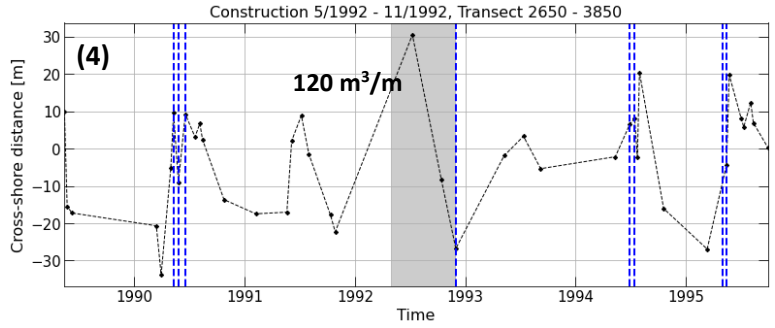

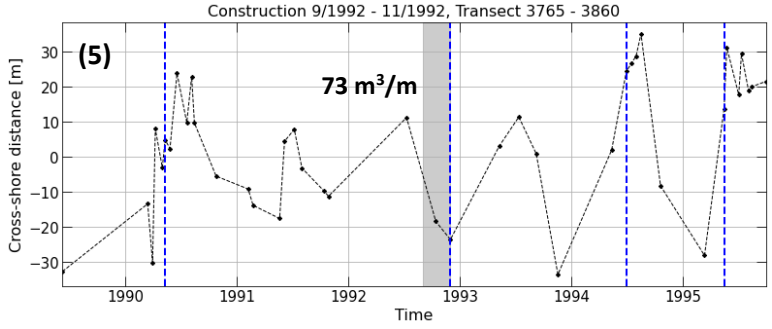

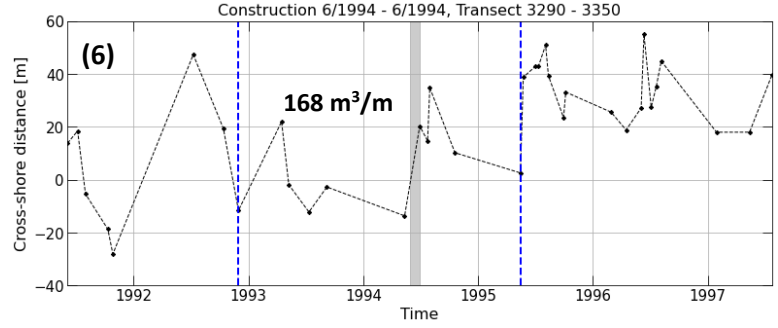

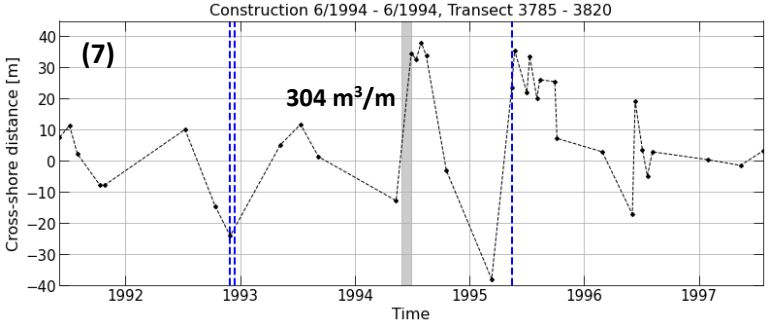

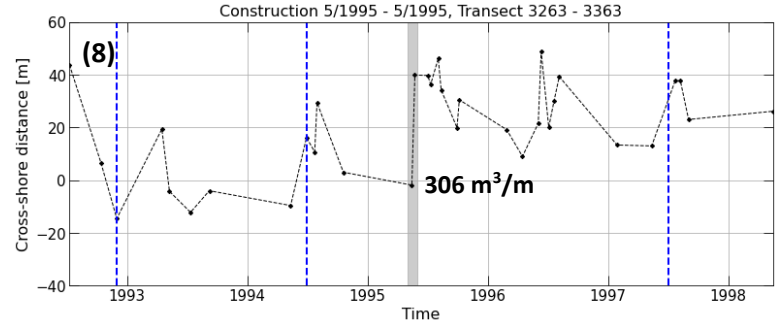

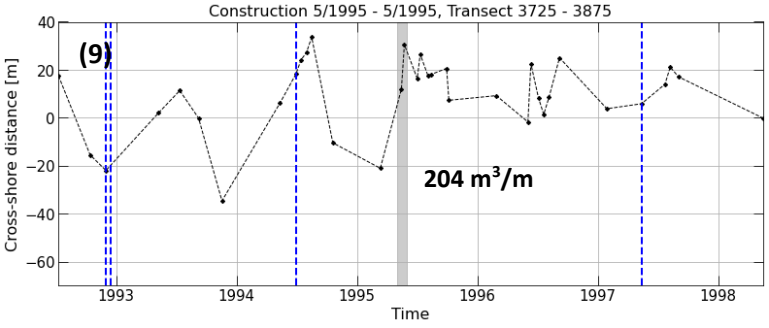

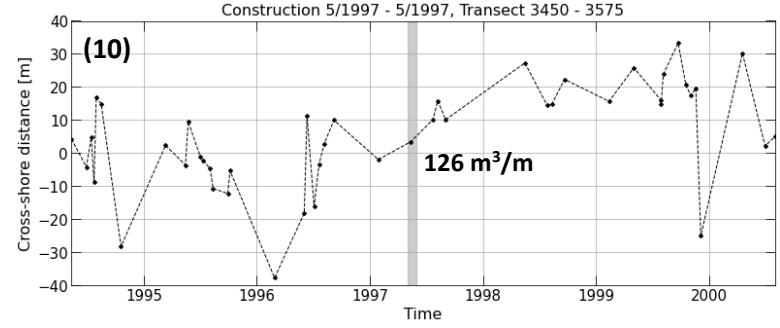

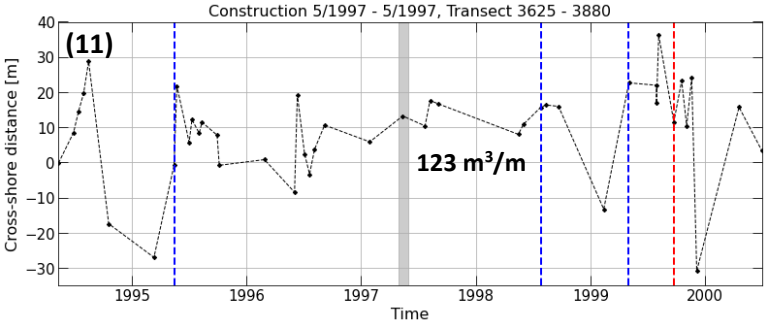

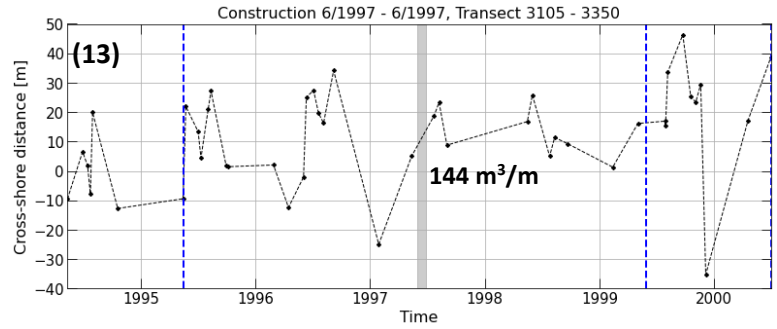
Construction 6/1997 - 6/1997, Transect 3105 - 3350
(13)
144 m³/m
Cross-shore distance [m]
Time

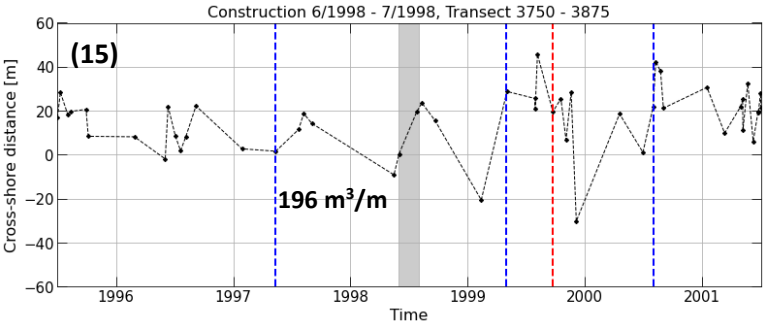
Construction 6/1998 - 7/1998, Transect 3750 - 3875
(15)
196 m³/m
Cross-shore distance [m]
Time

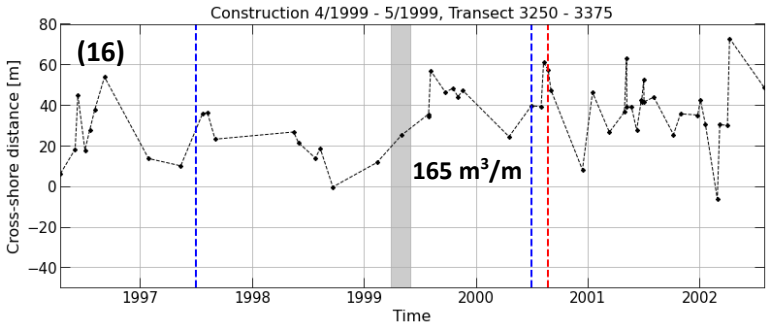
Construction 4/1999 - 5/1999, Transect 3250 - 3375
(16)
165 m³/m
Cross-shore distance [m]
Time

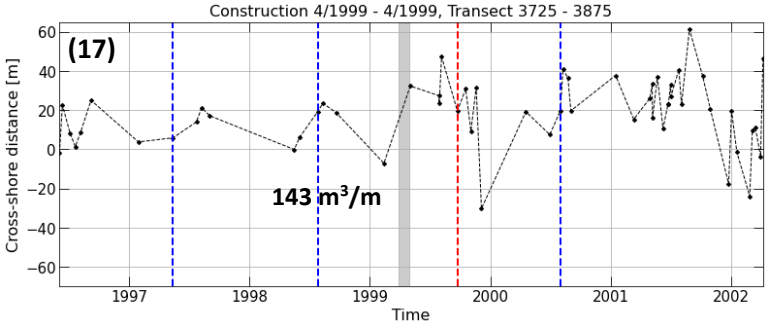
Construction 4/1999 - 4/1999, Transect 3725 - 3875
(17)
143 m³/m
Cross-shore distance [m]
Time

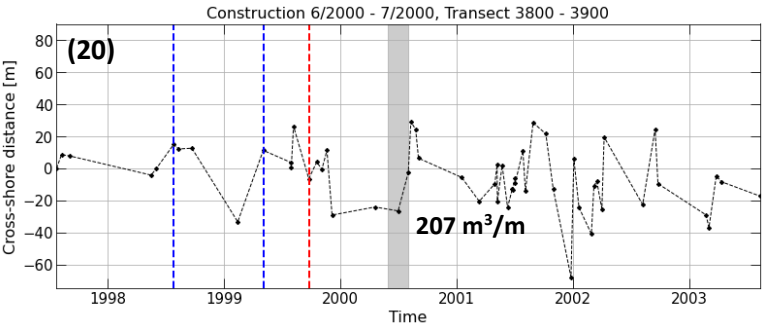
Construction 6/2000 - 7/2000, Transect 3800 - 3900
(20)
207 m³/m
Cross-shore distance [m]
Time

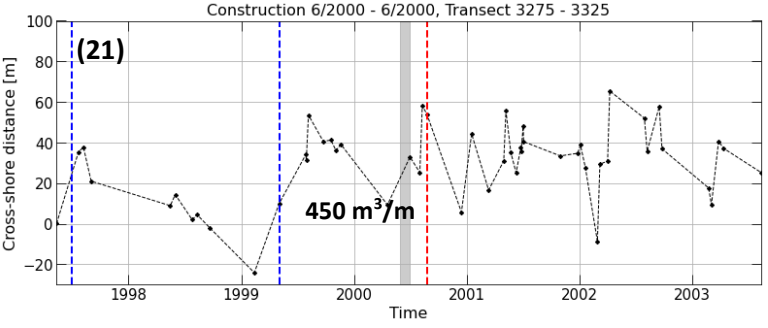
Construction 6/2000 - 6/2000, Transect 3275 - 3325
(21)
450 m³/m
Cross-shore distance [m]
Time

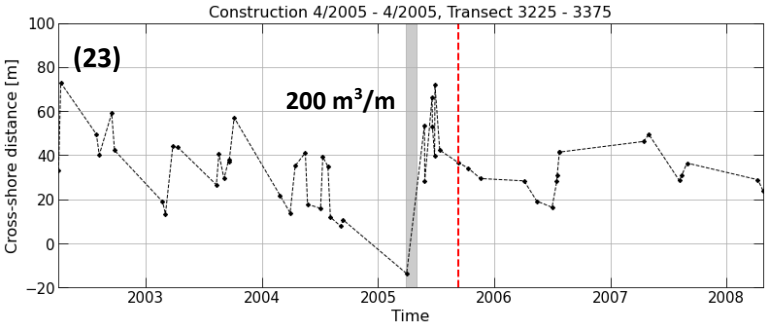
Construction 4/2005 - 4/2005, Transect 3225 - 3375
(23)
200 m³/m
Cross-shore distance [m]
Time

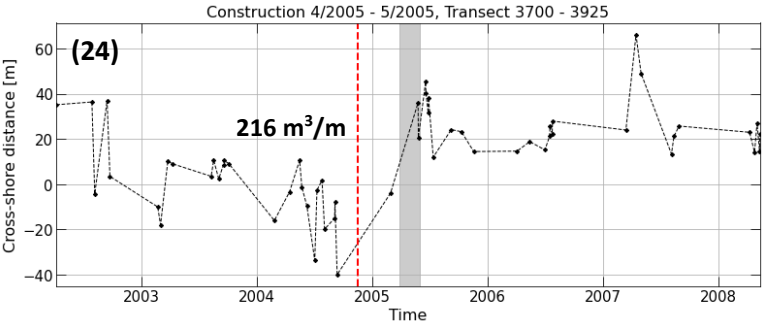
Construction 4/2005 - 5/2005, Transect 3700 - 3925
(24)
216 m³/m
Cross-shore distance [m]
Time

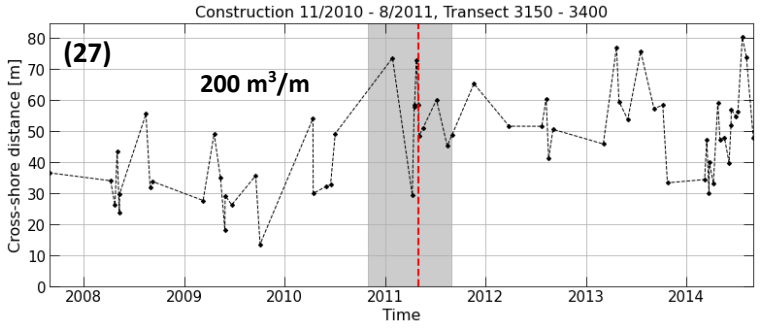
Construction 11/2010 - 8/2011, Transect 3150 - 3400
(27)
200 m³/m
Cross-shore distance [m]
Time

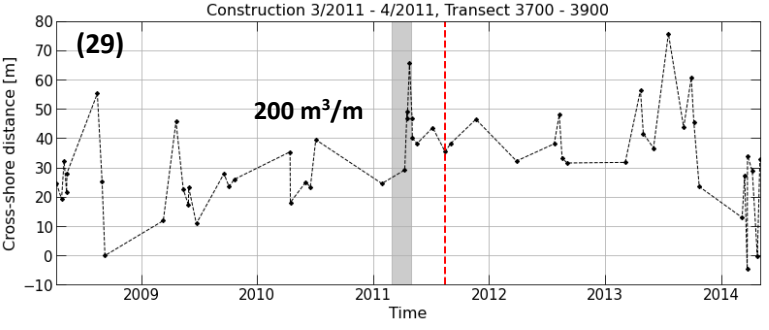
Construction 3/2011 - 4/2011, Transect 3700 - 3900
(29)
200 m³/m
Cross-shore distance [m]
Time

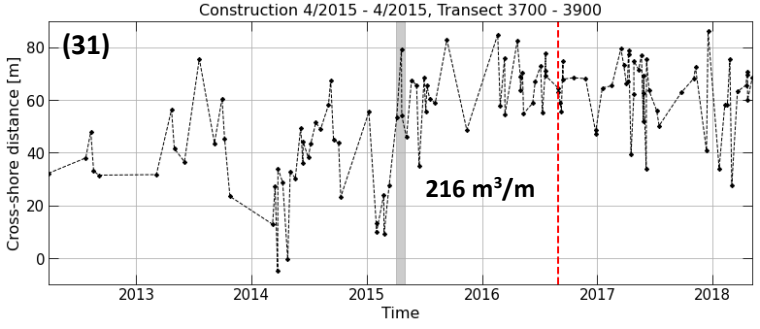
Construction 4/2015 - 4/2015, Transect 3700 - 3900
(31)
216 m³/m
Cross-shore distance [m]
Time

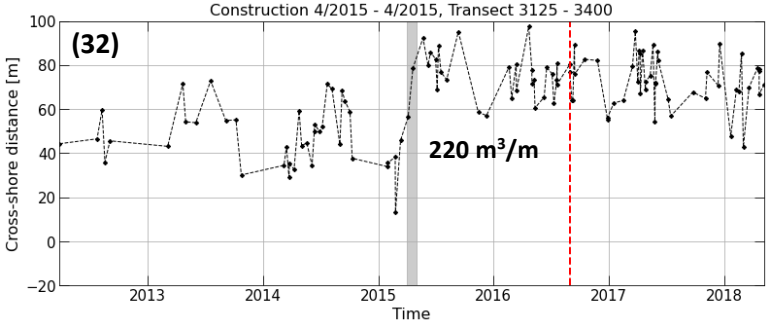
Construction 4/2015 - 4/2015, Transect 3125 - 3400
(32)
220 m³/m
Cross-shore distance [m]
Time

E.2 Areas 500 m northward (left figures) and southward (right figures) of the beach nourishments

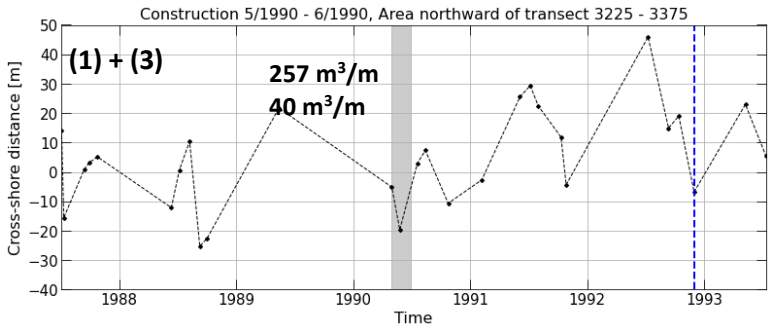

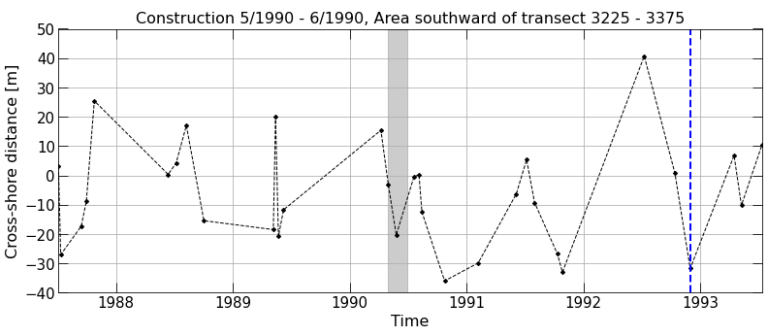

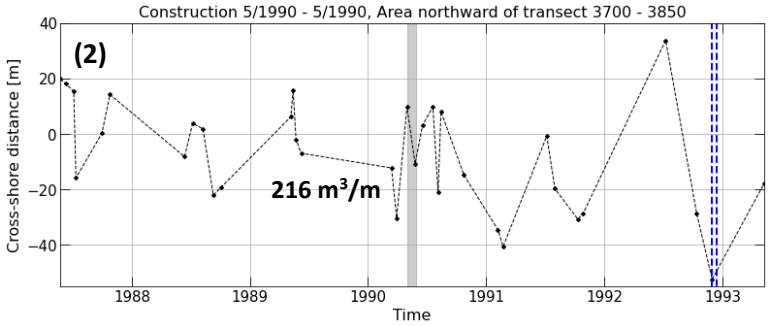

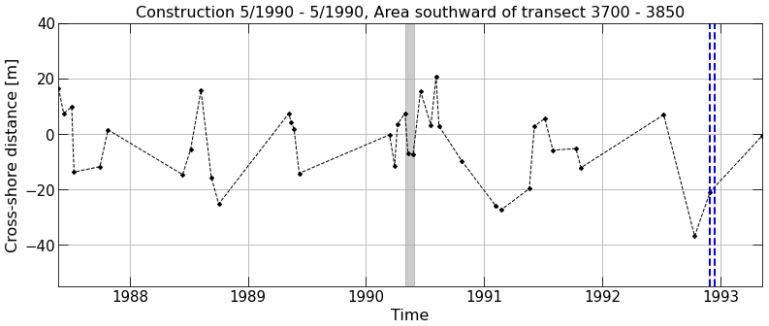

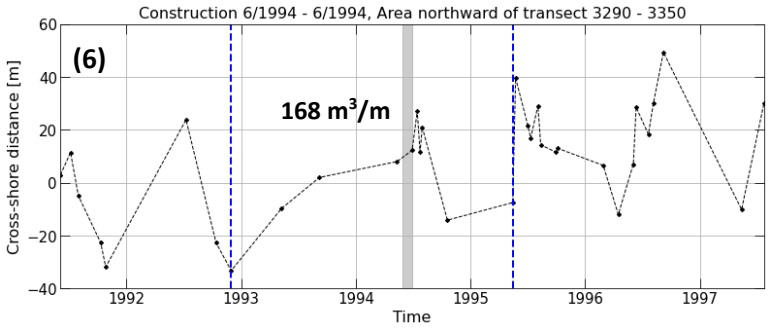

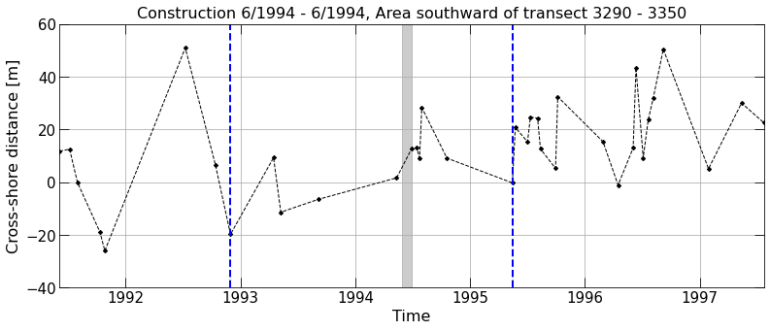

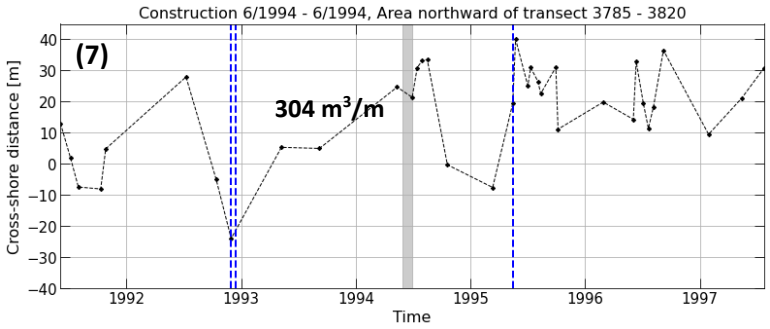

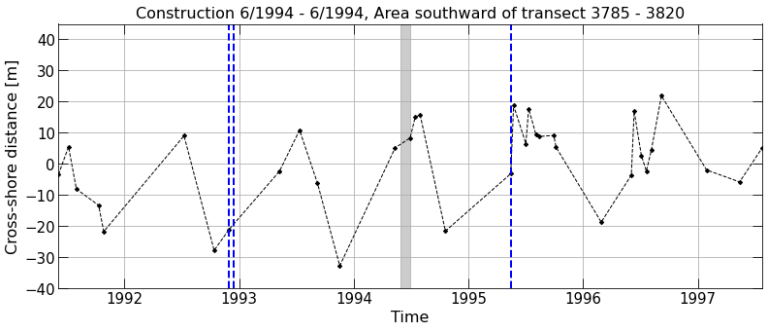

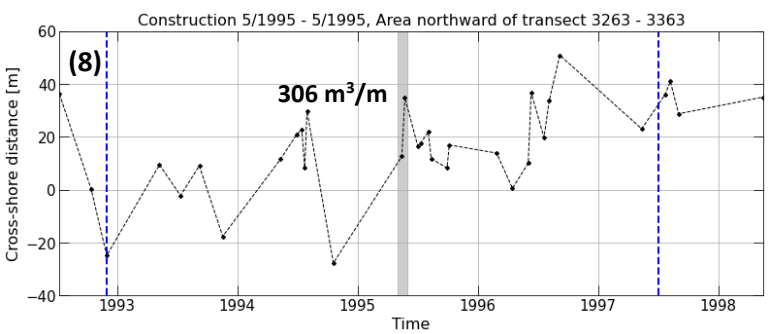

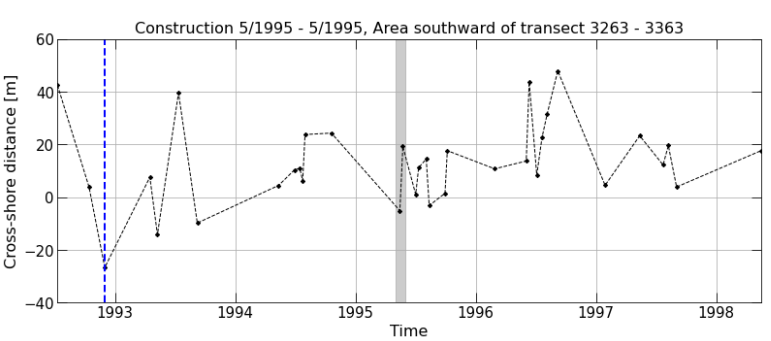

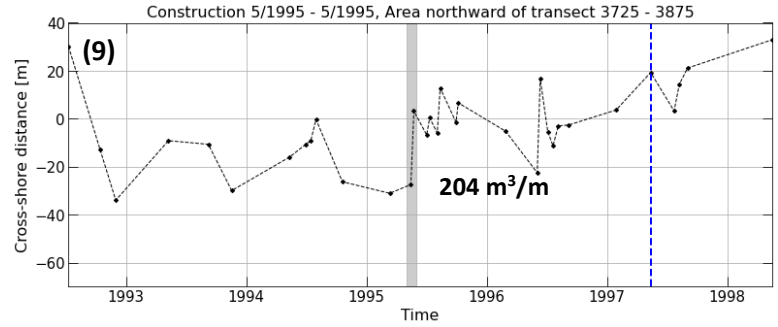
Construction 5/1995 - 5/1995, Area northward of transect 3725 - 3875
(9)
204 m³/m
Cross-shore distance [m]
Time

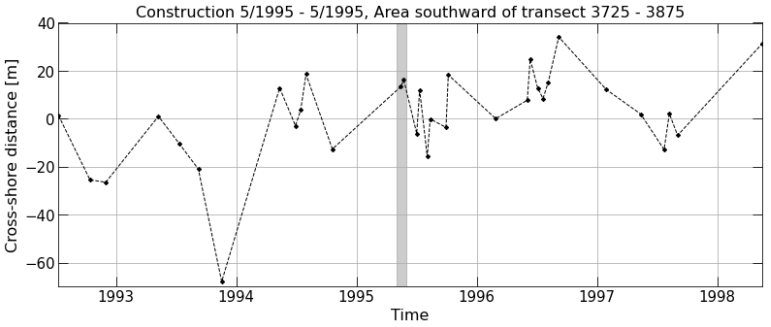
Construction 5/1995 - 5/1995, Area southward of transect 3725 - 3875
Cross-shore distance [m]
Time

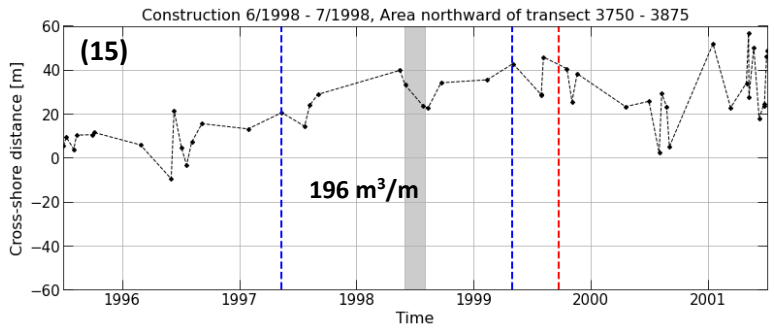
Construction 6/1998 - 7/1998, Area northward of transect 3750 - 3875
(15)
196 m³/m
Cross-shore distance [m]
Time

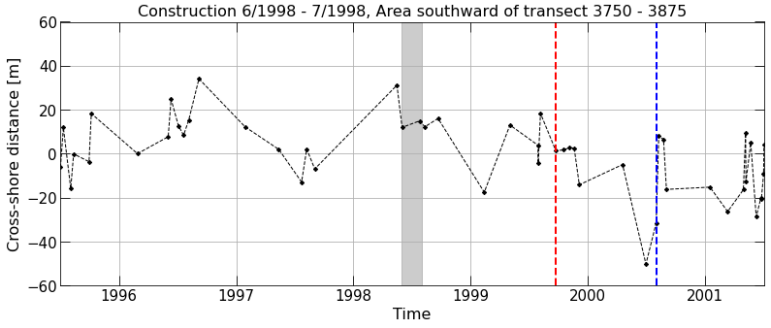
Construction 6/1998 - 7/1998, Area southward of transect 3750 - 3875
Cross-shore distance [m]
Time

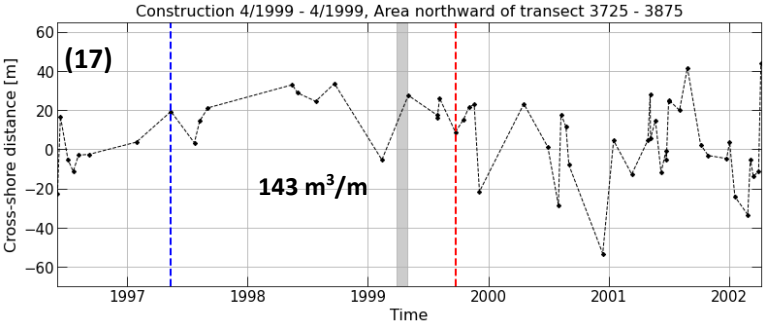
Construction 4/1999 - 4/1999, Area northward of transect 3725 - 3875
(17)
143 m³/m
Cross-shore distance [m]
Time

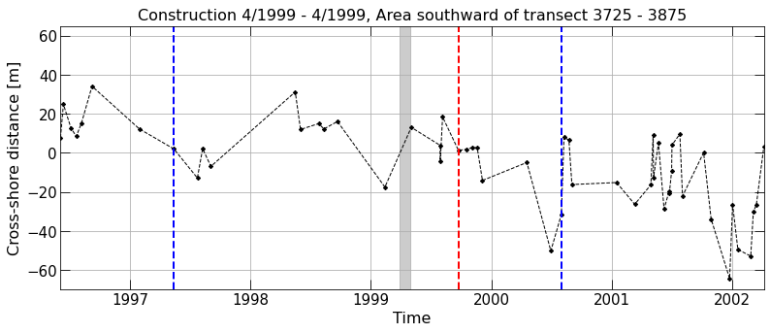
Construction 4/1999 - 4/1999, Area southward of transect 3725 - 3875
Cross-shore distance [m]
Time

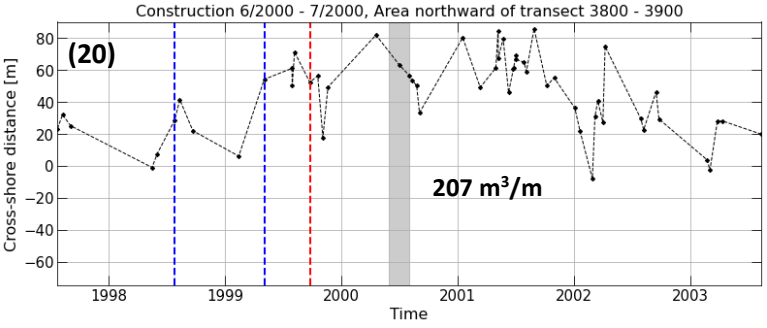
Construction 6/2000 - 7/2000, Area northward of transect 3800 - 3900
(20)
207 m³/m
Cross-shore distance [m]
Time

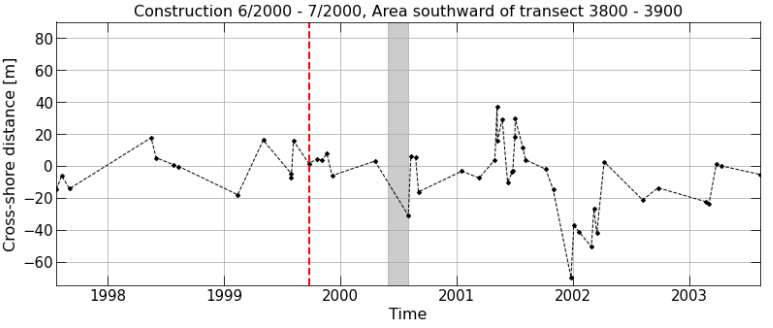
Construction 6/2000 - 7/2000, Area southward of transect 3800 - 3900
Cross-shore distance [m]
Time

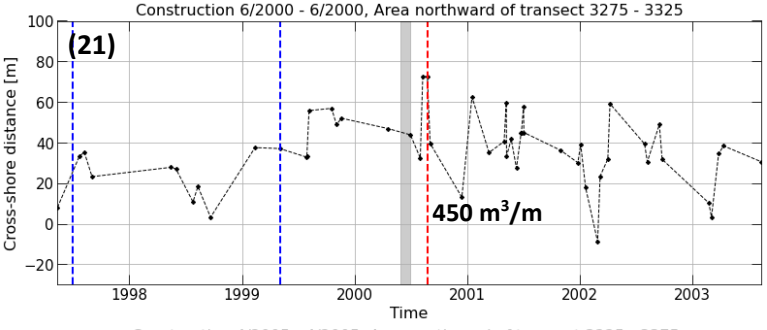
Construction 6/2000 - 6/2000, Area northward of transect 3275 - 3325
(21)
450 m³/m
Cross-shore distance [m]
Time

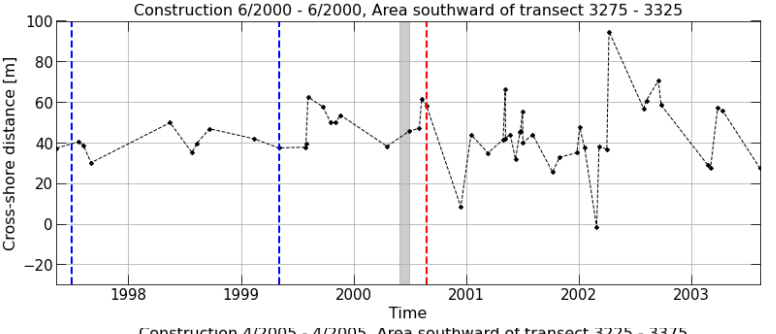
Construction 6/2000 - 6/2000, Area southward of transect 3275 - 3325
Cross-shore distance [m]
Time

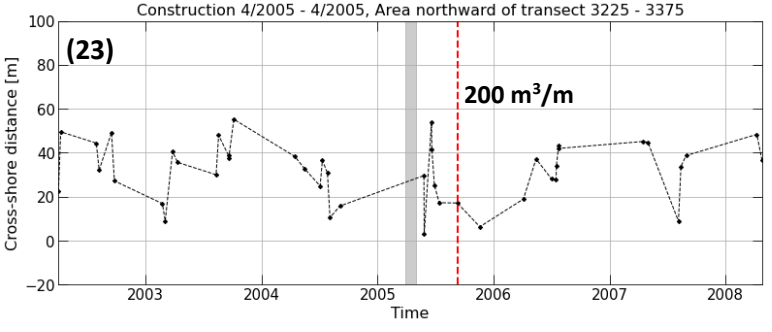
Construction 4/2005 - 4/2005, Area northward of transect 3225 - 3375
(23)
200 m³/m
Cross-shore distance [m]
Time

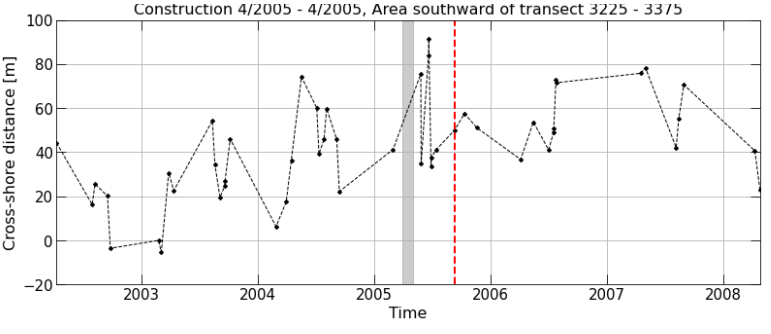
Construction 4/2005 - 4/2005, Area southward of transect 3225 - 3375
Cross-shore distance [m]
Time

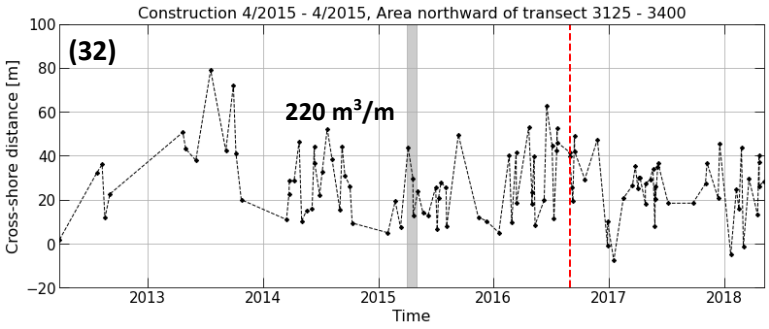

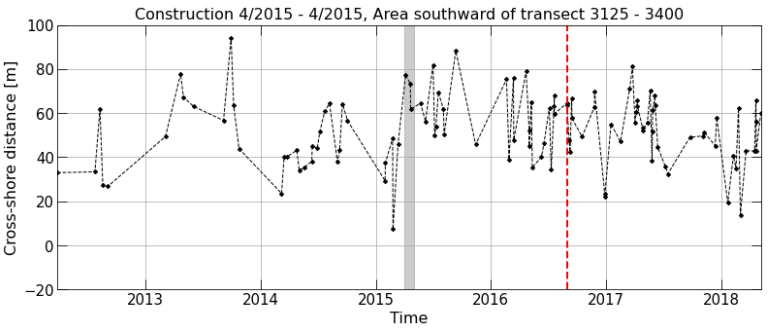

Two examples of areas 1000 m northward (left figures) and southward (right figures) of beach nourishments 8 and 15

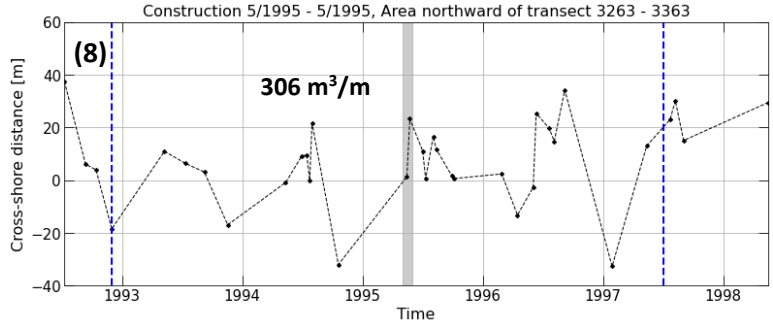

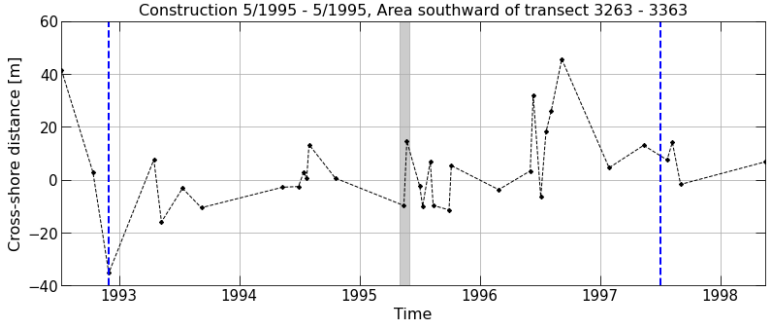

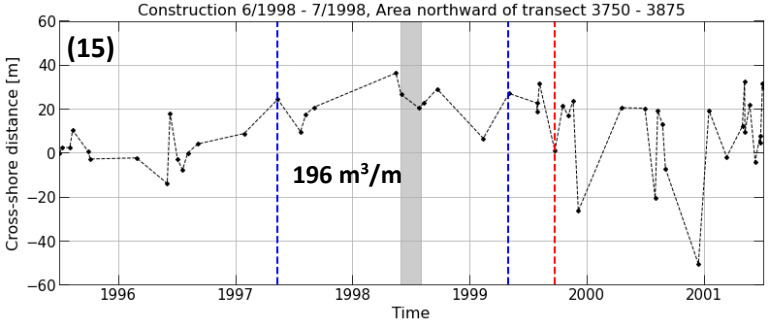

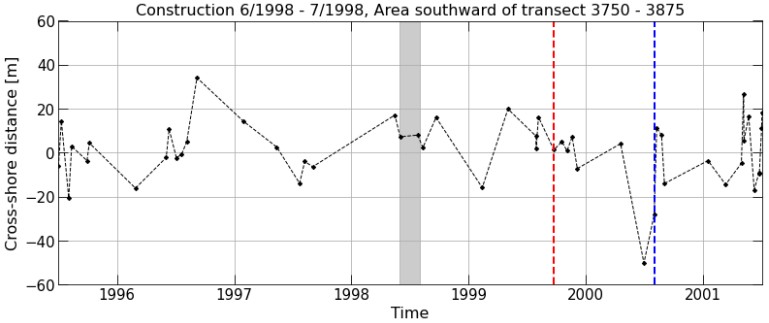

E.3 Shoreface nourishments

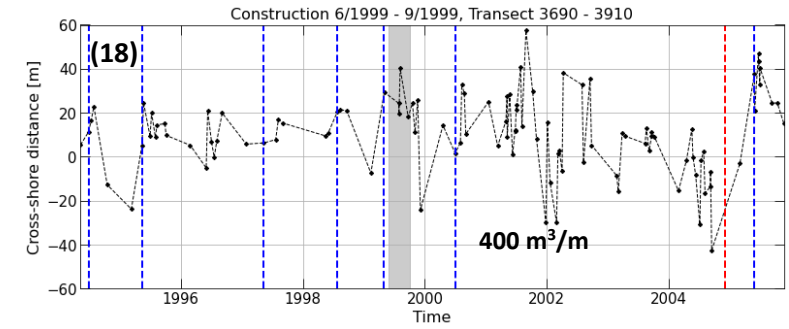

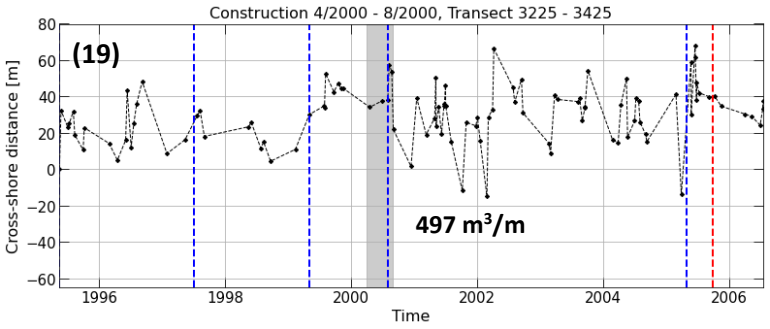

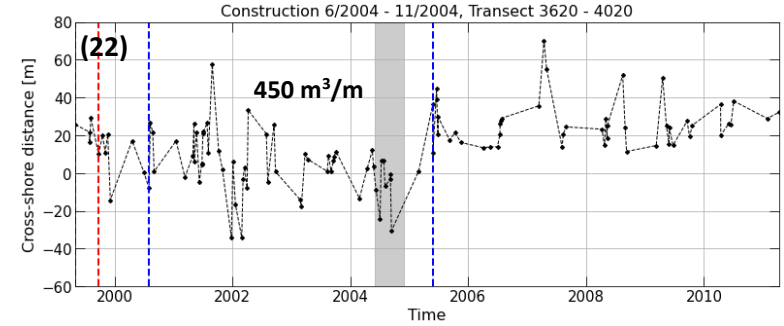

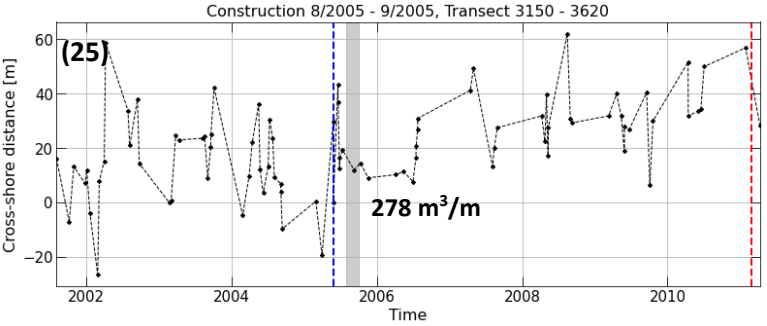

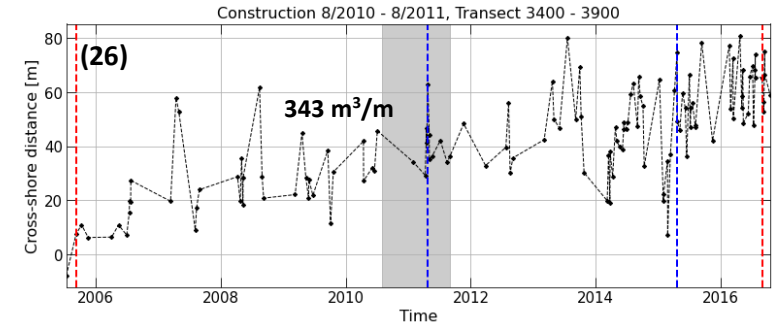

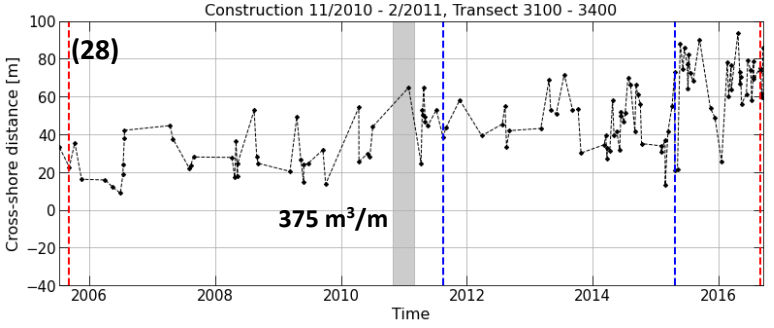

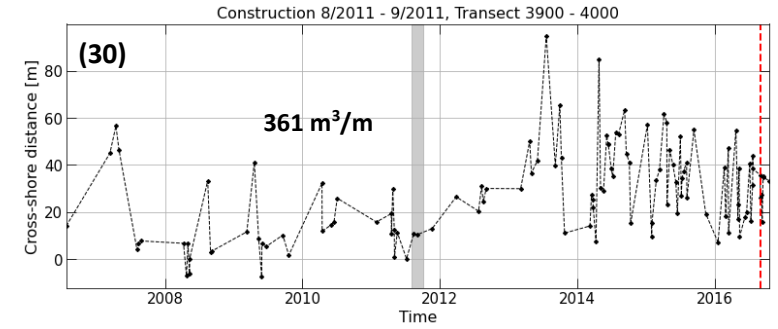

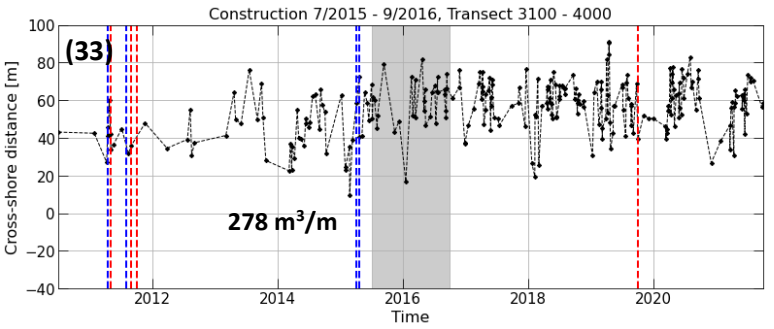

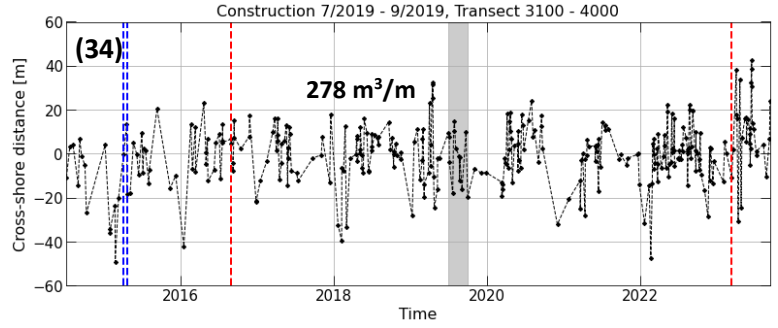

E.4 Areas 1000 m northward (left figures) and southward (right figures) of the shoreface nourishments.

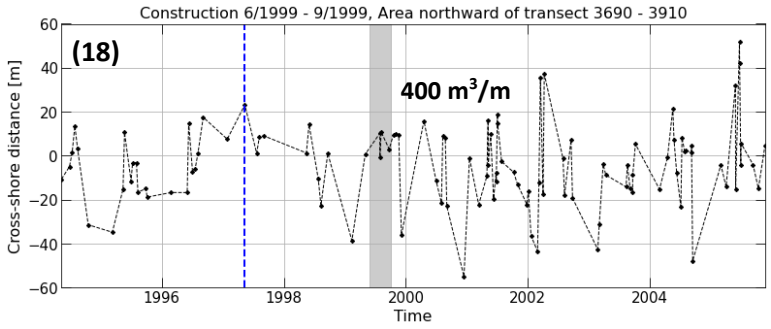

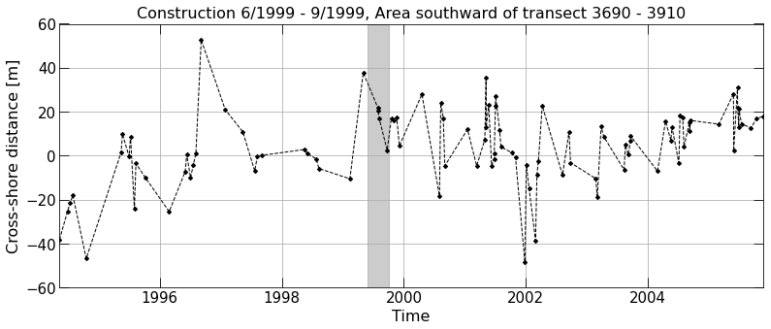

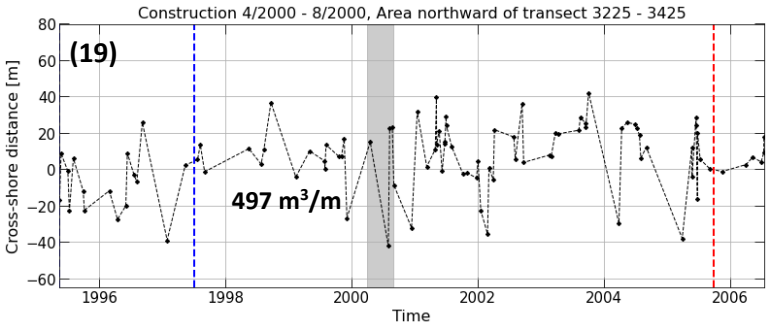

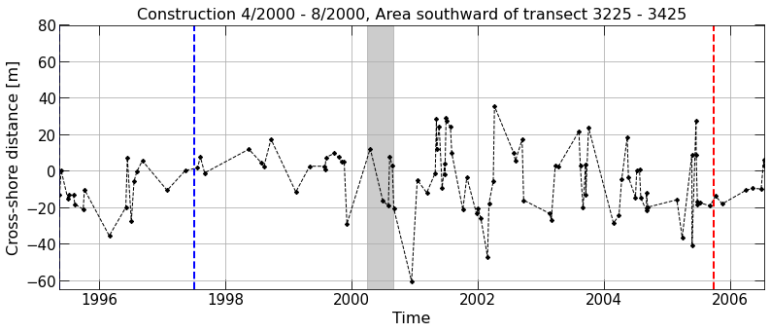

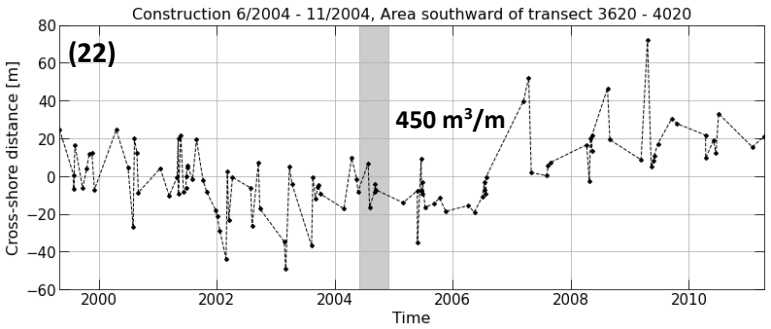

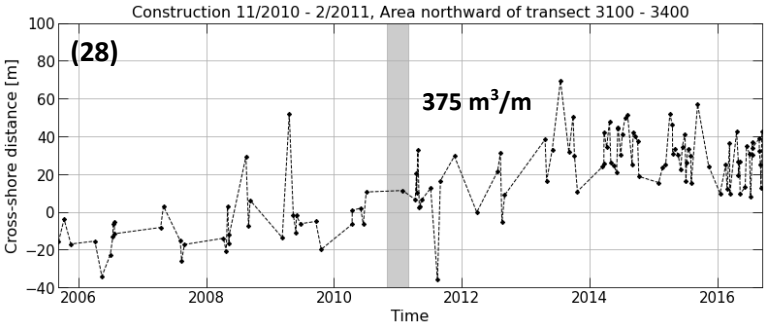

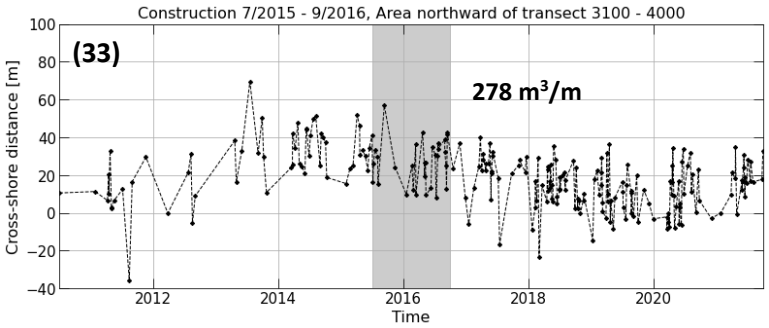

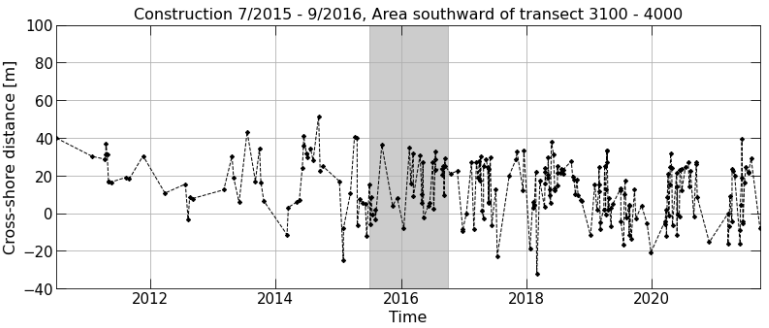

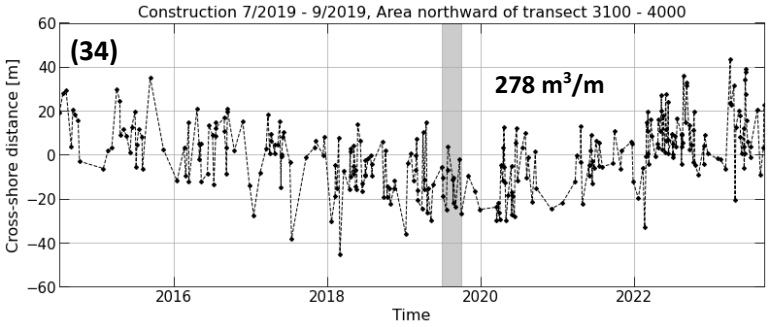
Construction 7/2019 - 9/2019, Area northward of transect 3100 - 4000
(34)
278 m³/m
Cross-shore distance [m]
Time
60
40
20
0
−20
−40
−60
2016
2018
2020
2022

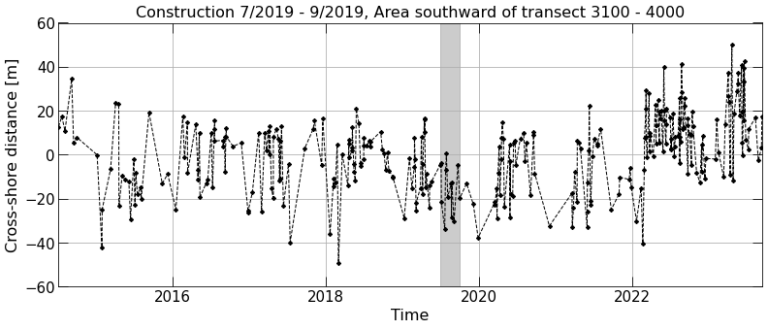
Construction 7/2019 - 9/2019, Area southward of transect 3100 - 4000
Cross-shore distance [m]
Time
60
40
20
0
−20
−40
−60
2016
2018
2020
2022